Bradford MM. 1976. A rapid and sensitive method for the quantitation of microgram quantities of protein utilizing the principle of protein-dye binding. Anal Biochem 772:248–254.
Castoria G, Barone MV, Di Domenico M, Bilancio A, Ametrano D, Migliaccio A, Auricchio F. 1999. Non-trascriptional action of oestradiol and progestin triggers DNA synthesis. EMBO J 18:2500–2510.
Castoria G, Migliaccio A, Bilancio A, Di Domenico M, de Falco A, Lombardi M, Fiorentino R, Varricchio L, Barone MV, Auricchio F. 2001. PI3-kinase in concert with Src promotes the S-phase entry of oestradiol-stimulated MCF-7 cells. EMBO J 20:6050–6059.
Cheng J, Lee EJ, Madison LD, Lazennec G. 2004. Expression of estrogen receptor β in prostate carcinoma cells inhibits invasion and proliferation and triggers apoptosis. FEBS Lett 566:169–172.
Couse JF, Korach KS. 1999. Reproductive phenotypes in the estrogen receptor-α knockout mouse. Ann Endocrinol 60:143–148.
Di Leo A, Messa C, Cavallini A, Linsalata M. 2001. Estrogens and colorectal cancer. Curr Drug Targets Immune Endocr Metabol Disord 1:1–12.
Dubal DB, Wilson ME, Wise PM. 1999. Estradiol: A protective and trophic factor in the brain. J Alzheimers Dis 1:265–274.
Fernando RI, Wimalasena J. 2004. Estradiol abrogates apoptosis in breast cancer cells through inactivation of BAD: Ras dependent non-genomic pathways requiring signaling through ERK and Akt. Mol Biol Cell 15:3266–3284.
Fiorelli G, Picariello L, Martineti V, Tonelli F, Brandi ML. 1999. Functional estrogen receptor β in colon cancer cells. Biochem Biophys Res Commun 261:521–527.
Geraldes P, Sirois MG, Tanguay J-F. 2003. Specific contribution of estrogen receptors on mitogen-activated protein kinase pathways and vascular cell activation. Circulation Res 93:399–405.
Han J, Lee JD, Bibbs L, Ulevitch RJ. 1994. A MAP kinase targeted by endotoxin and hyperosmolarity in mammalian cells. Science 265:808–811.
Harper SJ, LoGrasso P. 2001. Signalling for survival and death in neurones: The role of stress-activated kinases, JNK and p38. Cell Signal 13:299–310.
Horvath LG, Henshall SM, Lee CS, Head DR, Quinn DI, Makela S, Delprado W, Golovsky D, Brenner PC, O'Neill G, Kooner R, Stricker PD, Grygiel JJ, Gustafsson J-Å, Sutherland RL. 2001. Frequent loss of estrogen receptor-β expression in prostate cancer. Cancer Res 61:5331–5335.
Kang HJ, Soh Y, Kim MS, Lee EJ, Surh YJ, Kim HR, Kim SH, Moon A. 2003. Roles of JNK-1 and p38 in selective induction of apoptosis by capsaicin in Ras-transformed human breast epithelial cells. Int J Cancer 103:475–482.
Konstantinopoulos PA, Kominea A, Vandoros G, Sykiotis GP, Andricopoulos P, Varakis I, Sotiropoulou-Bonikou G, Papavassiliou AG. 2003. Oestrogen receptor beta (ERβ) is abundantly expressed in normal colonic mucosa, but declines in colon adenocarcinoma paralleling the tumour's dedifferentiation. Eur J Cancer 39:1251–1258.
Kousteni S, Bellido T, Plotkin LI, O'Brien CA, Bodenner DL, Han L, Han K, DiGregorio GB, Katzenellenbogen JA, Katzenellenbogen BS, Robertson PK, Weinstein RS, Jilka RL, Manolagas SC. 2001. Nongenotropic, sex-nonspecific signaling through the estrogen or androgen receptors: Dissociation from transcriptional activity. Cell 104:719–790.
Kuiper GG, Lemmen JG, Carlsson B, Corton JC, Safe SH, van der Saag PT, van der Burg B, Gustafsson J-Å. 1998. Interaction of estrogenic chemicals and phytoestrogens with estrogen receptor β. Endocrinology 139:4252–4263.
Lee H, Bai W. 2002. Regulation of estrogen receptor nuclear export by ligand-induced and p38-mediated receptor phosphorylation. Mol Cell Biol 22:5835–5845.
Lobenhofer EK, Huper G, Iglehart JD, Marks JR. 2000. Inhibition of mitogen-activated protein kinase and phosphatidylinositol 3-kinase activity in MCF-7 cells prevents estrogen-induced mitogenesis. Cell Growth Differ 11:99–110.
Marino M, Pallottini V, Trentalance A. 1998. Estrogens cause rapid activation of IP_3-PKC-α signal transduction pathway in HepG2 cells. Biochem Biophys Res Commun 245:254–258.
Marino M, Distefano E, Trentalance A, Smith CL. 2001. Estradiol-induced IP_3 mediate the estrogen receptor activity expressed in human cells. Mol Cell Endocrinol 182:19–26.
Marino M, Acconcia F, Bresciani F, Weisz A, Trentalance A. 2002. Distinct non genomic signal transduction pathways controlled by 17β-estradiol regulate DNA synthesis and cyclin D_1 gene transcription in HepG2 cells. Mol Biol Cell 13:3720–3729.
Marino M, Acconcia F, Trentalance A. 2003. Biphasic estradiol-induced AKT-phosphorylation is modulated by PTEN via MAP kinase in HepG2 cells. Mol Biol Cell 14:2583–2591.
Matthews J, Gustafsson J-Å. 2003. Estrogen signalling: A subtle balance between ERα and ERβ. Mol Interventions 3:281–292.
Moon WS, Chang K, Tarnawski AS. 2004. Overexpression of metastatic tumor antigen 1 in hepatocellular carcinoma: Relationship to vascular invasion and estrogen receptor-α. Hum Pathol 35:424–429.
Mori-Abe A, Tsutsumi S, Takahashi K, Toya M, Yoshida M, Du B, Kawagoe J, Nakahara K, Takahashi T, Ohmichi M, Kurachi H. 2003. Estrogen and raloxifene induce apoptosis by activating p38 mitogen-activated protein kinase cascade in synthetic vascular smooth muscle cells. J Endocrinol 178:417–426.
Ogawa S, Inoue S, Watanabe T, Orimo A, Hosoi T, Ouchi Y, Muramatsu M. 1998. Molecular cloning and characterization of human estrogen receptor βcx: A potential inhibitor of estrogen action in human. Nucleic Acids Res 26:3505–3512.
Paruthiyil S, Parmar H, Kerekatte V, Cunha GR, Firestone GL, Leitman DC. 2004. Estrogen receptor β inhibits human breast cancer cell proliferation and tumor formation by causing a G2 cell cycle arrest. Cancer Res 64:423–428.
Porras A, Zuluaga S, Black E, Valladares A, Alvarez AM, Ambrosino C, Benito M, Nebreda AR. 2004. p38α mitogen-activated protein kinase sensitizes cells to apoptosis induced by different stimuli. Mol Biol Cell 15:922–933.
Rapp UR, Rennefahrt U, Troppmair J. 2004. Bcl-2 proteins: Master switches at the intersection of death signaling and the survival control by Raf kinases. Biochim Biophys Acta 1644:149–158.
Razandi M, Pedram A, Greene GL, Levin ER. 1999. Cell membrane and nuclear estrogen receptors (ERs) originate from a single transcript: Studies of ERα and ERβ expressed in Chinese hamster ovary cells. Mol Endocrinol 13:307–319.
Razandi M, Pedram A, Levin ER. 2000a. Plasma membrane estrogen receptors signal to antiapoptosis in breast cancer. Mol Endocrinol 14:1434–1447.
Razandi M, Pedram A, Levin ER. 2000b. Estrogen signals to the preservation of endothelial cell form and function. J Biol Chem 275:38540–38546.
Razandi M, Oh P, Pedram A, Schnitzer J, Levin ER. 2002. ERs associate with and regulate the production of caveolin: Implications for signaling and cellular actions. Mol Endocrinol 16:100–115.
Roger P, Sahla ME, Makela S, Gustafsson J-Å, Baldet P, Rochefort H. 2001. Decreased expression of estrogen receptor beta protein in proliferative preinvasive mammary tumors. Cancer Res 61:2537–2541.
Shimada K, Nakamura M, Ispida E, Kishi M, Konishi N. 2003. Roles of p38- and c-jun NH2-terminal kinase-mediated pathways in 2-methoxyestradiol-induced p53 induction and apoptosis. Carcinogenesis 24:1067–1075.
Song RX, Santen RJ. 2003. Apoptotic action of estrogen. Apoptosis 8:55–60.
Song RX, Mor G, Naftolin F, McPherson RA, Song J, Zhang Z, Yue W, Wang J, Santen RJ. 2001. Effect of long-term estrogen deprivation on apoptotic responses of breast cancer cells to 17β-estradiol. J Nat Cancer Institute 93:1714–1723.
Song YS, Park HJ, Kim SY, Lee SH, Yoo HS, Lee HS, Lee MK, Oh KW, Kang SK, Lee SE, Hong JT. 2004. Protective role of Bcl-2 on β-amyloid-induced cell death of differentiated PC12 cells: Reduction of NF-κB and p38 MAP kinase activation. Neurosci Res 49:69–80.
Strom A, Hartman J, Foster JS, Kietz S, Wimalasena J, Gustafsson J-Å. 2004. Estrogen receptor beta inhibits 17β-estradiol-stimulated proliferation of the breast cancer cell line T47D. Proc Natl Acad Sci USA 101:1566–1571.
Sutherland RL, Reddel RR, Green MD. 1983. Effects of estrogens on cell proliferation and cell cycle kinetics: A hypothesis on the cell cycle effects of antiestrogens. Eur J Cancer Clin Oncol 19:307–318.
Talapatra S, Thompson CB. 2001. Growth factor signaling in cell survival: Implications for cancer treatment. J Pharmacol Exp Ther 298:873–878.
Tamura Y, Simizu S, Osada H. 2004. The phosphorylation status and anti-apoptotic activity of Bcl-2 are regulated by ERK and protein phosphatase 2A on the mitochondria. FEBS Lett 569:249–255.
Weihua Z, Andersson S, Cheng G, Simpson ER, Warner M, Gustafsson J-Å. 2003. Update on estrogen signaling. FEBS Lett 46:17–24.
Zhang CC, Shapiro DJ. 2000. Activation of the p38 mitogen-activated protein kinase pathway by estrogen or by 4-hydroxytamoxifen is coupled to estrogen receptor-induced apoptosis. J Biol Chem 275:479–486.
Zhang HM, Rao JN, Guo X, Liu L, Zou T, Turner DJ, Wang JY. 2004. Akt kinase activation blocks apoptosis in intestinal epithelial cells by inhibiting caspase-3 after polyamine depletion. J Biol Chem 279:22539–22547.
Zheng J, Ali A, Ramirez VD. 1996. Steroids conjugated to bovine serum albumin as tools to demonstrate specific steroid neuronal membrane binding sites. J Psych Neurosci 21:187–197.

Available online at www.sciencedirect.com
SCIENCE DIRECT
ELSEVIER
Biochemical and Biophysical Research Communications 338 (2005) 1950–1956
BBRC
www.elsevier.com/locate/ybbrc

A retrovirus restriction factor TRIM5α is transcriptionally regulated by interferons ☆

Kentaro Asaoka [a,b], Kazuhiro Ikeda [a], Toshiki Hishinuma [a], Kuniko Horie-Inoue [a], Satoru Takeda [b], Satoshi Inoue [a,c,*]

[a] Division of Gene Regulation and Signal Transduction, Research Center for Genomic Medicine, Saitama Medical School, Saitama, Japan
[b] Department of Obstetrics and Gynecology, Saitama Medical Center, Saitama Medical School, Saitama, Japan
[c] Department of Geriatric Medicine, Graduate School of Medicine, The University of Tokyo, Tokyo, Japan

Received 7 October 2005
Available online 11 November 2005

Abstract

TRIM5α is a member of tripartite motif protein family and recently identified as a restriction factor for retroviral infection in a species-specific manner. Human TRIM5α gene is located on chromosomal position 11p15 in a cluster with other TRIM genes including TRIM6, 21, 22, and 34. We show here that interferon (IFN) upregulates TRIM5α mRNA expression in HeLa and HepG2 cells by performing Northern blot analysis and quantitative real-time PCR. TRIM5α promoter activity was IFN inducible as confirmed by luciferase assay using a reporter plasmid that contained the 5′-flanking region of TRIM5α. Mutational analysis has revealed that IFNs activate TRIM5α promoter activity through a putative interferon-stimulated response element (ISRE). Intriguingly, another IFN-responsive protein signal transducer and activator of transcription factor 1 (STAT1) binds to the ISRE sequence as shown by electrophoretic mobility shift assay using HeLa cell extracts. We have raised a specific polyclonal antibody against TRIM5α and confirmed that TRIM5α protein expression is inducible by IFN-β in HeLa cells. These results lead us to define that the transcription and protein synthesis of TRIM5α could be modulated by IFN, suggesting that TRIM5α may play a role in an IFN-induced antiviral state against retrovirus infection.

Keywords: TRIM5α; Interferon; Interferon-stimulated response element; Signal transducer and activator of transcription factor 1

Tripartite motif (TRIM) proteins are composed of RING, B-box, and coiled-coil domains, but the functions of most TRIM proteins are not well understood [1]. TRIM5α is one of the six variants that are encoded by TRIM5 gene and includes a carboxyl-terminal SPRY domain lacking in other TRIM5 isoforms. TRIM5α has recently been shown to inhibit the infectivity of a range of different retroviruses in a species-specific manner and the carboxyl-terminal SPRY domain is a determinant for the species specificity of restriction. Human TRIM5α potently restricts N-tropic murine leukemia virus (MLV) and specifies an intermediate level of resistance to human immunodeficiency virus type 1 (HIV-1). In contrast, rhesus monkey TRIM5α potently restricts HIV-1 and exhibits a modest inhibition of N-MLV infection. Rhesus monkey TRIM5γ that lacks an intact SPRY domain, however, does not inhibit HIV-1 infection and even represses the ability of wild-type rhesus monkey TRIM5α. Notably, replacement of three amino acids in the amino-terminal variable region of human TRIM5α with the corresponding rhesus monkey TRIM5α residues resulted in a TRIM5α molecule that restricted HIV-1 nearly as efficiently as wild-type rhesus monkey TRIM5α [2].

The interferons (IFNs) are a family of secreted multifunctional proteins that exert a broad spectrum of

☆ *Abbreviations:* TRIM, tripartite motif; IFN, interferon; ISRE, interferon-stimulated response element; IRFE, IFN response factor binding element; IRF, interferon regulatory factor; STAT, signal transducer and activator of transcription factor; HIV-1, human immunodeficiency virus type 1; RNF, ring finger protein; RT-PCR, reverse transcription-polymerase chain reaction; EMSA, electrophoretic mobility shift assay.

* Corresponding author. Fax: +81 429 85 7209.
E-mail address: s_inoue@saitama-med.ac.jp (S. Inoue).

0006-291X/$ - see front matter © 2005 Elsevier Inc. All rights reserved.
doi:10.1016/j.bbrc.2005.10.173

biological functions including antiviral, antiproliferative, antitumor, and immunomodulatory activities [3]. They are subdivided into two types that activate transduction pathways via different cell surface receptors. Interferon regulatory factors (IRFs) have been identified together with signal transducers and activators of transcription (STAT) from studies on the type I IFN as well as IFN-stimulated gene (ISG) regulation and signaling. In response to such phenomena as viral infection, type I IFN (IFN-α/β) that is produced predominantly by B lymphocytes binds to its cognate receptor and activates receptor-associated Janus kinases Jak1 and Tyk2, leading to phosphorylation of STAT1 and STAT2. Tyrosine phosphorylated STAT1 and STAT2 form the transcriptionally active IFN-stimulated gene factor 3 by association with IRF-9 that recognizes interferon-stimulated response element (ISRE), present on the promoter of target genes [4]. Gene induction by type II IFN (IFN-γ) involves solely the phosphorylation of STAT1 by Jak1 and Jak2 kinases, leading to the generation of a STAT1 homodimer that is able to bind the IFN-γ-activated site (GAS element) to activate transcription [5,6].

We have previously cloned RING finger protein 21 (RNF21) and found that the mRNA expression of the medium form of RNF21 was upregulated by IFN-α and IFN-γ treatments [7]. RNF21 gene was mapped to chromosome 11p15.3-p15.4. The medium form of RNF21 is found to be a 488-amino acid protein that is encoded by TRIM34 gene, containing a carboxyl-terminal SPRY domain.

Based on the antiretroviral activities of TRIM5α as well as the structural similarity of TRIM5α with TRIM34, we suspected whether TRIM5α is an IFN-stimulated gene, which may play a role in the antiviral process of IFN against retroviral infection. We show here that TRIM5α is induced by both type I and type II IFNs and the IFN responsiveness is predominantly mediated through an ISRE sequence on the proximal promoter region of TRIM5α. Moreover, we have found that an IFN-stimulated transcription factor STAT1 may also be involved in a protein complex that binds to the ISRE on TRIM5α promoter.

Materials and methods

Cell culture. Human embryonic kidney 293T cells, human hepatoma HepG2 cells, and human cervical adenocarcinoma HeLa cells were purchased from American Type Culture Collection (Manassas, VA). Human endometrial cancer Ishikawa 3H12 No. 74 cells were a kind gift of Dr. M. Nishida. Cells were maintained in Dulbecco's modified Eagle's medium (DMEM) supplemented with 10% fetal calf serum (FCS) at 37 °C in 5% CO_2 and a humidified atmosphere.

Cloning of TRIM5α cDNA. Human full-length TRIM5α cDNA was cloned by reverse transcription-PCR. The template cDNA was generated from the Ishikawa cell total RNA using Superscript II reverse transcriptase (Invitrogen) with poly$(dT)_{20}$ primer according to the manufacturer's protocol. The TRIM5α cDNA was amplified with primers 5′-GAATTCG CTTCTGGAATCCTGGTTAATGTA-3′ and 5′-CTCGAGTCAAGA GCTTGGTGAGCACAGAGT-3′, inserted in-frame to Flag-tagged pcDNA3 (Invitrogen) at *Eco*RI and *Xho*I sites.

Computational analysis of TRIM5α sequence. Chromosomal localization and amino acid sequence comparison of TRIM5α were analyzed by Map Viewer and BLAST on the NCBI web site (http://www.ncbi.nlm.nih.gov). Following DNA sequences were retrieved from GenBank database on the NCBI web site: human TRIM5α (NM_033034), human TRIM6 (NM_001003818), human TRIM34 (NM_021616), and human TRIM22 (NM_006074).

Quantitative PCR and Northern blotting. HeLa cells and HepG2 cells were treated with IFN-α, IFN-β, IFN-γ or control vehicle (PBS) for 6 or 16 h and total RNAs were isolated using an ISOGEN reagent (Nippon Gene). Probes for Northern blot analysis were prepared by labeling the cloned human TRIM5α cDNAs with [^{32}P]dCTP using a Random Primer Labeling Kit (Takara Bio). Total RNAs (20 μg) were separated in 1% formaldehyde denaturing agarose gels and transferred to Hybond-NX membranes (Amersham Biosciences). Blotted membranes were hybridized with the ^{32}P-labeled probes in a hybridization buffer [0.1% sodium dodecyl sulfate (SDS), 50% formamide, 5× sodium saline citrate (SSC), 50 mM $NaPO_4$ (pH 6.8), 0.1% sodium pyrophosphate, 5× Denhardt's solution, and 50 μg/ml salmon sperm DNA] at 42 °C overnight. Membranes were then washed with 2× SSC, 0.1% SDS at 42 °C for 30 min and 0.2× SSC, 0.1% SDS at 42 °C for 30 min. Radioactivities of the signals were quantified using a Fuji FLA 3000 phosphoimaging analyzer (Fuji Photo Film). After hybridization, filters were stripped off the previous probes and rehybridized with a ^{32}P-labeled GAPDH cDNA as a loading control. Real-time quantitative RT-PCR (qPCR) for human TRIM5α mRNA was performed using an ABI Prism 7000 sequence detection system (Applied Biosystems) using SYBR Green as a fluorescence probe. The sequences of TRIM5α and 36B4 primers are as follows: TRIM5α forward primer, 5′-ACCTT GGGATCTGTGAACAAGAG-3′; TRIM5α reverse primer, 5′-GGA TTCCAGAAGCCATAGTAGCTATTC-3′; 36B4 forward primer, 5′-C CACGCTGCTGAACATGCT-3′; 36B4 reverse primer, 5′-GATGC TGCCATTGTCGAACA-3′. One microgram of total RNA from HeLa cells treated with IFN-β or vehicle was reverse-transcribed using poly$(dT)_{20}$ primer and SuperScript II (Invitrogen). The reaction mixture for qPCR was performed with 1% of reverse-transcribed product in the presence of 1× master mix reagents (3.5 mM $MgCl_2$, 300 μM deoxynucleoside-5′-triphosphate, 0.25 IU hot goldStart enzyme, and SYBR Green) (Applied Biosystems). qPCR analysis was performed for 40 cycles for TRIM5α as well 36B4 cDNA amplification to normalize RNA loading. The results were shown as means ± SD from triplicated experiments.

Cloning of promoter region of TRIM5α gene and luciferase assay. A 1-kb 5′-flanking region of the TRIM5α gene containing a putative ISRE and IFN response factor binding element (IRFE) was amplified by PCR using primers 5′-GAGGCTATGGTACATGGACCACAGTTCAGC-3′ and 5′-AGGAAATTCTTGCTCACACTCAGGGCAGGA-3′, and cloned into pGL3-basic vector (Promoter-Luc). pGL3-basic constructs containing the 1-kb TRIM5α promoter with 3-bp mutated ISRE and IRFE were generated by PCR mutagenesis technique and denoted as ISREm-Luc and IRFEm-Luc, respectively.

Luciferase assay was performed using HeLa cells (1×10^4 cells/well on 24-well plates) transfected with 0.1 μg of Promoter-Luc, ISREm-Luc or IRFEm-Luc together with 0.02 μg pRL-CMV (Promega) using a FuGENE 6 transfection reagent (Roche Diagnostics). Twelve hours after transfection, cells were treated with 500 U/ml IFN-α, IFN-β or the vehicle (PBS) for 24 h and luciferase activities were determined by a MicroLumatPlus microplate luminometer (Berthold Technologies) using a Dual-Luciferase Assay System (Promega). Data are expressed as means ± SD of three independent experiments performed in triplicate.

Electrophoretic mobility shift assay. Electrophoretic mobility shift assay (EMSA) was performed as described previously [8]. Whole cell extract from HeLa cells treated with IFN-β for 24 h were prepared using NP-40 lysis buffer. Protein concentrations were determined using a Bio-Rad protein assay reagent. Annealed oligonucleotides 5′-TCTT TCACTTTCC-3′ corresponding with the ISRE in the 5′-flanking region of TRIM5α gene were labelled using [γ-^{32}P]ATP (Amersham Biosciences) using a MEGA label kit (Takara Bio). Five micrograms of nuclear protein, a ^{32}P-labeled double-stranded probe (10,000 counts per minute), and 3 μl of 5× binding buffer [20% glycerol, 5 mM $MgCl_2$, 2.5 mM EDTA, 2.5 mM DTT, 250 mM NaCl, 50 mM Tris–HCl (pH 7.5), and 0.25 mg/ml poly(dI–dC).poly(dI–dC)] were mixed in a total volume of 15 μl. In competition assays, 50× unlabeled oligonucleotides of ISRE or mutated ISRE (TCTGGAACTTTCC) were added simultaneously with a probe. The mixture was incubated at 30 °C for 15 min and electrophoresed on 4% polyacrylamide gels in 0.5× TBE buffer. Radioactivities of gels were analyzed using a Fuji FLA 3000 phosphoimaging analyzer (Fuji Photo Film). For supershift experiments, a rabbit polyclonal anti-human STAT1 (Santa Cruz Biotechnology) or a normal rabbit IgG was incubated with the cell extracts for 20 min before the probes were added.

Generation of anti-TRIM5α antibody and Western blotting. Rabbit polyclonal anti-TRIM5α antibodies were generated by a synthetic peptide (MASGILVNVKEEVTC) corresponding to the amino-terminal amino acid sequence of human TRIM5α. The synthetic peptide was conjugated to keyhole limpet hemocyanin carrier protein and used as an immunogen. The specific antibody was purified from immune sera using columns of TRIM5α peptide coupled to Affigel 10 (Bio-Rad). For Western blot analysis, lysates from HeLa cells treated with IFN-β for 24 or 36 h were resolved by 10% denaturating SDS–polyacrylamide gel electrophoresis. Proteins were transferred to polyvinylidene fluoride (PVDF) transfer membranes (Immobilon-P, Millipore) and incubated with 500-fold diluted TRIM5α antibody for 2 h, followed by a reaction with horseradish peroxidase-conjugated anti-rabbit Ig (Amersham Biosciences) for 1 h at room temperature. The antibody–antigen complexes were detected using the enhanced chemiluminescence system (Amersham Biosciences).

Results

Chromosomal localization and domain structure of TRIM5 and its related genes

Human TRIM5 gene is located in chromosome 11p15 in a cluster with other TRIM genes including TRIM3, TRIM6, TRIM21, TRIM22, and TRIM34 (Fig. 1A, top). Especially, TRIM5, TRIM6, TRIM22, and TRIM34 are assembled at adjacent loci. Human TRIM5α consists of 493 amino acids encoded by the TRIM5 gene and contains a unique carboxyl-terminal SPRY domain that is not found in other TRIM5 isoforms. In mouse genome, the syntenic region for human 11p15 is present in distal region of chromosome 7 (Fig. 1A, bottom). Among mouse TRIM proteins on chromosome 7, Trim12 and 9230105E10Rik are the most closely related to human TRIM5α. These two mouse TRIM genes may be paralogs that arose from a duplication event during evolution [1]. The degree of variation between TRIM5α and Trim12/9230105E10Rik is, however, larger than that between TRIM5α and human TRIM6, indicating that there may be no ortholog of TRIM5α in mouse genome.

In terms of domain structure, TRIM5α displays higher identities to adjacent TRIM proteins in RING domain (66–77%) and B-box domain (71–93%), but lower identities in coiled-coil domain (43–53%) and SPRY domain (29–51%) (Fig. 1B). It is notable that the carboxyl-terminal SPRY domain has been recently shown as a variable region that determines the species specificity of retroviral restriction in primates [1].

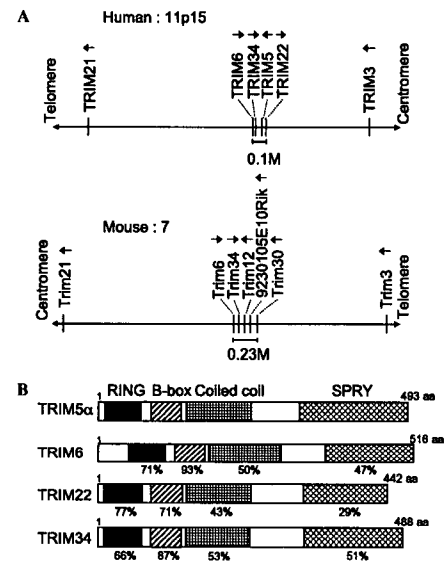

Fig. 1. Chromosomal localization and domain structure of TRIM5α. (A) Mapping of TRIM genes on human chromosome 11p15 (top) and mouse trim genes clustered in the conserved syntenic segment of 11p15, which is present in the distal region of mouse chromosome 7 (bottom). Six TRIM genes and seven trim genes are identified on 11p15 and its mouse orthologous region, respectively. TRIM5α is particularly adjacent to TRIM6, 22, and 34. No TRIM5α ortholog has been identified on mouse genome. (B) Comparison of domain structure of human TRIM proteins. Amino acid identities of domains between TRIM5α and other TRIM proteins are indicated as percentage.

Induction of TRIM5 mRNA by interferons

Since it is previously reported that TRIM21, TRIM22, and TRIM34 genes are upregulated by interferon [7], we examined whether TRIM5α expression is modulated by interferon. HeLa and HepG2 cells were treated with IFN-α, IFN-β, IFN-γ or control PBS (vehicle), and TRIM5α mRNA expression was investigated using Northern blot analysis or quantitative real-time PCR. Northern blot analysis showed that treatment with IFN-α, IFN-β or IFN-γ markedly upregulated TRIM5α mRNA levels in both HeLa and HepG2 cells (Fig. 2A). In quantitative real-time PCR, the TRIM5α mRNA level was elevated by 5- and 8-fold after 6- and 16-h treatment with IFN-β in HeLa cells (Fig. 2B). IFN-α or IFN-γ increased the TRIM5α mRNA level by 2-fold.

Promoter analysis of TRIM5α

It is known that interferon stimulates gene transcription through two IFN-responsive sequences, interferon-stimulated response elements (ISRE, consensus

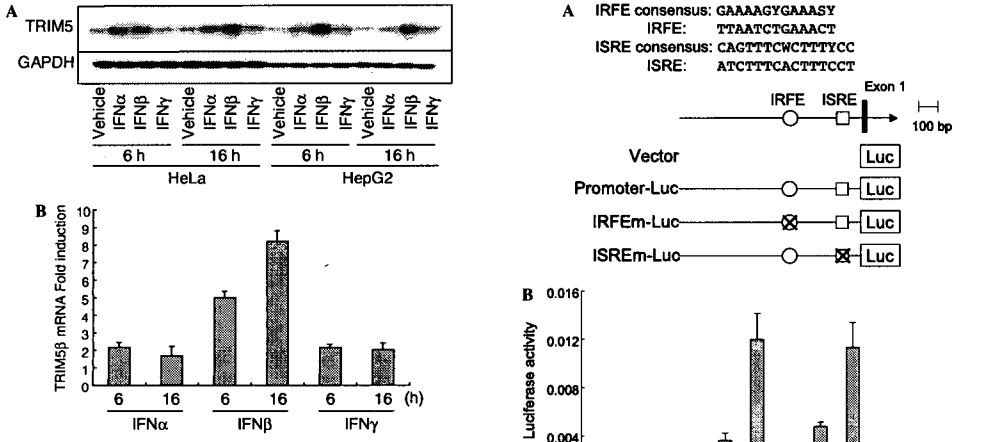

Fig. 2. Interferon-induced expression of TRIM5α mRNA. (A) HeLa and HepG2 cells are treated with IFN-α, IFN-β, IFN-γ, and the vehicle (PBS) for 6 or 16 h. Northern blot analysis was carried out using 20 μg total RNA and hybridized with ^{32}P-labeled cDNA for TRIM5α and GAPDH. (B) Real-time quantitative PCR was performed using cDNAs generated from the identical HeLa cell RNAs used in (A). Signal intensities of TRIM5α are normalized by the corresponding 36B4 signals and represented as fold induction over controls. Experiments are repeated three times and the results are represented as means ± SD.

Fig. 3. Functional interferon-stimulated response element (ISRE) on TRIM5α gene proximal promoter. (A) Schematic representation of luciferase reporter constructs containing 5′-flanking region of TRIM5α gene with or without mutation. Putative IFN response factor binding element (IRFE) and ISRE are shown by circles and squares, respectively. Crosses represent mutation in IRFE or ISRE. In consensus IRFE and ISRE sequences, S, W, and Y stand for G/C, A/T, and C/T, respectively. (B) Mutation in ISRE but not IRFE on TRIM5α gene promoter impairs IFN-stimulated luciferase activity. HeLa cells were plated at a density of 1×10^4 cells per well on 24-well plates and transfected with 0.2 μg of Promoter-Luc, ISREm-Luc or IRFEm-Luc together with 0.02 μg of pRL-CMV. Cells were treated with IFN-α, IFN-β or vehicle for 24 h, and luciferase assay was performed. Data are expressed as means ± SD of three independent experiments performed in triplicate.

sequence: CAGT TTCWCTTTYCC) or IFN response factor binding element (IRFE, consensus sequence: GAAAAGYGAAA SY), which are later shown to be recognized by the same complex [9,10]. In the proximal 5′-flanking region of TRIM5α gene (<1 kb upsteam to the transcription start site), we found a putative IRFE sequence (TTAATCTGAAACT) and an ISRE sequence (ATCTTT CACTTTCCT) by computational analysis (Fig. 3A). We then isolated the 1-kb proximal promoter region through genomic PCR and subcloned it into a luciferase reporter vector (Promoter-Luc). The reporter plasmids with 3-bp mutation in either IRFE or ISRE sequence were also constructed (IRFEm-Luc: TTAATCTTCCACT, ISREm-Luc: ATCTGGAACTTT CCT). Luciferase activities of HeLa cells transfected with Promoter-Luc or IRFEm-Luc were increased by both IFN-α and INF-β; the latter elicited a higher activation indeed (Fig. 3B). In contrast, the IFN-induced activation was not observed in cells expressed with ISREm-Luc. These results indicate that the putative ISRE sequence contributes to the interferon responsiveness of human TRIM5α promoter at least in HeLa cells.

STAT1 binds to ISRE on human TRIM5α proximal promoter

To confirm the sequence specificity of the ISRE sequence on human TRIM5α promoter and to identify a potential *trans*-acting factor that binds to the sequence, we performed electrophoretic mobility shift assay. HeLa cell extracts were incubated with a ^{32}P-labeled ISRE oligonucleotide in the presence or absence of competitive oligonucleotides (Fig. 4, left). A single DNA–protein band was detected on the polyacrylamide gel and the DNA–protein interaction was competed by a 50- and 100-fold excess of unlabeled ISRE oligonucleotide over the radiolabeled probe. As expected, no competition of DNA–protein binding was observed by the addition of a mutated ISRE oligonucleotide.

Signal transducer and activator of transcription (STAT) proteins are transcriptional factors that are known to be one of the key mediators in interferon signaling pathway [3,11,12]. STAT1 is a component of interferon-stimulated transcription factor 3 that serves as the ISRE recognition component [13]. We observed that the addition of anti-STAT 1 antibody exhibited a partial supershift of the

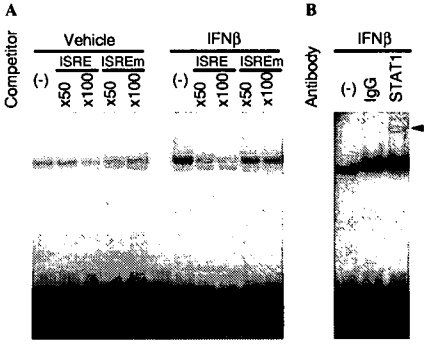

Fig. 4. Electrophoretic mobility shift assay of ISRE on TRIM5α gene promoter. (A) ^{32}P-labeled ISRE oligonucleotides were incubated with 5 μg of HeLa cell extracts treated with or without IFN-β for 24 h. A 50- or 100-fold excess of unlabeled ISRE oligonucleotides with or without mutation was added for competition. (B) Antibody interference with the mobility of the complex bound to the ISRE oligonucleotide. Arrowhead indicates the band shifted by anti-STAT1 antibody but not by normal IgG detected in IFN-β-stimulated HeLa cells probed with the labeled ISRE oligonucleotides.

ISRE–protein complex in HeLa cells treated with IFN-β, suggesting an involvement of STAT1 in the ISRE-bound complex on the human TRIM5α promoter.

IFN-induced expression of TRIM5α protein

To assess endogenous expression levels of human TRIM5α protein, we raised a rabbit polyclonal antibody against the carboxyl-terminal peptide of 15 amino acids. The specificity of the antibody was confirmed by Western blot analysis using 293T cells transfected with either empty vector or Flag-tagged TRIM5α (Fig. 5A). In HeLa cells, the upregulation of TRIM5α protein was observed at 24 and 36 h after treatment with IFN-β (Fig. 5B), consistent with the IFN-induced expression of TRIM5α mRNA (Fig. 2).

Discussion

Our results show that TRIM5α is a gene that can be induced by interferons, and this induction is dependent on the ISRE present in the proximal promoter region of the gene. By generating a specific antibody against TRIM5α, we showed that HeLa cells constitutively expressed TRIM5α protein and IFN-β upregulated endogenous expression of the protein in the cells. Moreover, we have identified that TRIM5α possesses a functional IFN response motif on its gene regulatory region.

The IFN-mediated upregulation of TRIM genes clustered on chromosome 11p15 has previously been shown at mRNA levels. TRIM21/Sjögren syndrome antigen A1 [3], TRIM22/Staf-50 [14], and TRIM34/RNF21 [7] can

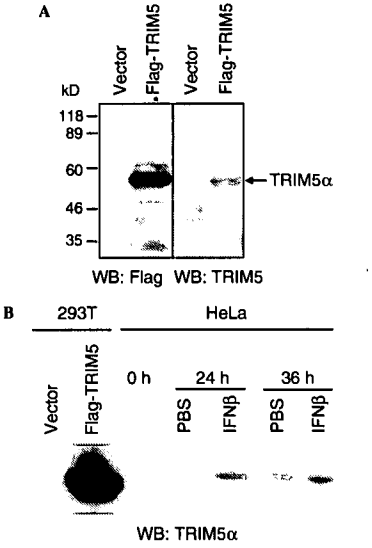

Fig. 5. IFN-β upregulates TRIM5α protein expression in HeLa cells. (A) Generation of a polyclonal antibody against human TRIM5α. Rabbits were immunized with a synthetic peptide corresponding to the amino-terminal peptide of TRIM5α. Lysates of 293T cells transfected with Flag-tagged TRIM5α were subjected to Western blot analysis probed with Flag M2 antibody (left panel) or the anti-TRIM5α antibody (right panel). (B) IFN-β-induced expression of TRIM5α protein in HeLa cells. HeLa cells were treated with IFN-β or vehicle for 24 and 36 h. TRIM5α protein expression was examined by Western blot analysis using the anti-TRIM5α antibody.

be induced by IFN. It is likely that the preference of IFN types and the time dependency of gene expression stimulated by distinct IFNs differ among TRIM family members. In microarray analysis of HT1080 cells stimulated for 6 h by distinct IFNs, TRIM21 has been identified as an upregulated gene either by IFN-α, IFN-β, or IFN-γ with the maximal response elicited by IFN-α, while TRIM22 has been identified as a type I IFN-stimulated gene without a significant increase by IFN-γ. TRIM34 exhibited a more rapid response of mRNA increase by IFN-α than by IFN-γ in HeLa cells and IFN-α-stimulated gene expression was inhibited by cycloheximide, suggesting that the upregulation requires the translation of some other protein(s). In the case of TRIM5α, we found that IFN-β was the most potent modulator of transcription while IFN-α and IFN-γ also induced a 2-fold upregulation of mRNA. Despite binding a common type I IFN receptor, it is intriguing that IFN-β manifests a preferential response than IFN-α in the TRIM5α gene expression. Indeed, more than 20 candidate genes preferentially induced by IFN-β were identified by oligonucleotide arrays and it is notable that STAT1 was one of those IFN-β-specific genes [3].

Although it is not determined whether IFN-stimulated gene expression of TRIM5α requires other protein synthesis, yet we consider that TRIM5α may be defined as a primary IFN-responsive gene whose promoter activity can be directly modulated by IFNs.

Among TRIM genes on 11p15, TRIM5, TRIM6, TRIM22, and TRIM34 are particularly assembled in a pinpoint region within 120 kb distance. TRIM5 and TRIM22 are adjacent to each other in a head-to-head direction with only a 4.8-kb distance. Considering that TRIM5 and TRIM22 orthologs are identified in nonhuman primates but not in rodents and that there might be a functional similarity in both genes, it is likely that the emergence of these genes have occurred after the rodent–primate divergence during evolution. Since both TRIM5 and TRIM22 can be induced by IFNs and TRIM22 has been reported to repress the transcription directed by HIV-1 long terminal repeat in transfected cells [14], both genes may particularly contribute to the establishment of innate immune systems against primate-specific retroviral infection. Moreover, the ISRE and the IFRE that we found on the proximal promoter of human TRIM5α may also be potential *cis*-acting elements that modulate TRIM22 transcription, as these sequences are located at ~4.7 kb upstream to the transcription start site of TRIM22.

Despite the recent advances of study regarding the restrictive function of TRIM5α in retroviral infection, the precise mechanism through which TRIM5α mediates species-specific restriction at a post-entry step has not been elucidated. Because the capsid protein is the viral determinant for susceptibility to the restriction and TRIM5α possesses a RING finger domain that is common among TRIM family members, one explanation is that TRIM5α may directly bind and ubiquitinate viral capsid proteins [15]. The localization of TRIM5α to cytoplasmic bodies [16] may be consistent with its ability to block retroviral infection shortly after entry of the viral capsid into the cytoplasm of the host cells. Although the structure and function of the carboxyl-terminal SPRY domain in TRIM5α need further study, the domain may play a role in the recognition of foreign ligands such as viral capsids through forming an immunoglobulin-like structure [17]. Four variable regions have been recently identified in the SPRY domain of TRIM5α and its related proteins in a comparative study of various primate species [1]. Since it has been shown that the TRIM5α SPRY domain exhibits lineage-specific length and species-specific sequence variation particularly at the variable regions, and the variation seems to have occurred at the timing of ancient retroviral epidemics, the diversity of the TRIM5α SPRY domain may have contributed to the establishment of innate intracellular defense systems against lethal retroviral infection during primate evolution.

Although the innate immunity has been paid relatively little attention and considered controversially in HIV infection, there are several lines of evidence that IFNs may contribute to play a significant role in this rapid host immune response against HIV infection. Asymptomatic long-term survivors with HIV infection had increased number of natural IFN-α-producing cells (IPCs) whereas patients with acquired immunodeficiency syndrome had decreased number of IPCs, suggesting that IPCs are important in controlling HIV replication [18]. IFN-β is known to block HIV-1 infection at a step prior to reverse transcription [19]. IFN-producing plasmacytoid dendritic cells (PDCs) do not generate high levels of IFN-α by HIV alone, whereas substantial type I IFN production occurs only after exposure of PDCs to HIV-infected cells [20]. We consider that TRIM5α may be involved in the IFN-mediated innate immunity against retroviral infection. Our data suggest that the IFN-stimulated TRIM5α transcription may be predominantly regulated through the pathway of type I IFN receptor, followed by the activation of JAK kinases and the recruitment of IFN-stimulated gene factor 3 on ISRE, the latter being composed of STAT1, STAT2, and IFN regulatory factor IRF-9. Further study will reveal the physiological relevance of the IFN-regulated TRIM5α transcription and the involvement of other regulatory factors in the signaling pathway.

Acknowledgments

We thank Dr. M. Nishida for kindly providing Ishikawa cells (Ishikawa 3H12 No. 74) and Dr. H. Ikeda for critical discussion. We also thank M. Nakamura for her technical assistance. This work was supported in part by Grants-in-Aid from the Ministry of Health, Labor and Welfare; from the Japan Society for the Promotion of Science. This work was supported in part by a grant of the Genome Network Project from the Ministry of Education, Culture, Sports, Science and Technology of Japan, and for Development of New Technology from The Promotion and Mutual Aid Corporation for Private Schools of Japan.

References

[1] B. Song, B. Gold, C. O'Huigin, H. Javanbakht, X. Li, M. Stremlau, C. Winkler, M. Dean, J. Sodroski, The B30.2(SPRY) domain of the retroviral restriction factor TRIM5α exhibits lineage-specific length and sequence variation in primates, J. Virol. 79 (2005) 6111–6121.

[2] M. Stremlau, M. Perron, S. Welikala, J. Sodroski, Species-specific variation in the B30.2(SPRY) domain of TRIM5α determines the potency of human immunodeficiency virus restriction, J. Virol. 79 (2005) 3139–3145.

[3] S.D. Der, A. Zhou, B.R. Williams, R.H. Silverman, Identification of genes differentially regulated by interferon α, β, or γ using oligonucleotide arrays, Proc. Natl. Acad. Sci. USA 95 (1998) 15623–15628.

[4] M. Matsumoto, N. Tanaka, H. Harada, T. Kimura, T. Yokochi, M. Kitagawa, C. Schindler, T. Taniguchi, Activation of the transcription factor ISGF3 by interferon-γ, Biol. Chem. 380 (1999) 699–703.

[5] T. Decker, D.J. Lew, J. Mirkovitch, J.E. Darnell Jr., Cytoplasmic activation of GAF, an IFN-γ-regulated DNA-binding factor, EMBO J. 10 (1991) 927–932.

[6] K. Shuai, C. Schindler, V.R. Prezioso, J.E. Darnell Jr., Activation of transcription by IFN-γ: tyrosine phosphorylation of a 91-kDa DNA binding protein, Science 258 (1992) 1808–1812.

[7] A. Orimo, N. Tominaga, K. Yoshimura, Y. Yamauchi, M. Nomura, M. Sato, Y. Nogi, M. Suzuki, H. Suzuki, K. Ikeda, S. Inoue, Muramatsu, Molecular cloning of ring finger protein 21 (RNF21)/interferon-responsive finger protein (ifp1), which possesses two RING-B box-coiled coil domains in tandem, Genomics 69 (2000) 143–149.

[8] K. Ikeda, S. Inoue, A. Orimo, M. Sano, T. Watanabe, K. Tsutsumi, M. Muramatsu, Multiple regulatory elements and binding proteins of the 5′-flanking region of the human estrogen-responsive finger protein (efp) gene, Biochem. Biophys. Res. Commun. 236 (1997) 765–771.

[9] R. Lu, W.C. Au, W.S. Yeow, N. Hageman, P.M. Pitha, Regulation of the promoter activity of interferon regulatory factor-7 gene. Activation by interferon snd silencing by hypermethylation, J. Biol. Chem. 275 (2000) 31805–31812.

[10] N. Tanaka, T. Taniguchi, The interferon regulatory factors and oncogenesis, Semin Cancer Biol. 10 (2000) 73–81.

[11] T. Taniguchi, A. Takaoka, A weak signal for strong responses: interferon-α/β revisited, Nat. Rev. Mol. Cell Biol. 2 (2001) 378–386.

[12] D.E. Levy, J.E. Darnell Jr., Stats: transcriptional control and biological impact, Nat. Rev. Mol. Cell Biol. 3 (2002) 651–662.

[13] C. Schindler, X.Y. Fu, T. Improta, R. Aebersold, J.E. Darnell Jr., Proteins of transcription factor ISGF-3: one gene encodes the 91-and 84-kDa ISGF-3 proteins that are activated by interferon α, Proc. Natl. Acad. Sci. USA 89 (1992) 7836–7839.

[14] C. Tissot, N. Mechti, Molecular cloning of a new interferon-induced factor that represses human immunodeficiency virus type 1 long terminal repeat expression, J. Biol. Chem. 270 (1995) 14891–14898.

[15] M. Stremlau, C.M. Owens, M.J. Perron, M. Kiessling, P. Autissier, J. Sodroski, The cytoplasmic body component TRIM5α restricts HIV-1 infection in Old World monkeys, Nature 427 (2004) 848–853.

[16] A. Reymond, G. Meroni, A. Fantozzi, G. Merla, S. Cairo, L. Luzi, D. Riganelli, E. Zanaria, S. Messali, S. Cainarca, A. Guffanti, S. Minucci, P.G. Pelicci, A. Ballabio, The tripartite motif family identifies cell compartments, EMBO J. 20 (2001) 2140–2151.

[17] M.H. Seto, H.L. Liu, D.A. Zajchowski, M. Whitlow, Protein fold analysis of the B30.2-like domain, Proteins 35 (1999) 235–249.

[18] V. Soumelis, I. Scott, F. Gheyas, D. Bouhour, G. Cozon, L. Cotte, L. Huang, J.A. Levy, Y.J. Liu, Depletion of circulating natural type 1 interferon-producing cells in HIV-infected AIDS patients, Blood 98 (2001) 906–912.

[19] V. Vieillard, I. Cremer, E. Lauret, W. Rozenbaum, P. Debre, B. Autran, E. De Maeyer, Interferon beta transduction of peripheral blood lymphocytes from HIV-infected donors increases Th1-type cytokine production and improves the proliferative response to recall antigens, Proc. Natl. Acad. Sci. USA 94 (1997) 11595–11600.

[20] J.A. Levy, I. Scott, C. Mackewicz, Protection from HIV/AIDS: the importance of innate immunity, Clin. Immunol. 108 (2003) 167–174.

14-3-3σ in Endometrial Cancer – A Possible Prognostic Marker in Early-Stage Cancer

Kiyoshi Ito,[1] Takashi Suzuki,[2] Jun-ichi Akahira,[1,2] Michiko Sakuma,[1] Sumika Saitou,[1] Satoshi Okamoto,[1] Hitoshi Niikura,[1] Kunihiro Okamura,[1] Nobuo Yaegashi,[1] Hironobu Sasano,[2] and Satoshi Inoue[3,4]

Abstract **Purpose:** We examined expression of 14-3-3σ, a regulator of cell proliferation, and evaluated its clinical significance in endometrioid endometrial carcinoma.

Experimental Design: One hundred three endometrioid endometrial adenocarcinoma cases were examined using immunohistochemistry with archival specimens. We correlated this finding with various clinicopathologic variables, including the status of estrogen receptor, progesterone receptor, and MIB-1 (Ki-57).

Results: 14-3-3σ Immunoreactivity was detected in 78 of 103 (75.3%) of carcinoma cases. No statistically significant correlation was detected between status of 14-3-3σ and any of clinicopathologic variables examined. There was, however, a statistically significant correlation between loss of 14-3-3σ expression and adverse clinical outcome of the patients ($P = 0.0007$). In the early stages of cancer (stages I and II), 14-3-3σ immunoreactivity was absent in 5 of 10 (50.0%) patients who showed recurrence during follow-up, whereas its absence was detected in only 13 of 68 (19.1%) disease-free patients in the same period. In addition, 14-3-3σ immunoreactivity was absent in 4 of 5 (80.0%) patients who died, whereas its absence was detected in only 14 of 73 (19.2%) patients who had lived during the same period. Patients whose tumors were negative for 14-3-3σ were at much greater risk to develop recurrent and/or mortal disease ($P = 0.0372$ and 0.0067). In multivariate analysis using the Cox proportional hazards model, absence of 14-3-3σ turned out to be statistically independent risk factor in disease-free survival and overall survival even in patients with early-stage disease ($P = 0.0321$ and 0.0191).

Conclusions: Results of our study showed that loss or absence of 14-3-3σ determined by immunohistochemistry may be an important tool to identify endometrial carcinoma cases at high risk of recurrence and/or death, who are otherwise not detected by current clinical and pathologic evaluation, especially in the early stages of the disease. In addition, results of 14-3-3σ immunohistochemistry in the early stage of endometrial carcinoma could contribute to planning postoperative follow-up and adjuvant therapy.

14-3-3 Proteins have been found to play important roles in the regulation of various cellular processes, such as cell cycle progression, cell growth, apoptosis, and signal transduction (1, 2). In humans, seven different 14-3-3 isoforms have been identified. 14-3-3σ, a member of this family, is induced by DNA damage and is required for a stable G_2 cell cycle arrest in epithelial cells. Loss of *14-3-3σ* expression results in malignant transformation *in vitro* and supports tumor formation *in vivo*, which suggests that this gene has tumor-suppressive properties. The *14-3-3σ* gene was originally identified as a p53-inducible gene responsive to DNA-damaging agents (3). In response to DNA damage, 14-3-3σ is induced in a p53-dependent manner and prevents the cdc2/cyclin B1 complex from entering the nucleus. We showed previously that 14-3-3σ undergoes proteolysis mediated by estrogen finger protein, which is a target of the estrogen receptor (ER) acting as an ubiquitin ligase of 14-3-3σ in breast carcinoma cells (4). In addition, 14-3-3σ is silenced by CpG methylation in a large proportion of human carcinomas (1, 2). The expression of 14-3-3σ is shown to be frequently lost in human epithelial carcinoma, breast, gastric, lung (5–7), etc. We also reported recently that decreased expression of 14-3-3σ was significantly associated with poor prognosis in epithelial ovarian cancer (8).

Endometrial carcinoma is the most common malignancy of the female genital tract, and its incidence has recently increased (9). In normal endometrium, 14-3-3σ protein was expressed weakly in epithelial glandular cells (10). However, the status of 14-3-3σ protein and its possible roles have never been examined in endometrial carcinoma. We reported previously the prognostic significance of p53 overexpression in endometrial cancer (11, 12). Therefore, decreased expression of 14-3-3σ may possibly have an important role in the development of endometrial cancer, because 14-3-3σ is directly regulated by p53.

To study the possible correlation between status of 14-3-3σ protein and prognosis of the patients, we examined its immunoreactivity in 103 cases of endometrioid endometrial cancer and correlated the findings with clinical outcome of the patients.

Authors' Affiliations: Departments of [1]Obstetrics and Gynecology and [2]Pathology, Tohoku University Graduate School of Medicine, Sendai, Japan; [3]Research Center for Genomic Medicine and Department of Molecular Biology, Saitama Medical School, Saitama, Japan; and [4]Department of Geriatric Medicine, Graduate School of Medicine, University of Tokyo, Tokyo, Japan

Received 1/26/05; revised 6/23/05; accepted 7/14/05.

The costs of publication of this article were defrayed in part by the payment of page charges. This article must therefore be hereby marked *advertisement* in accordance with 18 U.S.C. Section 1734 solely to indicate this fact.

Requests for reprints: Kiyoshi Ito, Department of Obstetrics and Gynecology, Tohoku University Graduate School of Medicine, 1-1 Seiryo-Machi, Aoba-Ku, Sendai 980-8574, Japan. Phone: 81-22-717-7254; Fax: 81-22-717-7258; E-mail: kito@mail.tains.tohoku.ac.jp.

doi:10.1158/1078-0432.CCR-05-0187

Table 1. Summary of primary antibodies used in this study

Antibody	Source	Optimal dilution	Antibody retrieval
14-3-3σ (polyclonal)	Santa Cruz Biotechnology	1:100	Autoclave*
ER (monoclonal)	Immunotech (Marseilles, France)	1:2	Autoclave*
PR (monoclonal)	Chemicon (Temecula, CA)	1:30	Autoclave*
Ki-67 (monoclonal)	Immunotech	1:50	Autoclave*
p53 (monoclonal)	Biomeda (Foster City, CA)	1:40	Autoclave*

*Heat in an autoclave for 5 minutes in citric acid buffer [2 mmol/L citric acid and 9 mmol/L trisodium citrate dehydrate (pH 6.0)]

Materials and Methods

Patients and tissues. Twenty-five normal cycling human endometria (15 proliferative phase and 10 secretory phase) and 103

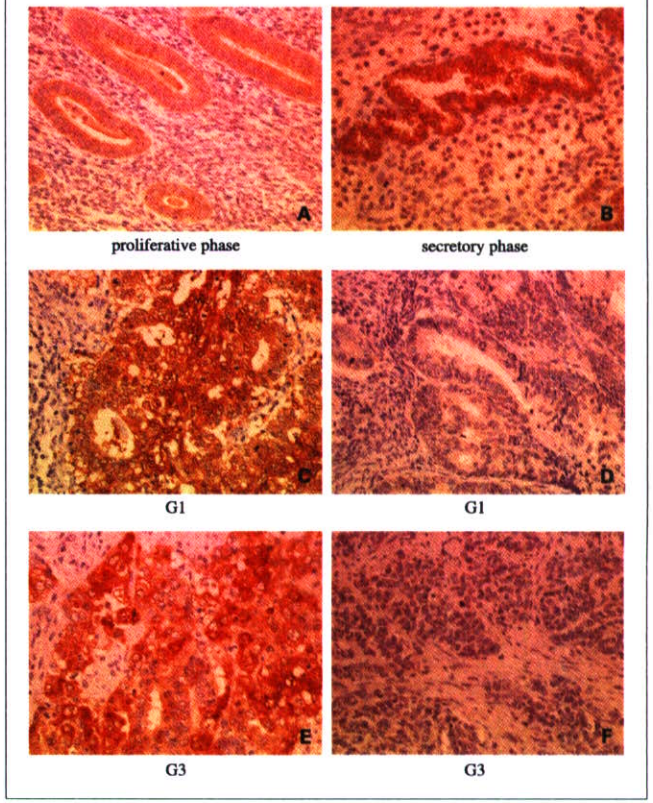

Fig. 1. Immunohistochemistry of 14-3-3σ expression: *A*, proliferative phase; *B*, secretory phase; *C* and *D*, endometrioid endometrial adenocarcinoma (G1); *E* and *F*, endometrioid endometrial adenocarcinoma (G3). 14-3-3σ Immunoreactivity was detected in the cytoplasm of glandular cells. 14-3-3σ Immunoreactivity was also detected in the cytoplasm of carcinoma cells. *C* and *E*, positive cases; *D* and *F*, negative cases. Original magnification, ×400.

endometrioid endometrial adenocarcinoma (49 well differentiated, 32 moderately differentiated, and 22 poorly differentiated; 66 stage I, 12 stage II, 22 stage III, and 3 stage IV) were retrieved from surgical pathology files of Tohoku University Hospital (Sendai, Japan). The protocol for this study was approved by the Ethics Committee at Tohoku University Graduate School of Medicine (Sendai, Japan). All carcinoma specimens were obtained from surgery. We obtained nonpathologic endometria from hysterectomy specimens performed due to carcinoma *in situ* of the uterine cervix at Tohoku University Hospital. All endometrial carcinoma specimens were obtained from hysterectomy. Median follow-up time of the patients examined in this study was 60 months (range, 2-148 months). Disease-free survival and overall survival were calculated from the time of initial surgery to recurrence and/or death or the date of last contact. Survival times of patients still alive or lost to follow-up were censored in December 2004. Clinicopathologic findings of these patients, including age, histology, stage, grade, and preoperative therapy, were retrieved by review of patient charts. A standard primary treatment for endometrial carcinoma at Tohoku University Hospital was surgery consisting of total abdominal hysterectomy, salpingo-oopholectomy, pelvic and/or para-aortic lymphadenectomy, and peritoneal washing cytology. A total of 85 of 103 (83%) patients underwent complete surgery. Six of 85 patients had lymph node metastasis. The remaining 18 (17%) patients underwent total abdominal hysterectomy and salpingo-oopholectomy without lymphadenectomy because of obesity and/or poor performance status. None of these patients had received preoperative chemotherapy and/or hormonal therapy or pelvic irradiation. No patient had used oral contraceptives. The lesions were classified according to the Histological Typing of Female Genital Tract Tumors by the WHO and staged according to the International Federation of Gynecology and Obstetrics system (13, 14). Sixty-eight of 103 patients received pelvic radiation therapy (50 Gy) or three to six courses of chemotherapy consisting of the cisplatin-based combination regimen CAP (60-70 mg/m^2 cisplatin, 40 mg/m^2 doxorubicin, and 500 mg/body cyclophosphamide) after operation. Patients who had early-stage and low-grade disease (stage Ia, grade 1; stage Ia, grade 2; and stage Ib, grade 1) and patients who were associated with poor performance status did not receive any adjuvant therapy. All specimens were routinely processed (i.e., 10% formalin fixed for 24-48 hours), paraffin embedded, and thin sectioned (3 μm).

Immunohistochemistry. Immunohistochemical analysis was done employing the streptavidin-biotin amplification method using a Histofine kit (Nichirei, Tokyo, Japan) as described previously in detail by the authors (15). Polyclonal antibody for 14-3-3σ (N-14) was purchased from Santa Cruz Biotechnology, Inc. (Santa Cruz, CA). The characteristics of the primary antibodies employed in this study are summarized in Table 1. For immunostaining of 14-3-3σ, p53, ERα, progesterone receptor (PR), and Ki-67, the slides were heated in an autoclave at 121°C for 5 minutes in citric acid buffer [2 mmol/L citric acid and 9 mmol/L trisodium citrate dehydrate (pH 6.0)] following deparaffinization for antigen retrieval. The dilutions of the primary antibodies used for our studies were as follows: 14-3-3σ, 1:100; p53, 1:40; ERα, 1:2; PR, 1:30; and Ki-67, 1:50. The antigen-antibody complex was visualized with 3,3′-diaminobenzidine solution [1 mmol/L 3,3′-diaminobenzidine, 50 mmol/L Tris-HCl buffer (pH 7.6), and 0.006% H_2O_2] and counterstained with hematoxylin. Tissue sections of nonneoplastic breast epithelial tissue were used as positive controls for 14-3-3σ, and breast cancer was also used as positive control for ERα. As a negative control, normal rabbit or mouse IgG was used instead of primary antibodies.

Semiquantitative analysis of immunohistochemical staining. For evaluation of ERα, PR, and Ki-67 immunoreactivity, labeling index was obtained in glandular or carcinoma cells as described by Utsunomiya et al. (16) with some modifications. In cases immunopositive for ERα, PR, and Ki-67, >1,000 glandular or carcinoma cells were counted in each case by two of the authors (K.I. and T.S.) independently after reviewing the slides and determining the areas of evaluation simultaneously with a double-headed microscope. The percentage of immunoreactivity (i.e., labeling index) was subsequently determined. Cases with interobserver differences of >5%, which occurred in 3% to 7% of the cases examined, were reevaluated together by two of the authors above using double-headed light microscopy. Intraobserver differences were <5% when examining the same selected fields of representative cases. The mean value was obtained in cases with interobserver differences of <5%. As immunoreactivities of 14-3-3σ and p53 were relatively homogeneous and clearly distinguishable as positive or negative, carcinoma cells were classified into the two groups without much differently (+, carcinoma cells with positive immunoreactivity; −, carcinoma cells with no immunoreactivity) by two of the same authors above.

Statistical analyses. Statistical analysis was done using SAS software version 5.0 (StatView, Cary, NC). The statistical difference between 14-3-3σ and characteristics of the patients was evaluated in a cross-table using the χ^2 test. Correlation between 14-3-3σ and p53, ERα, PR, and Ki-67 immunoreactivity was also assessed using Mann-Whitney *U* test.

Table 2. Correlation between 14-3-3σ immunoreactivity and clinicopathologic variables in endometrial cancer

	Total (n = 103)	14-3-3σ immunoreactivity		P
		Positive (n = 78)	Negative (n = 25)	
Age (median)	57.0	57.0	60.0	0.348
Grade, n (%)				
1	49 (47.6)	35	14	0.386
2	32 (31.0)	27	5	
3	22 (21.4)	16	6	
Stage				
I/II	78 (75.7)	60	18	0.815
III/IV	25 (24.3)	18	7	
p53 immunoreactivity				
Positive	15 (14.6)	11	4	0.055
Negative	88 (85.4)	67	21	
ER labeling index (median)	23.0	26.0	15.0	0.393
PR labeling index (median)	25.0	30.0	20.0	0.154
Ki-67 labeling index (median)	32.0	33.5	30.0	0.324

Table 3. Univariate analyses of predictors of disease-free survival and overall survival for 103 patients with endometrial cancer

Variable	Disease-free survival P	Overall survival P
14-3-3σ (positive vs negative)	0.0382	0.0041
Age (≦50 vs >50)	0.1159	0.0854
Stage (I/II vs III/IV)	0.2029	0.1163
Histologic grade (1-3)	0.0276	0.0063
p53 immunoreactivity (negative vs positive)	0.1601	0.0248
ER (positive vs negative)	0.0426	0.2643
PR (positive vs negative)	0.0004	0.0076
Ki-67 (positive vs negative)	0.4722	0.3449

Overall and disease-free survival curves were generated according to the Kaplan-Meier method, and the statistical significance was calculated using a log-rank test. Univariate and multivariate analyses were evaluated with Cox proportional hazards model. A result was considered significant when the $P < 0.05$.

Results

Normal cycling endometrium. 14-3-3σ Immunoreactivity was detected in the cytoplasm of glandular cells but not in the stromal cells of all the cases examined. Marked 14-3-3σ immunoreactivity was detected in the glandular cells of secretory phase mucosa compared with those of proliferative phase mucosa (Fig. 1A and B).

Association of 14-3-3σ expression with clinicopathologic variables and estrogen receptor α, progesterone receptor, Ki-67, and p53 immunoreactivity in patients with endometrial cancer. 14-3-3σ Immunoreactivity was detected in the cytoplasm of epithelial cancer cells, although ERα, PR, Ki-67, and p53 were confined exclusively to the nuclei of epithelial cells (Fig. 1C-F). 14-3-3σ Immunoreactivity was present in 78 of 103 (75.3%) cases of endometrioid endometrial carcinoma. The correlation between 14-3-3σ immunoreactivity and clinicopathologic variables, including ERα, PR, Ki-67, and p53 immunoreactivity, was examined. As seen in Table 2, no statistically significant correlation was detected between status of 14-3-3σ immunoreactivity and any of the variables examined in this study. The status of 14-3-3σ immunoreactivity tended to be inversely correlated with that of p53, but the correlation did not reach statistical significance. There were no statistically significant correlations between status of lymph node metastasis and 14-3-3σ expression (P = 0.1456).

Association of 14-3-3σ expression with disease-free survival and overall survival in patients with endometrial cancer. 14-3-3σ Immunoreactivity was evaluated as a prognostic variable in the 103 cases using univariate analysis (Table 3; Cox proportional hazards model). In 103 cases, 14-3-3σ immunoreactivity was absent in 7 of 16 patients (43.8%) who showed recurrence during follow-up, whereas loss of its immunoreactivity was detected only in 18 of 87 (20.7%) disease-free patients for the same clinical follow-up period. 14-3-3σ Immunoreactivity was also absent in 6 of 9 (66.7%) patients who died, whereas loss of its immunoreactivity was detected only in 19 of 94 (20.2%) patients who had lived during the same period. Patients whose tumors were associated with absence of 14-3-3σ expression were at much greater risk to develop recurrent and/or mortal disease (P = 0.0382 and 0.0041). Indicators of clinical outcome of the patients, including ER, PR, and p53 status and histologic grade, were likewise significantly associated with poor outcome. Patients whose tumors were negative for 14-3-3σ

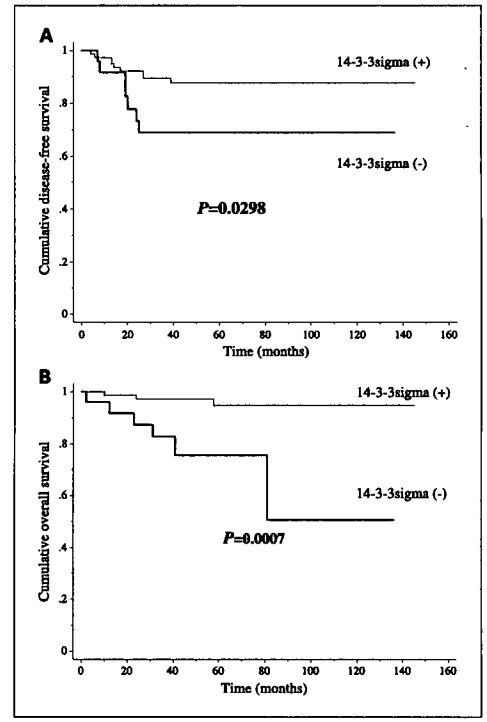

Fig. 2. *A*, correlation between 14-3-3σ immunoreactivity and recurrence for patients with endometrial cancer. *B*, correlation between 14-3-3σ immunoreactivity and survival for patients with endometrial cancer.

Table 4. Multivariate analyses of predictors of disease-free survival and overall survival for 103 patients with endometrial cancer

Variable	Disease-free survival		Overall survival	
	HR (95% CI)	P	HR (95% CI)	P
14-3-3σ (positive vs negative)	0.320 (0.114-0.894)	0.0297	0.185 (0.048-0.719)	0.0148
Stage (I/II vs III/IV)	0.687 (0.236-2.003)	0.4920	0.750 (0.190-2.964)	0.6810
Histologic grade (1-3)	1.473 (0.796-2.726)	0.2170	2.543 (1.030-6.281)	0.0431
p53 (negative vs positive)	0.587 (0.170-2.029)	0.3997	0.335 (0.089-1.261)	0.1058
ER (positive vs negative)	0.463 (0.168-1.273)	0.1356	1.134 (0.280-4.590)	0.8602
PR (positive vs negative)	0.142 (0.039-0.517)	0.0031	0.432 (0.091-2.049)	0.2904

NOTE: HR, hazard ratio; 95% CI, 95% confidence interval.

had also significantly worse disease-free survival and overall survival rates than 14-3-3σ-positive ones using log-rank tests (Fig. 2A and B; $P = 0.0298$ and 0.0007).

To determine whether the prognostic value of 14-3-3σ expression was independent of other risk factors associated with clinical outcome, we examined the data using multivariate analysis. The prognostic factors examined were 14-3-3σ, ER, PR, and p53 status, stage, and histologic grade. The findings are summarized in Table 4. Absence of 14-3-3σ expression was independently statistically significant as risk factor in disease-free survival and overall survival of the patients ($P = 0.0297$ and 0.0148). PR status was an independent risk factor only in disease-free survival, and histologic grade was an independent risk factor only in overall survival. ER status turned out not to be independent prognostic indicator in both disease-free survival and overall survival. Disease-free survival and overall survival were not significantly different between the two groups who received radiation therapy or chemotherapy (data not shown).

Significance of 14-3-3σ status in patients with early-stage disease of endometrial cancer. 14-3-3σ Expression was then evaluated as a prognostic variable in 78 cases with early-stage disease (stage I and II) using univariate analysis (Table 5; Cox proportional hazards model). In the total of 78 cases, 14-3-3σ immunoreactivity was absent in 5 of 10 (50.0%) patients who showed recurrence during follow-up, whereas loss of its immunoreactivity was detected only in 13 of 68 (19.1%) disease-free patients for the same period. 14-3-3σ Immunoreactivity was also not detected in 4 of 5 (80.0%) patients who died, whereas absence of its immunoreactivity was detected only in 14 of 73 (19.2%) patients who had lived during the same period. Patients whose tumors did not show 14-3-3σ immunoreactivity were at much greater risk to develop recurrent and/or mortal disease ($P = 0.0372$ and 0.0067). Patients whose tumors were negative for 14-3-3σ also had significantly worse disease-free survival and overall survival rates than 14-3-3σ-positive ones using log-rank tests (Fig. 3A and B; $P = 0.0251$ and 0.0002). In advanced-stage disease (stage III and IV), there was a trend for 14-3-3σ-negative cases to undergo aggressive biological behavior than 14-3-3σ-positive ones, although the differences did not reach statistical significance (data not shown). Multivariate analysis was done and summarized in Table 6. Absence of 14-3-3σ immunoreactivity was independently statistically significant as risk factor in disease-free survival and overall survival in patients with early-stage disease of endometrial carcinoma ($P = 0.0317$ and 0.0229).

Therefore, we examined the subgroup with completely surgically staged node-negative (International Federation of Gynecology and Obstetrics stage I and II) endometrial adenocarcinoma (Table 7). Absence of 14-3-3σ immunoreactivity still turned out to be independently statistically significant as risk factor in disease-free survival ($P = 0.0245$) although not significant in overall survival ($P = 0.0646$) of the patients.

Discussion

This is the first study that examined the status of 14-3-3σ protein and its possible roles in conjunction with clinical outcome of the patients in endometrial carcinoma. The *14-3-3σ* gene is well-known to be induced after DNA damage in a p53-dependent manner and to play an important role in the G_2 checkpoint by sequestering the cdc2/cyclin B1 complex (1, 2). An inactivation of 14-3-3σ is also currently considered to play an important role in tumor development and/or progression. However, it is also true that 14-3-3σ may play a different role in tumor development and/or progression among different human organs. In urinary bladder carcinoma, for example, 14-3-3σ is highly up-regulated in pure squamous cell carcinoma, whereas it is down-regulated in invasive bladder urothelial cell carcinoma (17). In breast carcinoma, loss of 14-3-3σ expression becomes marked in the progression from atypical hyperplastic lesions to ductal carcinoma *in situ* (18, 19). Loss of 14-3-3σ protein was also reported in prostate carcinoma and its precursors (20-22). Therefore, loss or absence of 14-3-3σ expression is generally considered an early event during carcinogenesis in both breast and prostate carcinoma (18-22). Ostergaard et al. (23) reported that less differentiated bladder squamous cell carcinoma was associated with decreased expression of 14-3-3σ. We showed recently that loss of 14-3-3σ expression was correlated with advanced disease and/or high-grade tumor and significantly associated with poor prognosis in epithelial ovarian carcinoma (8). In our present study, the frequency of absence of 14-3-3σ immunoreactivity in clinically early disease and/or low-grade tumor was similar with that in advanced-stage and/or high-grade tumor, although decreased status of 14-3-3σ immunoreactivity was significantly associated with poor prognosis in endometrioid endometrial cancer. These results suggest that the loss of 14-3-3σ expression in endometrioid endometrial cancer may be associated with an aggressive biological characteristics, which play an important role in prognosis and/or recurrence, although it could be a relatively early event during their carcinogenesis.

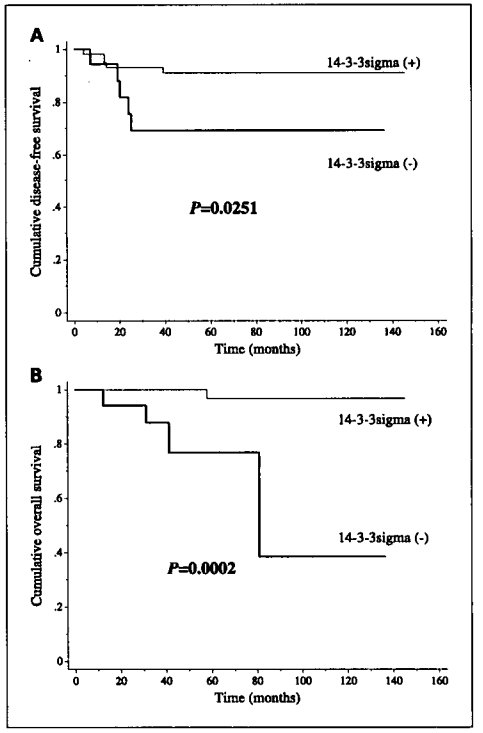

Fig. 3. *A*, correlation between 14-3-3σ immunoreactivity and recurrence for patients with early-stage (stage I and II) endometrial cancer. *B*, correlation between 14-3-3σ immunoreactivity and survival for patients with early-stage (stage I and II) endometrial cancer.

In our present study, there were no significant differences of the findings between cases of early-stage and advanced-stage cancer, although advanced-stage cancer cases tended to be associated with worse prognosis than early-stage cases. These findings are considered to be due to the following reasons: the relatively small number of advanced-stage cancer cases, especially only 3 stage IV cases, and the fact that 15 of 22 (70%) cases of stage III examined were stage IIIa. Cases of stage IIIa, especially cytologic stage IIIa (positive peritoneal cytology alone), has been shown to be associated with much better prognosis than those of stage IIIc (24, 25). However, it awaits further investigation for clarifying the possible role of decreased status of 14-3-3σ immunoreactivity in advanced-stage endometrial carcinoma cases.

Endometrial carcinoma is the most common pelvic gynecologic carcinoma, and 80% to 90% of all cases are in clinically early stage (26). Five-year survival data of the patients revealed ~10% to 20% mortality in early-stage disease (26). There have been many controversies on the possible use of adjuvant therapy in patients of early-stage endometrial carcinoma (27-31). Results of large randomized trial (the Post-Operative Radiation Therapy in Endometrial Carcinoma) showed no

Table 5. Univariate analyses of predictors of disease-free survival and overall survival for 78 patients with stage I and II endometrial cancer

Variable	Disease-free survival P	Overall survival P
14-3-3σ (positive vs negative)	0.0372	0.0067
Age (≤50 vs >50)	0.0856	0.2085
Histologic grade (1-3)	0.1527	0.1040
p53 immunoreactivity (negative vs positive)	0.6539	0.0870
ER (positive vs negative)	0.1368	0.9561
PR (positive vs negative)	0.0028	0.0001
Ki-67 (positive vs negative)	0.6605	0.8310

Table 6. Multivariate analyses of predictors of disease-free survival and overall survival for 78 patients with stage I and II endometrial cancer

Variable	Disease-free survival		Overall survival	
	HR (95% CI)	P	HR (95% CI)	P
14-3-3σ (positive vs negative)	0.241 (0.066-0.883)	0.0317	0.127 (0.022-0.752)	0.0229
Histologic grade (1-3)	1.469 (0.683-3.159)	0.3243	2.227 (0.749-6.619)	0.1496
p53 (negative vs positive)	1.182 (0.236-5.906)	0.8387	0.858 (0.149-4.931)	0.8635
ER (positive vs negative)	0.578 (0.161-2.077)	0.4011	2.272 (0.244-21.156)	0.4710
PR (positive vs negative)	0.115 (0.024-0.556)	0.0071	0.123 (0.012-1.280)	0.0795

Table 7. Multivariate analyses of predictors of disease-free survival and overall survival for 64 patients with completely surgically staged node-negative (FIGO stage I and II) endometrial cancer

Variable	Disease-free survival		Overall survival	
	HR (95% CI)	P	HR (95% CI)	P
14-3-3σ (positive vs negative)	0.189 (0.044-0.807)	0.0245	0.176 (0.028-1.111)	0.0646
Histologic grade (1-3)	1.708 (0.762-3.828)	0.1932	2.465 (0.774-7.853)	0.1270
p53 (negative vs positive)	1.007 (0.192-5.290)	0.9931	1.280 (0.172-9.554)	0.8095
ER (positive vs negative)	0.492 (0.121-2.005)	0.3223	2.326 (0.235-22.975)	0.4701
PR (positive vs negative)	0.060 (0.007-0.494)	0.0089	0.140 (0.013-1.509)	0.1050

Abbreviation: FIGO, International Federation of Gynecology and Obstetrics.

significant differences between survivals of the patients with or without adjuvant therapy in stage I endometrial adenocarcinoma. However, analysis of their study was limited because complete surgical staging was not a requirement for entry of the patients into the protocol (29). Very recently, Keys et al. showed no significant differences between survival of the patients with or without adjuvant therapy in completely surgically staged node-negative intermediate risk (International Federation of Gynecology and Obstetrics stage Ib, Ic, II occult) endometrial adenocarcinoma (Gynecologic Oncology Group study). The estimated 4-year survival was 86% in the group with no additional therapy arm and 92% for whole radiation therapy arm, with no statistical difference between these two groups (31). Therefore, identification of additional prognostic markers could provide the information to avoid unnecessary adjuvant therapy and to plan effective systemic treatment. Several studies have attempted to identify prognostic factors of the patients with early-stage endometrial cancer. However, none of them have provided satisfactory results. Fiumicino et al. (32) showed that microsatellite instability was an independent indicator of recurrence in early-stage endometrial adenocarcinoma, but Maxwell et al. (33) reported that microsatellite instability is rather a favorable prognostic factor. In addition, MacDonald et al. (34) and Basil et al. (35) both independently reported the lack of any correlation between microsatellite instability and clinical outcome in endometrial cancer. Recently, Powell et al. (36) examined the prognostic significance of rDNA methylation and showed that tumor rDNA level turned out to be significant prognostic factor for both disease-free survival and overall survival in early-stage endometrial cancer. Powell et al. therefore identified the prognostic indicator of early-stage endometrial carcinoma. However, their methods require sufficient quantity of frozen specimens, and patients with small tumors often did not have adequate tumor tissue for examination in clinical early stage of endometrial carcinoma, which may limit the clinical value of this interesting prognostic marker.

In our study, we studied archival or surgical pathology materials and analyzed a remarkable number of the cases with follow-up data to show possible correlation between absence of 14-3-3σ and adverse clinical outcome using immunohistochemistry, which is a simple and useful method in surgical pathology specimens. In early-stage endometrial cancer, 14-3-3σ immunoreactivity was not detected in 5 of 10 (50.0%) patients who had recurrence during clinical follow-up, whereas absence of its immunoreactivity was detected only in 13 of 68 (19.1%) disease-free patients during the same period. 14-3-3σ Immunoreactivity was not detected in 4 of 5 (80.0%) patients who died, whereas loss of its immunoreactivity was detected only in 14 of 73 (19.2%) patients who had lived for the same period of clinical follow-up. Absence of 14-3-3σ expression was independently statistically significant as risk factor in disease-free survival and overall survival in patients in the early stage of the disease. Additionally, even in the subgroup with completely surgically staged node-negative (International Federation of Gynecology and Obstetrics surgical stage I and II) endometrial adenocarcinoma, absence of 14-3-3σ immunoreactivity still turned out to be independently statistically significant as risk factor in disease-free survival although not significant in overall survival of the patients.

These findings all indicate that absence of 14-3-3σ protein determined by immunohistochemistry could be a very important tool to identify the patients at high risk of recurrence and/or death, who are otherwise not detected by current clinical and pathologic evaluation, especially in the early stage of endometrial carcinoma. In addition, results of 14-3-3σ immunohistochemistry in early stage of endometrial carcinoma could contribute to planning postoperative follow-up and adjuvant therapy.

References

1. Hermeking H. The 14-3-3 cancer connection. Nat Rev Cancer 2003;3:931–43.
2. Wilker E, Yaffe MB. 14-3-3 Proteins—a focus on cancer and human disease. J Mol Cell Cardiol 2004;37:633–42.
3. Hermeking H, Lengauer C, Polyak K, et al. 14-3-3σ is a p53-regulated inhibitor of G_2-M progression. Mol Cell 1997;1:3–11.
4. Urano T, Saito T, Tsukui T, et al. Efp targets 14-3-3σ for proteolysis and promotes breast tumour growth. Nature 2002;417:871–5.
5. Ferguson AT, Evron E, Umbricht CB, et al. High frequency of hypermethylation at the 14-3-3σ locus leads to gene silencing in breast cancer. Proc Natl Acad Sci U S A 2000;97:6049–54.
6. Suzuki H, Itoh F, Toyota M, Kikuchi T, Kakiuchi H, Imai K. Inactivation of the 14-3-3σ gene is associated with 5′ CpG island hypermethylation in human cancers. Cancer Res 2000;60:4353–7.
7. Osada H, Tatematsu Y, Yatabe Y, et al. Frequent and histological type-specific inactivation of 14-3-3σ in human lung cancers. Oncogene 2002;21:2418–24.
8. Akahira J, Sugihashi Y, Suzuki T, et al. Decreased expression of 14-3-3σ is associated with advanced disease in human epithelial ovarian cancer: its correlation with aberrant DNA methylation. Clin Cancer Res 2004;10:2687–93.
9. Parker SL, Tong T, Bolden S, Wingo PA. Cancer statistics. CA Cancer J Clin 1996;46:5–27.
10. Nakajima T, Shimooka H, Weixa P, et al. Immunohistochemical demonstration of 14-3-3σ protein in normal human tissues and lung cancers, and the preponderance of its strong expression in epithelial cells of squamous cell lineage. Pathol Int 2003;53:353–60.
11. Ito K, Sasano H, Matsunaga G, et al. Correlations between p21 expression and clinicopathological findings, p53 gene and protein alterations, and survival in patients with endometrial carcinoma. J Pathol 1997;183:318–24.
12. Ito K, Watanabe K, Nasim S, et al. Prognostic significance of p53 overexpression in endometrial cancer. Cancer Res 1994;54:4667–70.
13. Tavassoli FA, Devilee P. Pathology and genetics of tumours of the breast and female genital organs. In: WHO classification of tumours. WHO, Lyon; 2003. p.113–45.
14. Creasman WT. Announcement FIGO stages: 1988 revisions. Gynecol Oncol 1989;35:125–7.
15. Ito K, Suzuki T, Moriya T, et al. Retinoid receptors in the human endometrium and its disorders: a possible modulator of 17β-hydroxysteroid dehydrogenase. J Clin Endocrinol Metab 2001;86:2721–7.
16. Utsunomiya H, Suzuki T, Kaneko C, et al. The analyses of 17β-hydroxysteroid dehydrogenase isozymes in human endometrial hyperplasia and carcinoma. J Clin Endocrinol Metab 2001;86:3436–43.
17. Moreira JM, Gromov P, Celis JE. Expression of the tumor suppressor protein 14-3-3σ is down-regulated in invasive transitional cell carcinomas of the urinary bladder undergoing epithelial-to-mesenchymal transition. Mol Cell Proteomics 2004;3:410–9.
18. Simooka H, Oyama T, Sano T, Horiguchi J, Nakajima T. Immunohistochemical analysis of 14-3-3σ and related proteins in hyperplastic and neoplastic breast lesions, with particular reference to early carcinogenesis. Pathol Int 2004;54:595–602.
19. Umbricht CB, Evron E, Gabrielson E, Ferguson A, Marks J, Sukumar S. Hypermethylation of 14-3-3σ (stratifin) is an early event in breast cancer. Oncogene 2001;20:3348–53.
20. Cheng L, Pan CX, Zhang JT, et al. Loss of 14-3-3σ in prostate cancer and its precursors. Clin Cancer Res 2004;10:3064–8.
21. Urano T, Takahashi S, Suzuki T, et al. 14-3-3σ is down-regulated in human prostate cancer. Biochem Biophys Res Commun 2004;319:795–800.
22. Lodygin D, Diebold J, Hermeking H. Prostate cancer is characterized by epigenetic silencing of 14-3-3σ expression. Oncogene 2004;23:9034–41.
23. Ostergaard M, Rasmussen HH, Nielsen HV, et al. Proteome profiling of bladder squamous cell carcinomas: identification of markers that define their degree of differentiation. Cancer Res 1997;57:4111–7.
24. Kasamatsu T, Onda T, Katsumata N, et al. Prognostic significance of positive peritoneal cytology in endometrial carcinoma confined to the uterus. Br J Cancer 2003;88:245–50.
25. Tebeu PM, Popowski Y, Verkooijen HM, et al. Positive peritoneal cytology in early-stage endometrial cancer does not influence prognosis. Br J Cancer 2004;91:720–4.
26. Creasman WT, Odicino F, Maisonneuve P, et al. Carcinoma of the corpus uteri. Int J Gynaecol Obstet 2003;83 Suppl 1:79–118.
27. Ball HG. Do we know the best therapy for early endometrial cancer? Gynecol Oncol 1996;60:173–5.
28. Lanciano RM, Greven KM. Adjuvant treatment for endometrial cancer: who needs it? Gynecol Oncol 1995;57:135–7.
29. Creutzberg CL, van Putten WL, Koper PC, et al. Surgery and postoperative radiotherapy versus surgery alone for patients with stage-1 endometrial carcinoma: multicentre randomised trial. PORTEC Study Group. Post Operative Radiation Therapy in Endometrial Carcinoma. Lancet 2000;355:1404–11.
30. Orr JW, Jr., Roland PY, Leichter D, Orr PF. Endometrial cancer: is surgical staging necessary? Curr Opin Oncol 2001;13:408–12.
31. Keys HM, Roberts JA, Brunetto VL, et al. A phase III trial of surgery with or without adjunctive external pelvic radiation therapy in intermediate risk endometrial adenocarcinoma: a Gynecologic Oncology Group study. Gynecol Oncol 2004;92:744–51.
32. Fiumicino S, Ercoli A, Ferrandina G, et al. Microsatellite instability is an independent indicator of recurrence in sporadic stage I-II endometrial adenocarcinoma. J Clin Oncol 2001;19:1008–14.
33. Maxwell GL, Risinger JI, Alvarez AA, Barrett JC, Berchuck A. Favorable survival associated with microsatellite instability in endometrioid endometrial cancers. Obstet Gynecol 2001;97:417–22.
34. MacDonald ND, Salvesen HB, Ryan A, Iversen OE, Akslen LA, Jacobs IJ. Frequency and prognostic impact of microsatellite instability in a large population-based study of endometrial carcinomas. Cancer Res 2000;60:1750–52.
35. Basil JB, Goodfellow PJ, Rader JS, Mutch DG, Herzog TJ. Clinical significance of microsatellite instability in endometrial carcinoma. Cancer 2000;89:1758–64.
36. Powell MA, Mutch DG, Rader JS, Herzog TJ, Huang TH, Goodfellow PJ. Ribosomal DNA methylation in patients with endometrial carcinoma: an independent prognostic marker. Cancer 2002;94:2941–52.

CHAPTER 16

RING Finger-B Box-Coiled Coil (RBCC) Proteins as Ubiquitin Ligase in the Control of Protein Degradation and Gene Regulation

Kazuhiro Ikeda, Satoshi Inoue, Masami Muramatsu

Abstract

The protein family harboring the RING finger motif, defined as a linear array of conserved cysteines and histidines, has grown enormously in the last decade. The members of the family are involved in various biological processes including growth, differentiation, apoptosis, transcription and also in diseases and oncogenesis. It has been postulated that the RING finger domains have crucial roles in these phenomena themselves, in some cases, working with other domains in other proteins, although the precise mechanisms and common features of RING finger function have not been fully elucidated. However, most recently, an accumulating body of evidence has revealed that some of the RING finger proteins work as E3 ubiquitin ligases in ubiquitin-mediated specific protein degradation pathway. In this review, we focus on the RING finger protein with special reference to E3 ligase.

Structure of RING Finger

The RING finger protein sequence motif was first identified in the human gene RING1 – Really Interesting New Gene 1 – which is located proximal to the major histocompatibility region on chromosome 6.[1,2] The RING finger motif can be defined as a unique linear series of conserved cysteine and histidine residues: Cys-X_2-Cys-$X_{11\text{-}16}$-Cys-X-His-X_2-Cys -X_2-Cys-$X_{7\text{-}74}$-Cys-X_2-Cys (RING-CH or C_3HC_4 type), where X can be any amino acid (Fig. 1). So far, three-dimensional structures of RING domains from human PML (for promyelocytic leukemia protein),[3] immediate early equine herpes virus (IEEHV) protein,[4] human recombination-activating gene 1 protein (RAG1),[5] human MAT1 (for menage a trois-1 protein)[6] and human Cbl (for Casitas B-lineage lymphoma protein)[7] with a cognate ubiquitin-conjugating enzyme (E2) have been solved at atomic resolution. These studies have confirmed that the RING finger binds zinc ions in a similar manner as the classical zinc finger motif. Particularly, the RING finger is composed of a unique 'cross-brace' arrangement with two zinc ions and folds into a compact domain comprising a small central β sheet and an α helix. There are subfamilies of RING fingers which have Cys5 substituted with histidine (RING-H2) and a cysteine or histidine substituted with other metal binding residues such as aspartic acid and threonine.[8,9] Although the RING domain was initially found

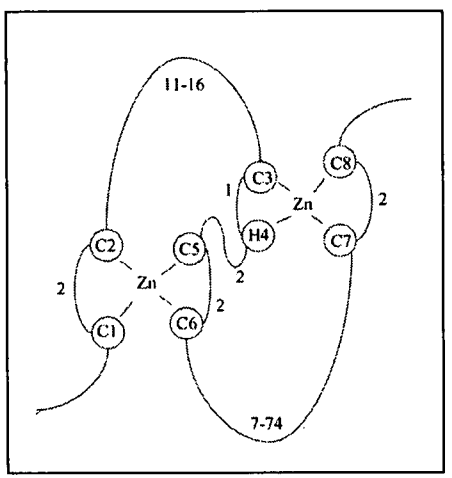

Figure 1. Schematic representation of the structure of RING finger domain. The metal-ligand residues, either cysteine (C) or histidine (H), are shown as numbered spheres. The numbers next to the loops connecting the metal-ligand residues indicate the minimum and maximum number of loop residues.

in only a few genes, more than 3000 proteins harboring the RING finger domain have been detected from diverse eukaryotes in the SMART database as of July 2003. Because of this evolutional conservation and variation in loop lengths, the RING domain appears to have a considerable flexibility within the rigid structure.

Family of RING Finger Protein

The RING fingers and their variants are generally located close to an amino or carboxyl terminus though there are no fixed rules. Most of the RING finger is associated with certain protein domains to form larger conserved motifs which may define the function of the protein, thus the family being divided into subfamilies along with the associated domains (Fig. 2). A similar domain architecture often corresponds with a similar function. For instance, TRAFs (for tumor necrosis factor (TNF) receptor-associated factors) 2-5 have an N-terminal RING domain followed by five zinc fingers, a coiled coil, and a C-terminal TRAF domain.[10] TRAF1 has all of these domains except for the RING. Members of TRAF family have been shown to be involved in TNF-related cytokine signal transduction through interactions between their TRAF domains and the intracytoplasmic parts of receptors of the TNF receptor family which are suicide receptors to transfer apoptotic signals into the cells.[11-13]

The inhibitors of apoptosis gene family, IAP1, IAP2 and XIAP, have a RING domain at their C termini and BIR (baculovirus IAP repeat) domain at their N termini. The BIR domains of the proteins bind and inhibit caspase.[14,15] Interestingly, the RING fingers of XIAP and IAP2 possess E3 ubiquitin ligase activity and are thought to be responsible for self-degradation when an apoptotic signal is transduced.[16] In addition, the anti-apoptotic activity of the protein is lost when the RING domain is mutated.[17]

There are interesting subfamilies uniquely possessing two RING fingers. Triad1 (for two RING fingers and DRIL1) and parkin have two RING finger domains separated by the double RING finger linked (DRIL) domain. Triad1 was identified as a nuclear RING finger protein, which is up-regulated during retinoic acid induced granulocytic differentiation of acute leukemia cells.[18] Parkin is a responsible gene for familial autosomal recessive Parkinson's disease.[19,20] Parkin binds to the E2 ubiquitin-conjugating enzymes through its C-terminal RING finger and has ubiquitin–protein ligase activity.[21] Parkin ubiquitinates and promotes the degradation of a putative G protein-coupled transmembrane polypeptide, Pael (parkin-associated endothelial-like) receptor, the insoluble form of which is accumulated in the brains of Parkinson's disease.[22] The insoluble parkin overexpressed in cells causes unfolded protein-induced cell death, whereas coexpression of Parkin suppresses the accumulation of Pael receptor and subsequent cell death.[21] Parkin also ubiquitinates and promotes the degradation of CDCrel-1 (for cell division cycle related-1) and itself.[23] Familial-linked mutations disrupt the ubiquitin–protein ligase function of Parkin and impair Parkin and CDCrel-1 degradation.

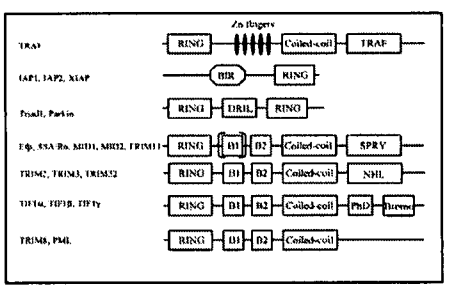

Figure 2. Structures of the RING finger protein family. Representative RING finger proteins with frequently associated domains are presented.

Function of RING Finger

It has been shown in early studies that the RING finger proteins have crucial roles in the growth, differentiation, transcription, signal transduction and oncogenesis.[24] For example, PML is fused to the retinoic acid receptor α (RARα) in acute promyelocytic leukemia (APL) translocation,[25-27] BRCA1 is mutated in early-onset breast cancer and ovarian cancer,[28] TIF1α is a positive cofactor of nuclear hormone receptors[29] and TRAF transduces signals from members of the TNF receptor superfamily to the transcription factor NF-κB.[14] Although those studies appear to show some essential roles played by the RING finger domains in the function of these proteins, the general function of the RING finger domain has not been resolved. However, recently, it was uncovered that the RING finger proteins are involved in the ubiquitin-mediated protein degradation pathway.

The ubiquitin-dependent protein degradation is a specific and sophisticated mechanism in which a target protein to be destroyed is tagged with the ubiquitin. Ubiquitination is accomplished by a complex process involving ubiquitin-activating enzyme (E1), ubiquitin-conjugating enzyme (E2) and ubiquitin ligase (E3).[30] Ubiquitin ligase mediates the transfer of ubiquitin from E2 to a substrate, marking it for degradation by the 26S proteosome. Therefore, E3 enzyme is thought to be important for the specific recognition of the substrate in the ubiquitination pathway. There is accumulating evidence that RING finger domains are identified in E3 complexes and proteins, suggesting the broad use of these domains for ubiquitination. As mentioned above, RING finger domain has the conserved cysteine and histidine residues. The C_3HC_4 type RING finger is found in several E3 proteins including Cbl,[31] BRCA1,[32] Efp (for estrogen-responsive finger protein)[33] and Mdm2 (for murine double minute 2).[34] The RING-H2 subtype is found in Rbx1 (for RING box protein 1) and Apc11 (for anaphase promoting complex (APC) subunit 11) in SCF (Skp1-Cullin-F-box) and APC E3 complexes,[35] respectively, and other ubiquitin ligases. Thus, evidence is accumulating that the RING finger proteins has crucial roles as an E3 ubiquitin ligase in diverse biological functions and diseases. Cbl is one of the initially identified E3 ligase which is involved in the regulation of various tyrosine kinase-linked receptors such as growth factor receptors (for example EGF and PDGF receptors), cytokine receptors and immuno-receptors (for example T-cell, B-cell and Fc-receptors).[36] Cbl recognizes activated protein tyrosine kinases and recruits E2 ubiquitin conjugating enzymes through its SH2 and RING finger domain, respectively. For EGF and PDGF receptors, increased recruitment of Cbl to the activated receptor complex leads to enhanced ubiquitination and degradation of the activated receptor. In contrast, oncogenic mutation in the Cbl RING finger which fails to bind E2 ubiquitin conjugating enzymes abrogates Cbl-mediated EGF receptor ubiquitination and degradation.[37] Thus, it appears that Cbl functions as an adapter to recruit the ubiquitination machinery to activated tyrosine kinase-linked receptors and stimulates receptor ubiquitination and degradation. This causes enhanced down-regulation of the receptor from the cell surface and attenuation of growth factor receptor signaling.

The RING finger protein Mdm2 is identified as an E3 ubiquitin ligase of the tumor-suppressor protein p53 which is a transcription factor and a potent inhibitor of the cell cycle. Mdm2 can bind to p53 and promote its ubiquitination and subsequent degradation by the proteasome.[38,39] It is also known that Mdm2 can ubiquitinate itself, suggesting that some of E3s self-regulate their own stability. The RING finger of Mdm2 is necessary for

Zinc Finger Proteins: From Atomic Contact to Cellular Function, edited by Shiro Iuchi and Natalie Kuldell.

both p53 ubiquitin and Mdm2 auto-ubiquitination. Substitution of the Mdm2 RING finger domain with the RING finger from another RING protein maintains the autoubiquination and degradation of Mdm2 but is not able to stimulate p53 ubiquitination. Moreover, mutations in the RING finger domain do not impair binding capacity between Mdm2 and p53. These observations suggest that the RING finger domain appears to be required for specific recognition of substrates in some degree, but is not generally involved in substrate binding.[40]

RBCC/TRIM Subfamily

Frequently, the RING is associated with cysteine-rich B-box domains followed by a predicted coiled coil domain. The B-box domain can be defined as a series of conserved cystein and histidine residues: B1 [Cys-X_2-Cys-X_{7-10}-Cys-X_2-Cys-X_{4-5}-Cys-X_2-Cys/His-X_{3-6}-His-X_{2-8}-His] and B2 [Cys-X_{2-4}-His/Cys-X_{4-9}-Cys-X_2-Cys/His-X_4-Cys/His-X_2-His/Cys] where X can be any amino acid. Structural analysis revealed that it consists of 15 or fewer β-strands.[41] The coiled coil is a common protein motif involving a number of α-helices wound around each other in a highly organized manner and is often used to control oligomerization.[42] These RING, one or two B-boxes and a coiled coil domain motifs are called RBCC or tripartite motif (TRIM)(Fig. 3).[43] This largest subfamily was first identified in a putative transcriptional regulator, Xenopus XNF7[24] and about 50 members have been identified since then. Though either one or two B-boxes are present, the spacing between the RING, B-boxes and the coiled coil is highly conserved with 38-40 residues between the RING and first B-box, and less than 10 amino acids between the second B-box and the coiled coil. There is no apparent homology among these separating sequences. According to the recent progress of genomic analysis, it was revealed that the chromosomal localization of the RBCC/TRIM subfamily genes has an intriguing feature. Although the genes encoding the RBCC/TRIM family members are dispersed throughout the genome, there are two distinct clusters on chromosomes 11p15 and 6p21-22 (Fig. 4). *TRIM22, SSA1/TRIM21, TRIM34, TRIM6, TRIM5, TRIM3* and *SS-56* are clustered in 11p15. *RFP/TRIM27, TRIM31, TRIM10, TRIM15, TRIM26, TRIM38, TRIM39, TRIM40* and *HZFW1* are clustered in 6p21-22. In particular, mRNAs for *TRIM 21, 22* and *34* are shown to be up-regulated by interferons.[44-46] These findings suggest that duplication of an ancestral *RBCC/TRIM* gene at these genomic loci may have occurred and, regulation and function may be conserved to some extents in these genes.[43]

The RBCC/TRIM proteins are associated with certain domains such as B30.2-like or SPRY, NHL, PHD and BROMO domains at their C-terminus. These additional domains may contribute to the function of the subfamily. The B30.2-like domain is a series of 160-170 amino acids containing three highly conserved motifs (LDP, WEVE and LDYE) which is named after the B30-2 exon within the human class I histocompatibility complex locus. The SPRY domain, which was originally named from SPla and the RYanodine Receptor, is composed of around 140 amino acids containing the latter two conserved motifs in B30.2-like domain. At present, the B30.2-like domain is considered as a subclass of the SPRY domain family. The SPRY domain is contained in many of the RBCC/TRIM subfamily including XNF-7, RPT-1, SSA-Ro and STAF50. The significantly conserved SPRY domains imply the biological importance of this gene, however the function of the SPRY domain is not known. The NHL domain name was derived from the three founding members: NCL-1, HT2A, and LIN-41.[47] NCL is involved in rRNA metabolism. HT2A was identified as an interacting partner of the

Gene		Structure
TRIM1	MID2, FXY2	SPRY
TRIM2	NARF	NHL
TRIM3	BERP, RNF22	NHL
TRIM4		SPRY
TRIM5		SPRY
TRIM6	IFP1 (long)	SPRY
TRIM7	GNIP1	SPRY
TRIM8	GERP, RNF27	
TRIM9		SPRY
TRIM10	HERF1, RNF9	SPRY
TRIM11	BIA1	SPRY
mTRIM12		
TRIM13	RFP2	
TRIM14		SPRY
TRIM15		SPRY
TRIM16	BEEP	SPRY
TRIM17	TERF	SPRY
TRIM18	MID1, FXY	SPRY
TRIM19	PML	
TRIM21	SSA/Ro	SPRY
TRIM22	STAF50	SPRY
TRIM23	ARD1	ARF
TRIM24	TIF1α	PHD, BROMO
TRIM25	EFP	SPRY
TRIM26	AFP	SPRY
TRIM27	RFP	SPRY
TRIM28	TIF1β, KAP1	PHD, BROMO
TRIM29	ATDC	
mTRIM30	mRPT1	SPRY
TRIM31	RING	
TRIM32	HT2A	NHL
TRIM33	TIF1γ	PHD, BROMO
TRIM34	IFP1 (middle)	SPRY
TRIM35	mNCR	SPRY
TRIM36		SPRY
TRIM37	MUL, TEF3	TRAF
TRIM38	RoRet, RNF15	SPRY
TRIM39	TFP	SPRY
TRIM40	RNF35	mSPRY
TRIM41		SPRY
TRIM42		FN3
TRIM43		SPRY
TRIM44	DIP8	
TRIM45		Filamin
TRIM46		FN3
TRIM47	GOA	SPRY
TRIM48		SPRY

Figure 3. RBCC/TRIM family genes. The gene names are listed in numerical order of *TRIM* genes followed by commonly used names in the second column. Their domain structures are schematically shown to the right.

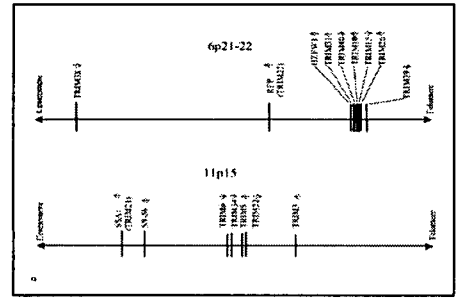

Figure 4. Clustered localization of the *RBCC/TRIM* genes in 6p21-22 and 11p15. *TRIM22, SSA1, TRIM34, TRIM6, TRIM5, TRIM3* and *SS-56* are clustered in 11p15, whereas *RFP, TRIM31, TRIM10, TRIM15, TRIM26, TRIM38, TRIM39, TRIM40* and *HZFW1* are clustered in 6p21-22. The sense strand orientations of each gene are indicated by the arrows.

HIV Tat protein and Lin41 is involved in posttranscriptional regulation of mRNA. The NHL motif has a slight homology with WD40 domain, suggesting a protein-protein interaction. The C-terminal PHD fingers and bromodomains are found in TIF1α and KAP1/TIF1β. The PHD domain is a motif characteristically defined by seven cysteines and a histidine that are highly homologous to the RING motif and is contained in some transcription factors. The PHD domain of MEKK1 (MEK kinase 1) exhibited E3 ubiquitin ligase activity toward ERK (extracellular signal-regulated protein kinase) 2, suggesting a negative regulatory mechanism for decreasing ERK1/2 activity.[48] The bromodomain is also found in transcription factors, can bind histones with acetylated lysines and appears to be involved in chromatin remodeling.[49] KAP1/TIF1β and TIF1α are involved in transcriptional regulation. Genes belonging to this RBCC/TRIM family are implicated in a variety of processes such as development and cell growth and are involved in several human diseases. PYRIN,[50] MID1 (Midline 1)[51] and MUL (for mulibrey nanism proteins)[52] are mutated in familial Mediterranean fever, X-linked Opitz/GBBB syndrome and mulibrey nanism, respectively, whereas PML, RFP (ret finger protein) and TIF1α acquire oncogenic activity when fused to RARα, RET or B-raf, respectively.

It has been shown that the RBCC/TRIM proteins can oligomerize through their coiled coil domains. In homodimerization of RFP proteins, the coiled coil region with the B-box but not the RING finger is required.[53] In this case, while the B-box is not an interacting interface itself, the mutation of conserved cysteine residues within the B-box affects the ability of RFP to multimerize, suggesting that its structural integrity is necessary for this interaction to occur.[53] The coiled coil domain of RFP is also necessary for interaction with Enhancer of polycomb protein (EPC) to repress gene transcription.[54] The homodimerization and binding with EPC occurs with the proximal coil in RFP protein. RFP also directly interacts and colocalizes with PML in a subset of the PML NBs (nuclear bodies).[55] This interaction is mediated by the RFP B-box and the distal two coils. The association of RFP with the PML NBs is altered by mutations that affect RFP/PML interaction and in APL patients-derived cells. These results indicate that RFP have an important role in regulating cellular growth and differentiation. MID1 protein, which is mutated in patients with Opitz GBBB syndrome, and the highly related gene MID2 also make both homo- and hetero-dimers mediated by the coiled coil motifs. The dimerization is a prerequisite for the association of MID and Alpha 4 (a regulatory subunit of PP2-type phosphatases) and the complex formation with microtubules which seems important for normal midline development.[56] In contrast, it has been shown that the entire RBCC/TRIM domain is required for hetero-oligomerization or binding natural ligands. The RBCC region of KAP1/TIF1β associates with the KRAB (Krüppel-associated box) transcriptional repressor domain of KOX-1.[57] From extensive studies of the interaction, it has been revealed that the interaction is specific for the KAP1 RBCC/TRIM domain. Namely, when each RBCC/TRIM motifs of KAP1 was swapped with other corresponding ones of MID1, KAP1 did not bind the KRAB domain any more. Therefore, each domain of the RBCC may function as an independent functional unit and have important roles in the specific recognition of interacting partners or oligomers formation. In other RBCC/TRIM proteins, only one copy of the B-box motif is present, but inspection of the whole family reveals a conserved residue spacing between the RING, B-box and coiled coil domains.[43] This strongly suggests that the overall architecture of the RBCC/TRIM motif is highly conserved, perhaps relating to the motif acting as a scaffold for higher-order protein-protein interactions.[57] Molecular modeling suggests that the position and orientation of the B-box (adjacent to the coiled coil) would be critical for the correct alignment of the α-helices that form the coiled coil. Interestingly, unlike the RING and coiled coil motifs, the B-box is only found in RBCC/TRIM family members suggesting that it is a critical determinant of the overall motif and its function.[43]

As mentioned above, the latest findings of RING fingers in E3 ubiquitin ligases imply that the members of this RBCC/TRIM subfamily are potential candidates for specific regulators/adopters in ubiquitin-dependent protein degradation. In fact, some genes belonging to the subfamily has been proven to act as E3 ligase. We next discuss such genes focusing on the recent findings.

Ring Fingers that Act As E3 Ligases

Efp

Estrogen-responsive finger protein (Efp) is a member of the RING-finger, B1 and B2-boxes, coiled coil and SPRY (RBCC-SPRY) subfamily in the RING finger family. Efp was isolated as an estrogen-responsive gene by genomic binding-site cloning using a recombinant estrogen receptor (ER) protein.[58] The estrogen-responsive element (ERE) to which ER can bind is found at the 3'-untranslated region (UTR) in the *Efp* gene and the gene's expression is predominantly detected in female reproductive organs including uterus, ovary and mammary gland[59] and in breast and ovarian cancers.[60] Estrogen-induced expression is found in the uterus, brain and mammary gland cells. *Efp* knockout mice have an underdeveloped uterus and estrogen responses of uterin cells from knockout mice are markedly attenuated, suggesting that Efp is necessary for estrogen-induced cell growth.[61] Moreover, tumor growth of breast cancer MCF7 cells implanted in female athymic mice has been demonstrated to be reduced by treatment with antisense Efp oligonucleotide. In contrast, Efp-overexpressing MCF7 cells in ovariectomized athymic mice generate tumors in the absence of estrogen.[33] These results indicate that Efp mediaes estrogen-dependent growth in breast cancer cells. We identified 14-3-3Σ which is responsible for reduced cell growth, as a binding factor to Efp and found an accumulation of 14-3-3Σ in *Efp* knockout mouse embryonic fibroblasts. Furthermore, it has been revealed that Efp is an ubiquitin ligase (E3) that targets proteolysis of 14-3-3Σ. Specifically, the RING which preferentially bound to ubiquitin-conjugating enzyme UbcH8 has been shown to be essential for the ubiquitination of 14-3-3Σ. Our findings provide an insight into the cell-cycle machinery and tumorigenesis of breast cancer by identifying 14-3-3Σ as a target for proteolysis by Efp, leading to cell proliferation. The degradation of 14-3-3Σ is subsequently followed by dissociation of the protein from cyclin–Cdk complexes, leading to cell cycle progression and tumor growth (Fig. 5).

MID1, MID2

Opitz GBBB syndrome (OS; Opitz syndrome) is a genetically and phenotypically complex disorder defined by characteristic facial anomalies, structural heart defects, as well as anal and genital anomalies.[62,63] A positional cloning approach has revealed a candidate gene designated *MID1*[51] which is a member of the RBCC-SPRY family. Most of the mutations identified so far in patients with Opitz syndrome cluster in the SPRY domain of

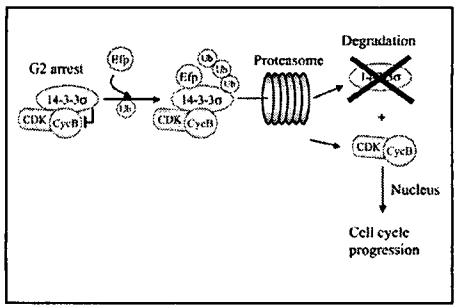

Figure 5. Models of Efp action as E3 ligase. Estrogen-induced RING finger protein Efp recognizes a cell cycle inhibitor 14-3-3Σ which keeps Cyclin B in cytoplasm. Efp modifies 14-3-3Σ with ubiquitin and the resulting ubiquitinated 14-3-3Σ is recruited to 26S proteosome to be destroyed. The dissociated cyclin B is now capable of entering the nucleus where it drives cell cycle.

MID1. It has been shown that MID1 associates with microtubules, whereas mutant forms of MID1 do not.[64] These results suggest that MID1 has a physiological role in microtubule dynamics.

Recently, the α4 protein, a regulatory subunit of protein phosphatase 2A (PP2A)[65] was isolated by yeast two-hybrid screening with MID1 as bait. It was demonstrated that the B-box 1 is sufficient for a strong interaction with α4. MID2,[66] which is highly similar to MID1, also binds α4. Cellular localizations of MID1 and α4 are coincident with cytoskeletal structures and MID1 with a mutation at the C terminus that mimics the mutant protein of some individuals with OS results in the formation of cytoplasmic clumps containing both proteins. The identified substrate for E3 ligase activity of MID1 is a cytosolic PP2A. In contrast, addition of a proteasome inhibitor to OS-derived fibroblasts expressing dysfunctional MID1 does not cause either enrichment of PP2A or accumulation of the enzyme's polyubiquitinated forms,[67] suggesting that MID1 mutations result in decreased proteolysis of the C subunit of PP2A in individuals with OS.

PML

PML also belongs to a subfamily of proteins containing a RBCC/TRIM motif.[43,68] PML has been implicated in the pathogenesis of acute promyelocytic leukemia that arises following a reciprocal chromosomal translocation that fuses the *PML* gene located on chromosome 15 with the retinoic acid receptor alpha (*RARα*) gene located on chromosome 17. The resulting PML-RARα fusion protein preserves most of the functional domains of both PML and RARα, but it lacks C-terminus of PML and N-terminus of RARα The fusion protein shows cell type- and promoter-specific differences from the wild type RARα,[25,26,69] while it maintains a responsiveness to retinoic acid. Overexpression of PML-RARα inhibits vitamin D3 and transforming growth factor β-induced differentiation and also reduces serum starvation-induced apoptosis in U937 cells.[70] In addition, dimerization of PML with PML-RARα is required to block differentiation.[71] Thus, PML-RARα is considered to function as a dominant negative protein by interfering with the function of PML and RARα.

In normal cells, cellular distribution of PML is found to form a discrete subnuclear compartment (nuclear body, NB)[72,73] or PML oncogenic domain.[74] Other proteins containing Sp100[75] and PLZF (for promyelocytic leukemia zinc finger)[76] have been reported to localize to the NBs. Interestingly, PLZF-RARα fusion protein is also found in a rare form of APL.[77] It is shown that the nuclear bodies were dispersed into a microspeckle pattern in APL cells but reformed with retinoic acid treatment by which APL cells differentiated into granulocytes. In addition, the NB is the preferred site where the early steps of transcription and replication of DNA virus occurs.[78] Therefore, the regulation of NB formation is thought to be involved in the pathogenesis of APL. Recently, PML is shown to be covalently modified by SUMO-1 (Small Ubiquitin-like Modifier-1) of ubiquitin-like proteins.[79] Mutations in the PML RING finger disrupt the nuclear body formation in vivo[3,69] and cause a failure of growth suppression,[80,81] apoptosis and anti-viral activities[82] of PML. The dependence on an intact RING finger for PML NBs formation implies specific protein interactions regulated by the RING structure. Recent studies have shown that PML RING interacting with the SUMO-1 E2 enzyme UBC9 is SUMO modified and the sumolylation of PML has an important role in regulating the formation of NBs.[83]

PML has two B-boxes (B1 and B2) adjacent to the RING domain. Mutations of conserved zinc-chelating residues in B1 and/or B2 boxes collapsed PML NB formation, whereas they did not affect PML oligomerization.[84] PML B-boxes are also involved in growth suppression.[80] It has been revealed that PML is sumoylated in B1 box which is responsible for binding of the 11S proteasomal subunit to PML NBs.[85]

The coiled coil region in PML is indispensable for multimerization or heterodimerization with PML-RARα,[69,71,86] formation of PML NB and growth suppression activity.[80] Notably, the important role of the coiled coil domain for the complex formation is also suggested from the studies of other RBCC/TRIM subfamily.[43,57]

TRIM8

TRIM8, a member of RBCC subfamily, is shown to interact with SOCS-1 (suppressor of cytokine signaling-1) which is induced by cytokines and inhibits cytokine signaling by binding to downstream signaling molecules such as JAK (Janus kinase) kinases.[87-89] The B-box coiled coil region of TRIM8 is sufficient for efficient interaction with SOCS-1, but the RING portion of the protein is not required for the binding. By contrast, both the SOCS box and the SH2 domain in SOCS-1 appear to be necessary for the interaction between SOCS-1 and TRIM8. It was found that exogenous coexpression of TRIM8/GERP with SOCS-1 decreased the stability of SOCS-1 protein and TRIM8 restored the IFN-γ-mediated transcription which was inhibited by the expression of SOCS-1.[90] These results suggest that TRIM8 is the putative E3 ligase for SOCS-1 and inhibits SOCS-1 function by targeting it for proteasomal degradation.

TRIM11

TRIM11 is a member of the protein family composed of a RING finger domain, which is a putative E3 ubiquitin ligase, a B-box domain, a coiled coil domain and a SPRY domain. A recent experiment with yeast two-hybrid screening has revealed that TRIM11 can interact with Humanin[91] which is a newly identified anti-apoptotic peptide that specifically suppresses Alzheimer's disease (AD)-related neurotoxicity. It is known that Bax

(Bcl2-associated X protein) has a crucial role in apoptosis. In response to death stimuli, Bax protein changes the conformation exposing membrane-targeting domains, translocates to mitochondrial membrane and releases the cytochrome c and other apoptogenic proteins. Indeed, Humanin is shown to bind with Bax and prevents the translocation of Bax from cytosol to mitochondria.[92] Moreover, Humanin blocks Bax association with isolated mitochondria and suppresses cytochrome c release. Therefore, Humanin seems to exert its anti-apoptotic effect by interfering the Bax function.

The coiled coil domain of TRIM11 is indispensable for the interaction with Humanin. The SPRY domain also contributes to the recognition of Humanin, whereas SPRY domain alone cannot. It was found that the intracellular level of Humanin was drastically reduced by the coexpression of TRIM11, and mutation of the RING finger domain or treatment with proteasome inhibitor attenuates the effect of TRIM11 on the intracellular level of Humanin.[91] These results suggest that the TRIM11 participates in the ubiquitin-mediated degradation of Humanin as an E3 ligase.

SSA/Ro (SSA1, TRIM21)

Sjögren syndrome is an autoimmune disease in which exocrine glands including salivary and lacrimal glands develop a chronic inflammation, and whose symptoms are dry eyes, dry mouth and fatigue. Autoantibodies to Ro recognize a ribonucleoprotein complex composed of small single-stranded RNAs and of one or more peptides. Although the Ro autoantigen is heterogeneous and found in most tissues and cells with differences in structure and quantity across tissues, it is detected in 35 to 50% of patients with systemic lupus erythematosus and in up to 97% of patients with Sjögren syndrome.[93] The 60-kD protein (Ro60) and the 52-kD protein (Ro52) were identified[94] and, another novel 56-kD protein (Ro56/SS-56) has been identified, recently.[95] Ro52 and Ro56 proteins belong to RBCC-SPRY subfamily. It is thought that the Ro autoantigen is involved in the regulation of transcription because it possesses functional domains associated with gene-regulation and binds to nucleic acids.[93] Its precise function is not understood, however. In a study, Ro52 was reported to be ubiquitinated in the cell.[96] The observation suggests that Ro52 may be downregulated by the ubiquitin–proteasome pathway in vivo. Interestingly, sera from patients with Sjögren syndrome showed heterogeneity in their reactivity to poly-ubiquitinated Ro52, probably because of their differing antigenic determinants. This heterogeneity of the reactivity may be associated with the varying clinical features found in Sjögren patients.

Conclusion

Here, we summarized the structural characteristics and functions of RING finger proteins specifically in terms of the E3 ligase activity. However, relatively few proteins have been really proven to function as E3 ligase. Thus, most RING finger proteins remain to be further investigated. Investigation of the RING finger proteins as a novel E3 ligase family will elucidate important mechanisms of cellular protein degradation and provide new insight into the physiological and pathophysiological roles of the pathway. Particularly, the molecular mechanisms of specific substrate recognition by E3 with the RING and other associated domains must be determined. Moreover, the RING finger proteins such as PML may possess unknown functions other than E3 ligase. Functional analysis of the RING finger proteins will help to understand biological roles of the family including the ubiquitin-mediated protein degradation pathway.

References

1. Freemont PS, Hanson IM, Trowsdale J. A novel cysteine-rich sequence motif. Cell 1991; 64(3):483-484.
2. Lovering R, Hanson IM, Borden KL et al. Identification and preliminary characterization of a protein motif related to the zinc finger. Proc Natl Acad Sci USA 1993; 90(6):2112-2116.
3. Borden KL, Boddy MN, Lally J et al. The solution structure of the RING finger domain from the acute promyelocytic leukaemia proto-oncoprotein PML. Embo J 1995; 14(7):1532-1541.
4. Barlow PN, Luisi B, Milner A et al. Structure of the C3HC4 domain by 1H-nuclear magnetic resonance spectroscopy. A new structural class of zinc-finger. J Mol Biol 1994; 237(2):201-211.
5. Bellon SF, Rodgers KK, Schatz DG et al. Crystal structure of the RAG1 dimerization domain reveals multiple zinc-binding motifs including a novel zinc binuclear cluster. Nat Struct Biol 1997; 4(7):586-591.
6. Gervais V, Busso D, Wasielewski E et al. Solution structure of the N-terminal domain of the human TFIIH MAT1 subunit: New insights into the RING finger family. J Biol Chem 2001; 276(10):7457-7464.
7. Zheng N, Wang P, Jeffrey PD et al. Structure of a c-Cbl-UbcH7 complex: RING domain function in ubiquitin-protein ligases. Cell 2000; 102(4):533-539.
8. Freemont PS. The RING finger. A novel protein sequence motif related to the zinc finger. Ann N Y Acad Sci 1993; 684:174-192.
9. Saurin AJ, Borden KL, Boddy MN et al. Does this have a familiar RING? Trends Biochem Sci 1996; 21(6):208-214.
10. Takeuchi M, Rothe M, Goeddel DV. Anatomy of TRAF2. Distinct domains for nuclear factor-kappaB activation and association with tumor necrosis factor signaling proteins. J Biol Chem 1996; 271(33):19935-19942.
11. Sato T, Irie S, Reed JC. A novel member of the TRAF family of putative signal transducing proteins binds to the cytosolic domain of CD40. FEBS Lett 1995; 358(2):113-118.
12. Cheng G, Cleary AM, Ye ZS et al. Involvement of CRAF1, a relative of TRAF, in CD40 signaling. Science 1995; 267(5203):1494-1498.
13. Rothe M, Sarma V, Dixit VM et al. TRAF2-mediated activation of NF-kappa B by TNF receptor 2 and CD40. Science 1995; 269(5229):1424-1427.
14. Takahashi R, Deveraux Q, Tamm I et al. A single BIR domain of XIAP sufficient for inhibiting caspases. J Biol Chem 1998; 273(14):7787-7790.
15. Liston P, Fong WG, Kelly NL et al. Identification of XAF1 as an antagonist of XIAP anti-Caspase activity. Nat Cell Biol 2001; 3(2):128-133.
16. Yang Y, Fang S, Jensen JP et al. Ubiquitin protein ligase activity of IAPs and their degradation in proteasomes in response to apoptotic stimuli. Science 2000; 288(5467):874-877.
17. Clem RJ, Miller LK. Control of programmed cell death by the baculovirus genes p35 and iap. Mol Cell Biol 1994; 14(8):5212-5222.
18. van der Reijden BA, Erpelinck-Verschueren CA, Lowenberg B et al. TRIADs: A new class of proteins with a novel cysteine-rich signature. Protein Sci 1999; 8(7):1557-1561.
19. Kitada T, Asakawa S, Hattori N et al. Mutations in the parkin gene cause autosomal recessive juvenile parkinsonism. Nature 1998; 392(6676):605-608.
20. Morett E, Bork P. A novel transactivation domain in parkin. Trends Biochem Sci 1999; 24(6):229-231.
21. Imai Y, Soda M, Inoue H et al. An unfolded putative transmembrane polypeptide, which can lead to endoplasmic reticulum stress, is a substrate of Parkin. Cell 2001; 105(7):891-902.
22. Imai Y, Soda M, Hatakeyama S et al. CHIP is associated with Parkin, a gene responsible for familial Parkinson's disease, and enhances its ubiquitin ligase activity. Mol Cell 2002; 10(1):55-67.

23. Zhang Y, Gao J, Chung KK et al. Parkin functions as an E2-dependent ubiquitin- protein ligase and promotes the degradation of the synaptic vesicle-associated protein, CDCrel-1. Proc Natl Acad Sci USA 2000; 97(24):13354-13359.
24. Reddy BA, Etkin LD, Freemont PS. A novel zinc finger coiled-coil domain in a family of nuclear proteins. Trends Biochem Sci 1992; 17(9):344-345.
25. Kakizuka A, Miller Jr WH, Umesono K et al. Chromosomal translocation t(15;17) in human acute promyelocytic leukemia fuses RAR alpha with a novel putative transcription factor, PML. Cell 1991; 66(4):663-674.
26. de The H, Lavau C, Marchio A et al. The PML-RAR alpha fusion mRNA generated by the t(15;17) translocation in acute promyelocytic leukemia encodes a functionally altered RAR. Cell 1991; 66(4):675-684.
27. Goddard AD, Borrow J, Freemont PS et al. Characterization of a zinc finger gene disrupted by the t(15;17) in acute promyelocytic leukemia. Science 1991; 254(5036):1371-1374.
28. Miki Y, Swensen J, Shattuck-Eidens D et al. A strong candidate for the breast and ovarian cancer susceptibility gene BRCA1. Science 1994; 266(5182):66-71.
29. Le Douarin B, Zechel C, Garnier JM et al. The N-terminal part of TIF1, a putative mediator of the ligand-dependent activation function (AF-2) of nuclear receptors, is fused to B-raf in the oncogenic protein T18. Embo J 1995; 14(9):2020-2033.
30. Hershko A, Ciechanover A. The ubiquitin system. Annu Rev Biochem 1998; 67:425-479.
31. Joazeiro CA, Wing SS, Huang H et al. The tyrosine kinase negative regulator c-Cbl as a RING-type, E2-dependent ubiquitin-protein ligase. Science 1999; 286(5438):309-312.
32. Lorick KL, Jensen JP, Fang S et al. RING fingers mediate ubiquitin-conjugating enzyme (E2)-dependent ubiquitination. Proc Natl Acad Sci USA 1999; 96(20):11364-11369.
33. Urano T, Saito T, Tsukui T et al. Efp targets 14-3-3 sigma for proteolysis and promotes breast tumour growth. Nature 2002; 417(6891):871-875.
34. Zhang Y, Xiong Y. Control of p53 ubiquitination and nuclear export by MDM2 and ARF. Cell Growth Differ 2001; 12(4):175-186.
35. Seol JH, Feldman RM, Zachariae W et al. Cdc53/cullin and the essential Hrt1 RING-H2 subunit of SCF define a ubiquitin ligase module that activates the E2 enzyme Cdc34. Genes Dev 1999; 13(12):1614-1626.
36. Galisteo ML, Dikic I, Batzer AG et al. Tyrosine phosphorylation of the c-cbl proto-oncogene protein product and association with epidermal growth factor (EGF) receptor upon EGF stimulation. J Biol Chem 1995; 270(35):20242-20245.
37. Thien CB, Walker F, Langdon WY. RING finger mutations that abolish c-Cbl-directed polyubiquitination and downregulation of the EGF receptor are insufficient for cell transformation. Mol Cell 2001; 7(2):355-365.
38. Haupt Y, Maya R, Kazaz A et al. Mdm2 promotes the rapid degradation of p53. Nature 1997; 387(6630):296-299.
39. Kubbutat MH, Jones SN, Vousden KH. Regulation of p53 stability by Mdm2. Nature 1997; 387(6630):299-303.
40. Geyer RK, Yu ZK, Maki CG. The MDM2 RING-finger domain is required to promote p53 nuclear export. Nat Cell Biol 2000; 2(9):569-573.
41. Chen Y, Chen CF, Riley DJ et al. Aberrant subcellular localization of BRCA1 in breast cancer. Science 1995; 270(5237):789-791.
42. Lupas A. Coiled coils: New structures and new functions. Trends Biochem Sci 1996; 21(10):375-382.
43. Reymond A, Meroni G, Fantozzi A et al. The tripartite motif family identifies cell compartments. Embo J 2001; 20(9):2140-2151.
44. Tissot C, Mechti N. Molecular cloning of a new interferon-induced factor that represses human immunodeficiency virus type 1 long terminal repeat expression. J Biol Chem 1995; 270(25):14891-14898.
45. Der SD, Zhou A, Williams BR et al. Identification of genes differentially regulated by interferon alpha, beta, or gamma using oligonucleotide arrays. Proc Natl Acad Sci USA 1998; 95(26):15623-15628.
46. Orimo A, Tominaga N, Yoshimura K et al. Molecular cloning of ring finger protein 21 (RNF21)/interferon-responsive finger protein (ifp1), which possesses two RING-B box-coiled coil domains in tandem. Genomics 2000; 69(1):143-149.
47. Slack FJ, Ruvkun G. A novel repeat domain that is often associated with RING finger and B-box motifs. Trends Biochem Sci 1998; 23(12):474-475.
48. Lu Z, Xu S, Joazeiro C et al. The PHD domain of MEKK1 acts as an E3 ubiquitin ligase and mediates ubiquitination and degradation of ERK1/2. Mol Cell 2002; 9(5):945-956.
49. Dhalluin C, Carlson JE, Zeng L et al. Structure and ligand of a histone acetyltransferase bromodomain. Nature 1999; 399(6735):491-496.
50. Ancient missense mutations in a new member of the RoRet gene family are likely to cause familial Mediterranean fever. The International FMF Consortium. Cell 1997; 90(4):797-807.
51. Quaderi NA, Schweiger S, Gaudenz K et al. Opitz G/BBB syndrome, a defect of midline development, is due to mutations in a new RING finger gene on Xp22. Nat Genet 1997; 17(3):285-291.
52. Avela K, Lipsanen-Nyman M, Idanheimo N et al. Gene encoding a new RING-B-box-Coiled-coil protein is mutated in mulibrey nanism. Nat Genet 2000; 25(3):298-301.
53. Cao T, Borden KL, Freemont PS et al. Involvement of the rfp tripartite motif in protein-protein interactions and subcellular distribution. J Cell Sci 1997; 110(Pt 14):1563-1571.
54. Shimono Y, Murakami H, Hasegawa Y et al. RET finger protein is a transcriptional repressor and interacts with enhancer of polycomb that has dual transcriptional functions. J Biol Chem 2000; 275(50):39411-39419.
55. Cao T, Duprez E, Borden KL et al. Ret finger protein is a normal component of PML nuclear bodies and interacts directly with PML. J Cell Sci 1998; 111(Pt 10):1319-1329.
56. Trockenbacher A, Suckow V, Foerster J et al. MID1, mutated in Opitz syndrome, encodes an ubiquitin ligase that targets phosphatase 2A for degradation. Nat Genet 2001; 29(3):287-294.
57. Peng H, Begg GE, Schultz DC et al. Reconstitution of the KRAB-KAP-1 repressor complex: A model system for defining the molecular anatomy of RING-B box-coiled-coil domain-mediated protein-protein interactions. J Mol Biol 2000; 295(5):1139-1162.
58. Inoue S, Orimo A, Hosoi T et al. Genomic binding-site cloning reveals an estrogen-responsive gene that encodes a RING finger protein. Proc Natl Acad Sci USA 1993; 90(23):11117-11121.
59. Orimo A, Inoue S, Ikeda K et al. Molecular cloning, structure, and expression of mouse estrogen-responsive finger protein Efp. Colocalization with estrogen receptor mRNA in target organs. J Biol Chem 1995; 270(41):24406-24413.
60. Ikeda K, Orimo A, Higashi Y et al. Efp as a primary estrogen-responsive gene in human breast cancer. FEBS Lett 2000; 472(1):9-13.
61. Orimo A, Inoue S, Minowa O et al. Underdeveloped uterus and reduced estrogen responsiveness in mice with disruption of the estrogen-responsive finger protein gene, which is a direct target of estrogen receptor alpha. Proc Natl Acad Sci USA 1999; 96(21):12027-12032.
62. Opitz JM. G syndrome (hypertelorism with esophageal abnormality and hypospadias, or hypospadias-dysphagia, or "Opitz-Frias" or "Opitz-G" syndrome)—perspective in 1987 and bibliography. Am J Med Genet 1987; 28(2):275-285.
63. Robin NH, Opitz JM, Muenke M. Opitz G/BBB syndrome: Clinical comparisons of families linked to Xp22 and 22q, and a review of the literature. Am J Med Genet 1996; 62(3):305-317.
64. Gaudenz K, Roessler E, Quaderi N et al. Opitz G/BBB syndrome in Xp22: Mutations in the MID1 gene cluster in the carboxy-terminal domain. Am J Hum Genet 1998; 63(3):703-710.
65. Jerome LA, Papaioannou VE. DiGeorge syndrome phenotype in mice mutant for the T-box gene, Tbx1. Nat Genet 2001; 27(3):286-291.
66. Cainarca S, Messali S, Ballabio A et al. Functional characterization of the Opitz syndrome gene product (midin): Evidence for homodimerization and association with microtubules throughout the cell cycle. Hum Mol Genet 1999; 8(8):1387-1396.

67. Short KM, Hopwood B, Yi Z et al. MID1 and MID2 homo- and heterodimerise to tether the rapamycin-sensitive PP2A regulatory subunit, alpha 4, to microtubules: Implications for the clinical variability of X-linked Opitz GBBB syndrome and other developmental disorders. BMC Cell Biol 2002; 3(1):1.
68. Borden KL. RING fingers and B-boxes: Zinc-binding protein-protein interaction domains. Biochem Cell Biol 1998; 76(2-3):351-358.
69. Kastner P, Perez A, Lutz Y et al. Structure, localization and transcriptional properties of two classes of retinoic acid receptor alpha fusion proteins in acute promyelocytic leukemia (APL): Structural similarities with a new family of oncoproteins. Embo J 1992; 11(2):629-642.
70. Grignani F, Ferrucci PF, Testa U et al. The acute promyelocytic leukemia-specific PML-RAR alpha fusion protein inhibits differentiation and promotes survival of myeloid precursor cells. Cell 1993; 74(3):423-431.
71. Grignani F, Testa U, Rogaia D et al. Effects on differentiation by the promyelocytic leukemia PML/RARalpha protein depend on the fusion of the PML protein dimerization and RARalpha DNA binding domains. Embo J 1996; 15(18):4949-4958.
72. Weis K, Rambaud S, Lavau C et al. Retinoic acid regulates aberrant nuclear localization of PML-RAR alpha in acute promyelocytic leukemia cells. Cell 1994; 76(2):345-356.
73. Koken MH, Puvion-Dutilleul F, Guillemin MC et al. The t(15;17) translocation alters a nuclear body in a retinoic acid-reversible fashion. Embo J 1994; 13(5):1073-1083.
74. Dyck JA, Maul GG, Miller Jr WH et al. A novel macromolecular structure is a target of the promyelocyte-retinoic acid receptor oncoprotein. Cell 1994; 76(2):333-343.
75. Szostecki C, Guldner HH, Netter HJ et al. Isolation and characterization of cDNA encoding a human nuclear antigen predominantly recognized by autoantibodies from patients with primary biliary cirrhosis. J Immunol 1990; 145(12):4338-4347.
76. Koken MH, Reid A, Quignon F et al. Leukemia-associated retinoic acid receptor alpha fusion partners, PML and PLZF, heterodimerize and colocalize to nuclear bodies. Proc Natl Acad Sci USA 1997; 94(19):10255-10260.
77. Chen Z, Brand NJ, Chen A et al. Fusion between a novel Kruppel-like zinc finger gene and the retinoic acid receptor-alpha locus due to a variant t(11;17) translocation associated with acute promyelocytic leukaemia. Embo J 1993; 12(3):1161-1167.
78. Ishov AM, Maul GG. The periphery of nuclear domain 10 (ND10) as site of DNA virus deposition. J Cell Biol 1996; 134(4):815-826.
79. Kamitani T, Nguyen HP, Kito K et al. Covalent modification of PML by the sentrin family of ubiquitin-like proteins. J Biol Chem 1998; 273(6):3117-3120.
80. Fagioli M, Alcalay M, Tomassoni L et al. Cooperation between the RING + B1-B2 and coiled-coil domains of PML is necessary for its effects on cell survival. Oncogene 1998; 16(22):2905-2913.
81. Mu ZM, Chin KV, Liu JH et al. PML, a growth suppressor disrupted in acute promyelocytic leukemia. Mol Cell Biol 1994; 14(10):6858-6867.
82. Regad T, Saib A, Lallemand-Breitenbach V et al. PML mediates the interferon-induced antiviral state against a complex retrovirus via its association with the viral transactivator. Embo J 2001; 20(13):3495-3505.
83. Kamitani T, Kito K, Nguyen HP et al. Identification of three major sentrinization sites in PML. J Biol Chem 1998; 273(41):26675-26682.
84. Borden KL, Lally JM, Martin SR et al. In vivo and in vitro characterization of the B1 and B2 zinc-binding domains from the acute promyelocytic leukemia protooncoprotein PML. Proc Natl Acad Sci USA 1996; 93(4):1601-1606.
85. Lallemand-Breitenbach V, Zhu J, Puvion F et al. Role of promyelocytic leukemia (PML) sumolation in nuclear body formation, 11S proteasome recruitment, and As2O3-induced PML or PML/retinoic acid receptor alpha degradation. J Exp Med 2001; 193(12):1361-1371.
86. Le XF, Yang P, Chang KS. Analysis of the growth and transformation suppressor domains of promyelocytic leukemia gene, PML. J Biol Chem 1996; 271(1):130-135.
87. Chen XP, Losman JA, Rothman P. SOCS proteins, regulators of intracellular signaling. Immunity 2000; 13(3):287-290.
88. Haque SJ, Harbor PC, Williams BR. Identification of critical residues required for suppressor of cytokine signaling-specific regulation of interleukin-4 signaling. J Biol Chem 2000; 275(34):26500-26506.
89. Terstegen L, Maassen BG, Radtke S et al. Differential inhibition of IL-6-type cytokine-induced STAT activation by PMA. FEBS Lett 2000; 478(1-2):100-104.
90. Toniato E, Chen XP, Losman J et al. TRIM8/GERP RING finger protein interacts with SOCS-1. J Biol Chem 2002; 277(40):37315-37322.
91. Niikura T, Hashimoto Y, Tajima H et al. A tripartite motif protein TRIM11 binds and destabilizes Humanin, a neuroprotective peptide against Alzheimer's disease-relevant insults. Eur J Neurosci 2003; 17(6):1150-1158.
92. Guo B, Zhai D, Cabezas E et al. Humanin peptide suppresses apoptosis by interfering with Bax activation. Nature 2003; 423(6938):456-461.
93. Sibilia J. Ro(SS-A) and anti-Ro(SS-A): An update. Rev Rhum Engl Ed 1998; 65(1):45-57.
94. Itoh Y, Reichlin M. Autoantibodies to the Ro/SSA antigen are conformation dependent. I: Anti-60 kD antibodies are mainly directed to the native protein; anti-52 kD antibodies are mainly directed to the denatured protein. Autoimmunity 1992; 14(1):57-65.
95. Billaut-Mulot O, Cocude C, Kolesnitchenko V et al. SS-56, a novel cellular target of autoantibody responses in Sjogren syndrome and systemic lupus erythematosus. J Clin Invest 2001; 108(6):861-869.
96. Fukuda-Kamitani T, Kamitani T. Ubiquitination of Ro52 autoantigen. Biochem Biophys Res Commun 2002; 295(4):774-778.

14

Immunohistochemical Detection of EBAG9/RCAS1 Expression in Hepatocellular Carcinoma

Taku Aoki, Hiroshi Imamura, Masatoshi Makuuchi, and Satoshi Inoue

Introduction

Identification of EBAG9/RCAS1

Estrogen receptor–binding fragment-associated gene 9 (*EBAG9*) is an estrogen-responsive gene that has been isolated from a CpG island library of MCF-7 human breast cancer cells by the genomic binding-site cloning method (Watanabe *et al.*, 1998). The complementary deoxyribonucleic acid (cDNA) of human EBAG9 encodes an open reading frame (ORF) of 213 amino acids. An estrogen-responsive element (ERE) is located in the 5′ flanking region of the EBAG9 gene, and its transcript is directly up-regulated by estrogen (Tsuchiya *et al.*, 2001; Watanabe *et al.*, 1998).

The receptor-binding cancer antigen expressed on SiSo cells (RCAS1) was originally isolated as the antigen recognized by 22-1-1 antibody against human uterine adenocarcinoma cell line SiSo (Sonoda *et al.*, 1996) and was later found to be identical to EBAG9 (EBAG9/RCAS1) (Nakashima *et al.*, 1999). Based on *in vitro* observation, RCAS1 has been assumed to act as a ligand for a putative receptor present on normal peripheral lymphocytes, such as T, B, and natural killer (NK) cells. RCAS1 has also been found to inhibit the growth of activated $CD3^+$ T lymphocytes and NK cells and to induce apoptotic cell death (Nakashima *et al.*, 1999). Based on these observations, it has been speculated that EBAG9/RCAS1 is involved in the escape of tumor cells from immune system action.

EBAG9/RCAS1 Expression in Normal Tissue and Cancer Tissue

Two antibodies have been used to assess the expression of EBAG9/RCAS1 in various tissues and cell lines. The first is the 22-1-1 monoclonal antibody established by cell fusion between mouse myeloma cells and spleen cells derived from mice immunized with human uterine cervical adenocarcinoma cell line, SiSo (Sonoda *et al.*, 1996). Immunoreactivity to this antibody has been detected in normal human tissues, such as uterine endometrial glands (Sonoda *et al.*, 2000), goblet cells of bronchi and bronchioles (Iwasaki *et al.*, 2000; Izumi *et al.*, 2001), and gastric mucosa (Kubokawa *et al.*, 2001). Immunoreactivity has also been reported in various cancer tissues, including cancer of the uterus (Kaku *et al.*, 1999; Sonoda *et al.*, 1996; Sonoda *et al.*, 1998; Sonoda *et al.*, 2000), ovary (Sonoda *et al.*, 1996), lung (Iwasaki *et al.*, 2000; Izumi *et al.*, 2001; Oizumi *et al.*, 2002), stomach (Kubokawa *et al.*, 2001), skin (Takahashi *et al.*, 2001), gallbladder (Oshikiri *et al.*, 2001), esophagus (Nakakubo *et al.*, 2002), pancreas (Hiraoka *et al.*, 2002), bile duct

Handbook of Immunohistochemistry and *in situ* Hybridization of Human Carcinomas,
Volume 3. Molecular Genetics, Liver Carcinoma, and Pancreatic Carcinoma

(Enjoji *et al.*, 2002; Suzuoki *et al.*, 2002), and liver (Noguchi *et al.*, 2001).

We raised a rabbit polyclonal anti-EBAG9 antibody against a glutathione-*S*-transferase (GST)-EBAG9 fusion protein (Tsuchiya *et al.*, 2001), and the antibody has been shown to react with human and mouse EBAG9 and yield a 32-kD band in Western Blot analysis. The intensity of the band has been shown to be reduced by prior incubation of the antibody with recombinant EBAG9 protein (Suzuki *et al.*, 2001). Immunostaining with this polyclonal antibody has shown that EBAG9 is expressed in various tissues from normal mice, including liver (Tsuchiya *et al.*, 2001), and tissues from normal humans, such as mammary gland tissue (Suzuki *et al.*, 2001) and prostate tissue (Takahashi *et al.*, 2003). EBAG9 has also been shown to be widely distributed in human breast cancer and prostate cancer (Suzuki *et al.*, 2001; Takahashi *et al.*, 2003).

Because the reports referred to earlier have documented that expression of EBAG9/RCAS1 is more remarkable in cancer tissues than in normal tissues, EBAG9/RCAS1 has attracted attention as a potential cancer-associated antigen. Its expression is generally thought to be related to tumor invasiveness and to be associated with poor patient prognosis in cancer of the uterus (Kaku *et al.*, 1999), lung (Iwasaki *et al.*, 2000; Izumi *et al.*, 2001; Oizumi *et al.*, 2002), gallbladder (Oshikiri *et al.*, 2001), esophagus (Nakakubo *et al.*, 2002), pancreas (Hiraoka *et al.*, 2002), bile duct (Suzuoki *et al.*, 2002), and prostate (Takahashi *et al.*, 2003).

Stepwise Evolution of Hepatocellular Carcinoma and EBAG9/RCAS1 Expression in Hepatocellular Carcinoma

Hepatocellular carcinoma (HCC) is one of the most common malignancies worldwide, ranking 5th in frequency in the world (Parkin *et al.*, 2001). Although HCC is more prevalent in Asia and Africa, its incidence is on the rise in Western countries (El-Serag and Mason, 1999; El-Serag *et al.*, 2003; Taylor-Robinson *et al.*, 1997). The condition HCC has the unique characteristic of developing and progressing in a typical multistep manner—that is, from early HCC (Liver Cancer Study Group of Japan, 2000; Takayama *et al.*, 1998), through early-advanced HCC, to advanced HCC (Kojiro and Nakashima, 1999). Most early HCCs are small, well-differentiated nodules with low proliferative activity, but when they progress to a more advanced stage, they transform into moderately to poorly differentiated cancers and undergo a rapid increase in size. During this process (tumor dedifferentiation and proliferation), HCCs acquire malignant potential as reflected by intrahepatic metastasis and vascular invasion (see later discussion). This transformation occurs nonuniformly within a given tumor nodule, resulting in the simultaneous presence of well-differentiated and moderately to poorly differentiated lesions within the same nodule. This produces what histologists refer to as a "nodule-in-nodule" or "mosaic" appearance (Kojiro and Nakashima, 1999). As mentioned earlier, HCC frequently invades blood vessels, especially the portal system, resulting in intrahepatic metastasis. Many previous reports have documented vascular invasion and intrahepatic metastasis as unfavorable prognostic factors.

In this chapter, we describe immunohistochemical detection of EBAG9/RCAS1 expression in noncancerous liver tissue and in HCC tissue, especially the methodologic aspects. We used a rabbit polyclonal anti-EBAG9 antibody (Tsuchiya *et al.*, 2001). In view of the pathologic features of HCC and the results of previous studies on EBAG9/RCAS1 as a cancer marker, we paid particular attention to the multistep evolution of HCC, including the following: 1) process of tumor dedifferentiation, 2) cancer proliferative activity, and 3) ability to metastasize. The overall results have previously been reported by our group elsewhere (Aoki *et al.*, 2003).

MATERIALS

Liver Samples

Samples of HCC tissue and adjacent noncancerous liver tissue from 143 cases of HCC were analyzed immunohistochemically. Testing for hepatitis B virus surface antigen was positive in 23 patients, and testing for anti-hepatitis C virus (HCV) antibody was positive in 100 patients. The liver tissue was obtained during surgery in our department between October 1994 and December 1998. Ten liver biopsy specimens obtained for preoperative evaluation of potential liver transplant donors, and 10 liver biopsy specimens obtained to assess patients who were serologically anti-HCV antibody positive were also made available for the analysis as noncancerous samples. The biopsy specimens from the patients who were HCV antibody positive were kindly provided by Dr. Jyunichi Fukushima (Department of Pathology, Teikyo University School of Medicine, Tokyo, Japan).

Materials for Immunohistochemistry

1. 10% formalin for fixation.
2. Xylene: for dewaxing.
3. Ethanol: diluted to 50%, 70%, 90%, and 95% with distilled water.

4. Tris-buffered saline (TBS): 6.06 g TRIZMA Base and 8.77 g NaCl; brought to a volume of 1 L with deionized distilled water and adjusted to pH 7.6 with HCl.

5. 10 mM Na-citrate solution (pH 6.0): 2.10 g citric acid brought to a volume of 1 L with deionized distilled water and adjusted to pH 6.0 with 6 M NaOH.

6. 0.3% hydrogen peroxide (H_2O_2) in 100% methanol: 150 ml of 100% methanol was mixed with 1.5 ml of 30% H_2O_2.

7. Fetal calf serum (FCS): stored at –20°C.

8. Primary antibody: rabbit polyclonal anti-EBAG9 antibody (Tsuchiya *et al.*, 2001) diluted 1:40 in 10% FCS-TBS or normal rabbit immunoglobulin (IgG) diluted 1:800 in 10% FCS-TBS.

9. Envision (Dako, Glostrup, Denmark; for rabbit polyclonal antibody).

10. 3,3'-diaminobenzidine tetrahydrochloride (DAB) working solution mixed with Tris-HCl (pH 7.5) and 0.02% H_2O_2.

11. 50% Mayer's hematoxylin: for counterstaining.

METHOD

Liver Tissue Preparation

Resected liver specimens were fixed in 10% formalin, cut into blocks, and embedded in paraffin. They were then sliced into 4-μm sections and mounted on glass slides.

Protocol for EBAG9/RCAS1 Immunostaining

1. Dip the slides in xylene for 3 min 3×.
2. Dip the slides in 100% ethanol for 3 min 2×.
3. Dip the slides in 95% ethanol for 3 min 2×.
4. Rinse the slides in TBS for 5 min.
5. Dip the slides in 10 mM Na-citrate solution (pH 6.0) and then heat them in an autoclave at 125°C for 5 min.
6. Rinse the slides in TBS for 5 min. at room temperature.
7. Block endogenous peroxide by dipping the slides in 0.3% hydrogen peroxide (H_2O_2) in 100% methanol for 30 min.
8. Rinse the slides in TBS for 5 min 3×.
9. Block nonspecific binding by incubating the sections in 10% FCS-TBS for 30 min in a moist chamber.
10. Incubate the sections in primary antibody (rabbit polyclonal antibody for EBAG9) or control rabbit IgG diluted in 10% FCS-TBS in a moist chamber at 4°C overnight.
11. Wash the slides quickly in TBS 3× at room temperature.
12. Rinse the slides in TBS for 5 min.
13. Incubate the sections in Envision (Dako; for rabbit polyclonal antibody) for 1 hr in a moist chamber at room temperature.
14. Rinse the slides in TBS for 5 min 3× at room temperature.
15. Visualize the staining with 3,3'-DAB: apply the working solution and stop the reaction as soon as adequate color develops (usually 2–3 min).
16. Counterstain the sections in 50% Mayer's hematoxylin.
17. Wash the slides in tap water for 5 min.
18. Dip the slides in graded ethanol solutions (50%, 70%, 90%, and 100%) and then in xylene (each for 3 min).
19. Place coverslips on the sections. They are now ready for final examination under a light microscope.

RESULTS AND DISCUSSION

EBAG9 Expression in Normal and Chronically Diseased Liver

Noncancerous hepatocytes, including hepatocytes from normal liver, chronic HCV-related hepatitis, or cirrhotic liver, displayed a low but significant level of EBAG9 immunoreactivity (Figure 43a). High-power magnification revealed punctate staining concentrated specifically near the cell membrane bordering adjacent hepatocytes (not shown). The distribution of the EBAG9 staining was homogeneous and regular throughout the tissue, suggesting that it becomes localized in the cells.

EBAG9/RCAS1 has been detected in various normal human tissues, e.g., uterine endometrial glands (Sonoda *et al.*, 2000), goblet cells of bronchi and bronchioles (Iwasaki *et al.*, 2000; Izumi *et al.*, 2001), mammary glands (Suzuki *et al.*, 2001), and gastric mucosa (Kubokawa *et al.*, 2001), suggesting that EBAG9/RCAS1 is expressed and secreted by gland cells. Thus, the polarity of EBAG9/RCAS1 expression in noncancerous liver tissue suggests that it is related to some physiologic function, e.g., glandular secretion, in normal liver tissue.

EBAG9 Expression in Hepatocellular Carcinoma

EBAG9 Expression at the Cell Level

The EBAG9 immunoreactivity of HCC cells varied. Some exhibited weak immunoreactivity, similar to that of noncancerous hepatocytes (enhancement-negative cells) (Figure 43b), whereas others displayed enhanced immunoreactivity (enhancement-positive cells)

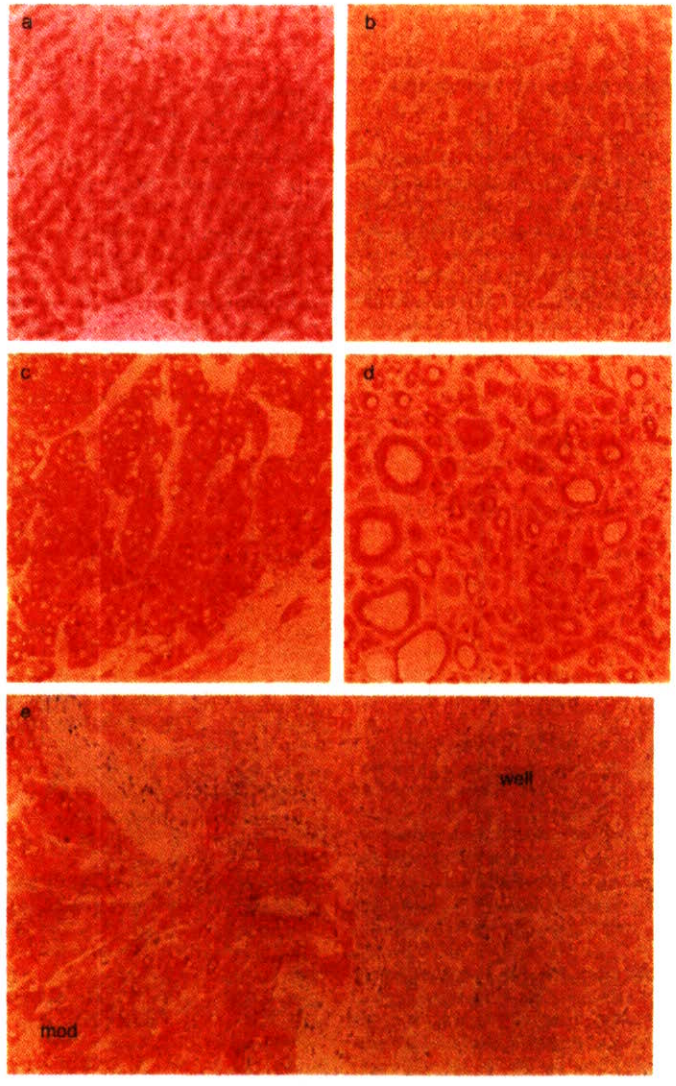

Figure 43. **a:** Normal liver tissue showing weak EBAG9 immunoreactivity. The staining pattern is homogeneous and regular throughout the tissue (200X). **b:** A well differentiated hepatocellular carcinoma (HCC) classified as EBAG9-negative. The pattern of expression is similar to the pattern in noncancerous tissue (200X). **c:** An EBAG9-positive case of moderately differentiated HCC (trabecular type) (200X). Immunoreactivity is detected over the entire surface of the cancer cells and in their cytoplasm. **d:** Pseudoglandular type of moderately differentiated HCC displaying intense expression on the apical surface of the cells (200X). **e:** A tumor with a "nodule-in-nodule" appearance showing intense staining in the interior, moderately differentiated region ("mod"), contrasting with weak staining in the outer, well-differentiated region ("well") (100X).

(Figure 43c). The staining pattern in enhancement-negative cancer cells showed regular distribution of EBAG9-positive granules, similar to the pattern in noncancerous hepatocytes. By contrast, in the majority of enhancement-positive cells there was intense staining over the entire surface of the cell as well as in the cytoplasm. Coarse, thickened granules were dispersed throughout the cytoplasm, and the regularity of the granule distribution noted in the noncancerous hepatocytes was lost. This finding was consistent with observations in the cells of invasive ductal carcinoma of the breast showing that normal mammary gland cells expressed EBAG9/RCAS1 only on their apical surface, whereas carcinoma cells exhibit enhanced expression without a polar distribution (Suzuki *et al.*, 2001). The apical surfaces of the pseudoglands stained strongly in the pseudoglandular type of moderately differentiated HCC (Figure 43d).

Intranodular Distribution of Enhanced EBAG9 Immunoreactivity

The proportion and distribution of enhancement-positive cancer cells were highly variable from nodule to nodule (range 5–100%). It is interesting that, "nodule-in-nodule" tumors, i.e., those consisting of a combination of well-differentiated lesion and a less-differentiated lesion, displayed different immunoreactivity in the two regions, with the less-differentiated intensely immunoreactive region contrasting clearly with the weakly immunoreactive well-differentiated region (Figure 43e).

Semiquantitative Classification of EBAG9 Expression in Hepatocellular Carcinoma Sections

Based on the observations described earlier, HCC section was classified in a semiquantitative manner as follows:

1. Negative (−): sections in which all the cancer cells were identified as enhancement-negative.
2. Borderline (±): sections in which 1–5% of the malignant cells were enhancement-positive, or, sections showing uniformly positive but very weak immunoreactivity.
3. Positive (+): sections in which more than 5% of enhancement-positive cancerous cells.

As a result, 35 of the 143 sections examined (24.5%) were classified as negative, 24 (16.8%) as borderline, and 84 (58.7%) as positive.

Correlation between EBAG9 Expression and Pathologic Variables

For purposes of analysis, the borderline group and negative group were combined and compared with the positive group. The relationship between EBAG9 immunoreactivity and various clinicopathologic parameters was analyzed by comparing the EBAG9-positive group (n = 84) with the EBAG9-negative/borderline group (n = 59), as shown in Table 17. Enhanced EBAG9 immunoreactivity was more frequently observed in the less-differentiated tumors (P = 0.01), and EBAG9 immunoreactivity was significantly correlated with the Ki-67 labeling index. However, there was no significant correlation between enhanced EBAG9 expression and tumor invasiveness (Kosuge *et al.*, 1993; intrahepatic metastasis and/or vascular invasion) (P = 0.86). No other clinical or pathologic variables were significantly correlated with enhanced EBAG9 expression, and no significant correlation was established between enhanced EBAG9 expression and disease-free survival evaluated by the Kaplan-Meier method and log-rank test (P = 0.17) (Figure 44).

EBAG9/RCAS1 Expression in the Process of Stepwise Hepatocellular Carcinoma Progression

Our results showed that enhanced EBAG9/RCAS1 expression is closely correlated with degree of tumor differentiation and increased Ki-67 labeling index. Ki-67 is now widely used as a marker of cell proliferation, including in human studies (Gerdes *et al.*, 1984; Scholzen and Gerdes, 2000). Thus, our findings suggest that enhanced EBAG9/RCAS1 expression is associated with HCC tumor progression as represented by dedifferentiation and proliferation. It is interesting that, tumors showing a "nodule-in-nodule" appearance displayed intense expression in the less-differentiated region and weak expression in the more highly differentiated region (Figure 43e), suggesting that enhancement of EBAG9/RCAS1 expression parallels tumor dedifferentiation.

In contrast to a previous report (Noguchi *et al.*, 2001), EBAG9/RCAS1 was unassociated with tumor metastasis in our series. All of our results lead us to conclude that EBAG9/RCAS1 is closely associated with tumor dedifferentiation and proliferation but not with tumor metastasis. In other words, EBAG9/RCAS1 appears to be more related to growth of the primary tumor than to development of tumor metastases. Our results therefore imply that enhanced EBAG9/RCAS1 expression is an intermediate event in the multistep progression of HCC and is unrelated to the final event, which is characterized by the frequent occurrence of vascular invasion and resultant intrahepatic metastasis. Because enhanced EBAG9 expression was not significantly associated with patient disease-free survival, EBAG9 may not be a prognostic factor in patients with HCC. Nevertheless, we consider it to be of value as a

Table 17. Association between EBAG9 Immunoreactivity and Clinicopathologic Parameters

Parameters	Number of Patients	Intensity of EBAG9 Immunoreactivity: Negative/Borderline (%)	Intensity of EBAG9 Immunoreactivity: Positive (%)	P
Age (years)[a]		62.2±11.6	61.8±10.6	.44
<65	75	28 (37.3)	47 (62.7)	
≥65	68	31 (45.6)	37 (54.4)	.39
Sex				
Male	107	40 (37.4)	67 (62.6)	
Female	36	19 (52.8)	17 (47.2)	.12
HBsAg				
+	23	10 (43.5)	13 (56.5)	
−	120	49 (40.8)	71 (59.2)	.82
HCV Ab				
+	100	42 (42.0)	58 (58.0)	
−	43	17 (39.5)	26 (60.5)	.85
Child-Turcotte-Pugh Score				
A	110	43 (39.1)	67 (60.9)	
B	33	16 (48.5)	17 (51.5)	.42
AFP (ng/ml)[b]		51 [2-436000]	55 [2-69000]	.57
≤20	48	17 (35.4)	31 (64.6)	
>20	95	42 (44.2)	53 (55.8)	.37
DCP (AU/ml)[b]		62.5 [11-80000]	76.0 [10-77520]	.10
≤62.5	76	36 (47.4)	40 (52.6)	
>62.5	67	23 (34.3)	44 (65.7)	.12
Degree of tumor differentiation				
Well	25	16 (64.0)	9 (36.0)	
Moderately/poorly	118	43 (36.4)	75 (63.6)	.01
Tumor size (cm)[a]		2.8 [0.8-15.5]	3.4 [1.0-16.0]	.29
≤2.0	38	20 (52.6)	18 (47.4)	
>2.0	105	39 (37.1)	66 (62.9)	.12
Tumor number				
Solitary	79	35 (44.3)	44 (55.7)	
Multifocal	64	24 (37.5)	40 (62.5)	.49
IM and/or VI				
Positive	58	23 (39.6)	35 (60.3)	
Negative	85	36 (42.4)	49 (57.6)	.86
Fibrous capsular formation/infiltration				
Positive/positive	79	30 (38.0)	49 (62.0)	
Positive/negative	27	13 (48.1)	14 (51.9)	
Negative	37	16 (43.2)	21 (56.8)	.62
Background liver disease				
Liver fibrosis	5	1 (20.0)	4 (80.0)	
Chronic hepatitis	40	13 (32.5)	27 (67.5)	
Liver cirrhosis	98	45 (45.9)	53 (54.1)	.21
	143	59 (41.3)	84 (58.7)	

[a]Data expressed as average ± SD
[b]Data expressed as median value [range]
HBsAg, HBsAg-positive; HCV Ab, HCV Ab-positive; AFP, alpha-fetoprotein; DCP, des-γ-carboxy prothrombin; IM, intrahepatic metastasis; VI, vascular invasion
Cited from Reference Aoki *et al.*, 2003 with permission.

pathologic marker of a specific stage of HCC tumor progression.

In conclusion, we observed weak but discretely localized expression of EBAG9/RCAS1 in noncancerous normal and chronically diseased liver tissue, suggesting that EBAG9/RCAS1 is expressed in a positionally regulated fashion. We also found enhanced expression in about half of the HCCs examined, and we found that the enhanced expression was characterized by loss of the localized staining pattern. Enhanced EBAG9/RCAS1 expression was correlated with tumor dedifferentiation and proliferation and not with metastasis.

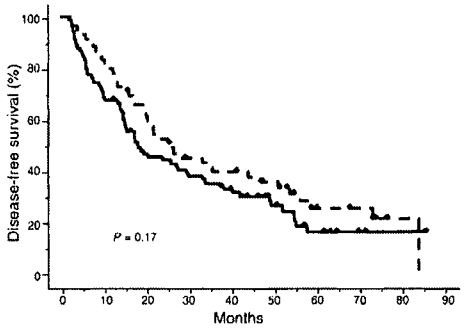

Figure 44. The Kaplan-Meier curves for disease-free survival in the EBAG9-positive group (*solid line*, $n = 84$) and EBAG9-negative/borderline group (*broken line*, $n = 59$). There is no significant difference between the two groups ($P = 0.17$).

Future investigation of EBAG9/RCAS1 function should help clarify the mechanism of HCC progression.

References

Aoki, T., Inoue, S., Imamura, H., Fukushima, J., Takahashi, S., Urano, T., Hasegawa, K., Ogushi, T., Ouchi, Y., and Makuuchi, M. 2003. EBAG9/RCAS1 expression in hepatocellular carcinoma: Correlation with tumour dedifferentiation and proliferation. *Eur. J. Cancer 39*:1552–1561.

Enjoji, M., Nakashima, M., Nishi, H., Choi, I., Oimomi, H., Sugimoto, R., Kotoh, K., Taguchi, K., Nakamuta, M., Nawata, H., and Watanabe, T. 2002. The tumor-associated antigen, RCAS1 can be expressed in immune-mediated diseases as well as in carcinomas of biliary tract. *J. Hepatol. 36*:786–792.

El-Serag, H.B., and Mason, A.C. 1999. Rising incidence of hepatocellular carcinoma in the United States. *N. Engl. J. Med. 340*:745–750.

El-Serag, H.B., Davila, J.A., Peterson, N.J., and McGlynn, K.A. 2003. The continuing increase in the incidence of hepatocellular carcinoma in the United States: An update. *Ann. Intern. Med. 139*:817–823.

Gerdes, J., Lemke, H., Baisch, H., Wacker, H.H., Schwab, U., and Stein, H. 1984. Cell cycle analysis of a cell proliferation-associated human nuclear antigen defined by the monoclonal antibody Ki-67. *J. Immunol. 133*:1710–1715.

Hiraoka, K., Hida, Y., Miyamoto, M., Oshikiri, T., Suzuoki, M., Nakakubo, Y., Shinohara, T., Itoh, T., Shichinohe, T., Kondo, S., Kasahara, N., and Katoh, H. 2002. High expression of tumor-associated antigen RCAS1 in pancreatic ductal adenocarcinoma is an unfavorable prognostic marker. *Int. J. Cancer 99*:418–423.

Iwasaki, T., Nakashima, M., Watanabe, T., Yamamoto, S., Inoue, Y., Yamanaka, H., Matsumura, A., Iuchi, K., Mori, T., and Okada, M. 2000. Expression and prognostic significance in lung cancer of human tumor-associated antigen RCAS1. *Int. J. Cancer 89*:488–493.

Izumi, M., Nakanishi, Y., Yoshino, I., Nakashima, M., Watanabe, T., and Hara, N. 2001. Expression of tumor-associated antigen RCAS1 correlates significantly with poor prognosis in nonsmall cell lung carcinoma. *Cancer 92*:446–451.

Kaku, T., Sonoda, K., Kamura, T., Hirakawa, T., Sakai, K., Amada, S., Ogawa, S., Kobayashi, H., Nakashima, M., Watanabe, T., and Nakano, H. 1999. The prognostic significance of tumor-associated antigen 22-1-1 expression in adenocarcinoma of the uterine cervix. *Clin. Cancer Res. 5*:1449–1453.

Kojiro, M., and Nakashima, O. 1999. Histopathologic evaluation of hepatocellular carcinoma with special reference to small early stage tumors. *Semin. Liver Dis. 19*:287–296.

Kosuge, T., Makuuchi, M., Takayama, T., Yamamoto, J., Shimada, K., and Yamasaki, S. 1993. Long-term results after resection of hepatocellular carcinoma: Experience of 480 cases. *Hepato-gastroenterol. 40*:328–332.

Kubokawa, M., Nakashima, M., Yao, T., Ito, K., Harada, N., Nawata, H., and Watanabe, T. 2001. Aberrant intracellular localization of RCAS1 is associated with tumor progression of gastric cancer. *Int. J. Oncol. 19*:695–700.

Liver Cancer Study Group of Japan. 2000. *The General Rules for the Clinical and Pathological Study of Primary Liver Cancer.* 4th ed. Tokyo: Kanehara & Co. Ltd., 28–34.

Nakakubo, Y., Hida, Y., Miyamoto, M., Hashida, H., Oshikiri, T., Kato, K., Suzuoki, M., Hiraoka, K., Ito, T., Morikawa, T., Okushiba, S., Kondo, S., and Katoh, H. 2002. The prognostic significance of RCAS1 expression in squamous cell carcinoma of the oesophagus. *Cancer Lett. 177*:101–105.

Nakashima, M., Sonoda, K., and Watanabe, T. 1999. Inhibition of cell growth and induction of apoptotic cell death by the human tumor-associated antigen RCAS1. *Nat. Med. 5*:938–942.

Noguchi, K., Enjoji, M., Nakamuta, M., Nakashima, M., Nishi, H., Choi, I., Taguchi, K., Kotoh, K., Shimada, M., Sugimachi, K., Tsuneyoshi, M., Nawata, H., and Watanabe, T. 2001. Expression of a tumor-associated antigen RCAS1 in hepatocellular carcinoma. *Cancer Lett. 168*:197–202.

Oizumi, S., Yamazaki, K., Nakashima, M., Watanabe, T., Homnura, F., Ogura, S., Nishimura, M., and Dosaka-Akita, H. 2002. RCAS1 expression: A potential prognostic marker for adenocarcinoma of the lung. *Oncology 62*:333–339.

Oshikiri, T., Hida, Y., Miyamoto, M., Hashida, H., Katoh, K., Suzuoki, M., Nakakubo, Y., Hiraoka, K., Shinohara, T., Itoh, T., Kondo, S., and Katoh, H. 2001. RCAS1 as a tumour progression marker: An independent negative prognostic factor in gallbladder cancer. *Br. J. Cancer 85*:1922–1927.

Parkin, D.M., Bray, F., Ferlay, J., and Pisani, P. 2001. Estimating the world cancer burden: GLOBOCAN 2000. *Int. J. Cancer 94*:153–156.

Scholzen, T., and Gerdes, J. 2000. The Ki-67 protein: From the known and the unknown. *J. Cell Physiol. 182*:311–322.

Sonoda, K., Nakashima, M., Kaku, T., Kamura, T., Nakano, H., and Watanabe, T. 1996. A novel tumor-associated antigen expressed in human uterine and ovarian carcinomas. *Cancer 77*:1501–1509.

Sonoda, K., Kaku, T., Kamura, T., Nakashima, M., Watanabe, T., and Nakano, H. 1998. Tumor-associated antigen 22-1-1 expression in the uterine cervical squamous neoplasias. *Clin. Cancer Res. 4*:1517–1520.

Sonoda, K., Kaku, T., Hirakawa, T., Kobayashi, H., Amada, S., Sakai, K., Nakashima, M., Watanabe, T., and Nakano, H. 2000. The clinical significance of tumor-associated antigen RCAS1 expression in the normal, hyperplastic, and malignant uterine endometrium. *Gynecol. Oncol. 79*:424–429.

Suzuki, T., Inoue, S., Kawabata, W., Akahira, J., Moriya, T., Tsuchiya, F., Ogawa, S., Muramatsu, M., and Sasano, H. 2001.

EBAG9/RCAS1 in human breast carcinoma: A possible factor in endocrine-immune interactions. *Br. J. Cancer 85*:1731–1737.

Suzuoki, M., Hida, Y., Miyamoto, M., Oshikiri, T., Hiraoka, K., Nakakubo, Y., Shinohara, T., Itoh, T., Okushiba, S., Kondo, S., and Katoh, H. 2002. RCAS1 expression as a prognostic factor after curative surgery for extrahepatic bile duct carcinoma. *Ann. Surg. Oncol. 9*:388–393.

Takahashi, H., Iizuka, H., Nakashima, M., Wada, T., Asano, K., Ishida-Yamamoto, A., and Watanabe, T. 2001. RCAS1 antigen is highly expressed in extramammary Paget's disease and in advanced stage squamous cell carcinoma of the skin. *J. Dermatol. Sci. 26*:140–144.

Takahashi, S., Urano, T., Tsuchiya, F., Fujimura, T., Kitamura, T., Ouchi, Y., Muramatsu, M., and Inoue, S. 2003. EBAG9/RCAS1 expression and its prognostic significance in prostatic cancer. *Int. J. Cancer 106*:310–315.

Takayama, T., Makuuchi, M., Hirohashi, S., Sakamoto, M., Yamamoto, J., Shimada, K., Kosuge, T., Okada, S., Takayasu, K., and Yamasaki, S. 1998. Early hepatocellular carcinoma as an entity with a high rate of surgical cure. *Hepatology 28*:1241–1246.

Taylor-Robinson, S.D., Foster, G.R., Arora, S., Hargreaves, S., and Thomas, H.C. 1997. Increase in primary liver cancer in the UK, 1979–94. *Lancet 350*:1142–1143.

Tsuchiya, F., Ikeda, K., Tsutsumi, O., Hiroi, H., Momoeda, M., Taketani, Y., Muramatsu, M., and Inoue, S. 2001. Molecular cloning and characterization of mouse EBAG9, homolog of a human cancer associated surface antigen: Expression and regulation by estrogen. *Biochem. Biophys. Res. Commun. 284*:2–10.

Watanabe, T., Inoue, S., Hiroi, H., Orimo, A., Kawashima, H., and Muramatsu, M. 1998. Isolation of estrogen-responsive genes with a CpG island library. *Mol. Cell Biol. 18*:442–449.

Oncogene (2005) 24, 4754–4764

www.nature.com/onc

Tyrosine phosphorylation of paxillin affects the metastatic potential of human osteosarcoma

Kotaro Azuma[1,2], Masamitsu Tanaka[1], Takamasa Uekita[1], Satoshi Inoue[2], Jun Yokota[3], Yasuyoshi Ouchi[2] and Ryuichi Sakai*,[1]

[1]*Growth Factor Division, National Cancer Center Research Institute, 5-1-1 Tsukiji, Chuo-ku, Tokyo 104-0045, Japan;* [2]*Department of Geriatric Medicine, Graduate School of Medicine, The University of Tokyo, 7-3-1, Hongo, Bunkyo-ku, 113-8655, Tokyo, Japan;* [3]*Division of Biology, National Cancer Center Research Institute, 5-1-1 Tsukiji, Chuo-ku, Tokyo 104-0045, Japan*

To acquire information on signal alteration corresponding to the changes in metastatic potential, we analysed protein tyrosine phosphorylation of low- and high-metastatic human osteosarcoma HuO9 sublines, which were recently established as the first metastatic model of human osteosarcoma. Tyrosine phosphorylation of proteins around 60, 70, and 120–130 kDa was enhanced in high-metastatic sublines. Among these proteins, the protein around 70 kDa, which was most remarkably phosphorylated, was identified as paxillin, a scaffold protein in integrin signaling. Activity of Src family kinase correlated well with metastatic potential, and a Src family kinase inhibitor, PP2, not only abolished tyrosine phosphorylation of paxillin but also impaired the motility of high-metastatic sublines. The expression of paxillin was also elevated in high-metastatic sublines, and knocking down of paxillin expression by RNAi method resulted in attenuated motility of high-metastatic cells. We also demonstrated that the phosphorylated form of paxillin is essential for the migration-promoting effect in human osteosarcoma. These findings suggest that enhanced activity of Src family kinases and overexpression of paxillin synergistically contribute to the high metastatic potential of human osteosarcoma through the hyperphosphorylation of paxillin.
Oncogene (2005) **24**, 4754–4764. doi:10.1038/sj.onc.1208654; published online 2 May 2005

Keywords: osteosarcoma; pulmonary metastasis; paxillin; tyrosine phosphorylation; Src family kinase; motility

Introduction

Multiple steps of tumor metastasis are regulated by various external stimuli such as hormones, cytokines and extracellular matrices. As major mediators of these stimuli, both receptor and nonreceptor tyrosine kinases play important roles to elicit intracellular signal transduction in response to the metastatic environment of tumor cells (Pawson, 2004). Various processes such as cell adhesion, anchorage-independent growth, cell motility, and cell invasion, which are essential components of tumor metastasis, are regulated by tyrosine phosphorylation. Indeed, the activation of Src family tyrosine kinases is frequently found during proliferation and metastasis of human cancers (Yeatman, 2004), indicating that tumor progression is reflected by the activity of tyrosine kinase and phosphorylation states of substrates in metastatic tumors.

Osteosarcoma is a primary malignant bone tumor that usually affects teenagers and frequent metastasis to the lungs is a clinical characteristic of osteosarcoma. As many as 20% of patients are estimated to have pulmonary metastases at the time of diagnosis and their prognosis is extremely poor with 10–20% 5-year survival rate (Meyers *et al.*, 1993; Tsuchiya *et al.*, 2002). Even though patients did not have metastases at the time of diagnosis, 35–50% of them developed pulmonary metastases during treatment (Huth and Eilber, 1989; Ward *et al.*, 1994). For this reason, pulmonary metastasis of osteosarcoma requires effective prevention and treatment.

Investigation of pulmonary metastasis of human osteosarcoma was impeded by the lack of a proper metastatic model of human osteosarcoma cell lines. Recently, Kimura *et al.* (2002) established human osteosarcoma cell lines with high metastatic potential to the lungs for the first time. From parental HuO9 cells, M112 and M132 were established as high-metastatic sublines, which developed more than 200 macroscopic metastatic nodules in the lungs after injection of 2×10^6 cells into the tail vein of nude mice. On the other hand, L12 and L13 are low-metastatic sublines established by the dilution plating method from the same parent HuO9 cells (Nakano *et al.*, 2003). These sublines developed only 0–15 macroscopic nodules in the lungs after injection of 2×10^6 cells and all mice survived up to 200 days.

In order to acquire information on signal alteration corresponding to the changes in metastatic potential, we compared the profile of protein tyrosine phosphorylation by utilizing these HuO9-derived sublines. A 68 kDa cytoskeletal protein, paxillin, was identified as a molecule that shows the most outstanding difference in phosphorylation state between low- and high-metastatic sublines among several phosphotyrosine-containing proteins that are differentially phosphorylated in these sublines. Paxillin has no intrinsic enzymatic activity, but it has multiple domains that interact with cytoskeletal and signaling molecules, and functions as a scaffold protein at focal adhesions (Turner, 2000; Schaller, 2001). Paxillin contains two critical tyrosine phosphorylation sites at Tyr 31 and Tyr 118 (Schaller and Parsons, 1995). These phosphotyrosines are considered to serve as docking sites for other signaling molecules, but it remains controversial whether these phosphotyrosines have promoting effect or inhibitory effect on cell motility.

In this study, we show overexpression and hyperphosphorylation of paxillin in high-metastatic sublines of human osteosarcoma, indicating that, in the case of human osteosarcoma, tyrosine phosphorylation of paxillin has a promoting effect for cell migration. We also demonstrate that elevated activity of Src family kinases in high-metastatic sublines is essential for the enhanced motility for these osteosarcoma cells, suggesting the contribution of Src family kinase activity to the high metastatic potential of human osteosarcoma.

*Correspondence: R Sakai; E-mail: rsakai@gan2.res.ncc.go.jp
Received 8 October 2004; revised 21 January 2005; accepted 25 February 2005; published online 2 May 2005

Results

General enhancement of tyrosine phosphorylation in high-metastatic HuO9 sublines

First, we confirmed the difference in motility between low- and high-metastatic sublines using Cell Culture Insert. High-metastatic sublines, M112 and M132, showed more than six times as high motility as low-metastatic sublines, L12 and L13 (data not shown). This result indicates that the motility of HuO9 sublines indeed correlates with their metastatic potential as previously reported (Nakano *et al.*, 2003).

To clarify the factors that determine the metastatic potential of HuO9 sublines, we compared expression patterns of phosphotyrosine-containing proteins between low- and high-metastatic sublines (Figure 1). General enhancement of tyrosine phosphorylation was observed in high-metastatic sublines, M112 and M132, as well as parental HuO9, which also has rather high metastatic potential (Nakano *et al.*, 2003). Among several phosphotyrosine-containing proteins showing elevated phosphorylation in high-metastatic sublines, the most striking difference was a broad band around 70 kDa (marked b in Figure 1). In addition, there were several other minor phosphotyrosine-containing proteins differentially expressed between low- and high-metastatic sublines, such as proteins around 60 kDa (marked c in Figure 1) and 120–130 kDa (marked a in Figure 1). These differences in tyrosine phosphorylation were consistent at different time points after plating (6 and 24 h) with and without fibronectin coating (Supplementary Figure 1 and data not shown).

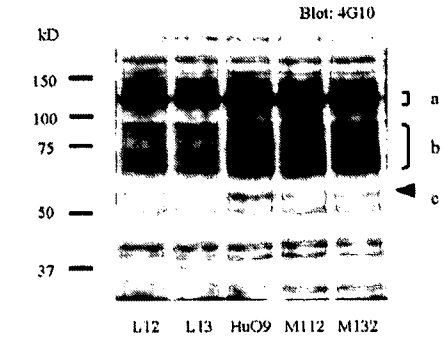

Figure 1 Elevated tyrosine phosphorylation of several proteins in high-metastatic sublines of HuO9 cells. Low-metastatic sublines (L12, L13), high-metastatic sublines (M112, M132) and parental HuO9 cells plated on plastic culture dishes for longer than 48 h were lysed for immunoblotting with anti-phosphotyrosine antibody 4G10. Hyperphosphorylated proteins in high-metastatic sublines are indicated on the right (a, b, c)

As candidate proteins of the difference around 120–130 kDa tyrosine phosphorylation, p130^{Cas} and focal adhesion kinase (FAK) were examined using phospho-specific antibodies (Figure 2). p130^{Cas} is a docking protein involved in the integrin signaling. We generated phospho-specific antibodies against several putative phosphorylation sites of p130^{Cas} and used them for the analysis. As a result, elevated phosphorylation of Tyr 762 was found in high-metastatic sublines (2.5 times as much as low-metastatic sublines), while phosphorylation of Tyr 460 of p130^{Cas} did not show obvious correlation with metastatic potential (Figure 2a). Tyr 460 represents tandem YDXP motifs in the substrate domain of p130^{Cas}, which binds (Crk) (Sakai *et al.*, 1994) or Nck (Schlaepfer *et al.*, 1997), and Tyr 762 consists of YDYV motif, which serves as a Src-binding site when phosphorylated (Nakamoto *et al.*, 1996). Expression of p130^{Cas} did not vary significantly among each subline (Figure 2a).

FAK is a nonreceptor tyrosine kinase, which is also involved in the integrin signaling, and its Tyr 397 is autophosphorylated when FAK is activated (Schaller *et al.*, 1994). The expression of FAK and phosphorylation on Tyr 397 of FAK were analysed. However, no remarkable elevation of tyrosine-phosphorylated FAK was detected in high-metastatic sublines (Figure 2b).

To identify the phosphotyrosine-containing protein around 60 kDa, the expression level and tyrosine phosphorylation of Src family kinases was examined. Among the members of Src family kinases, only Fyn kinase had the tendency of hyperphosphorylation in high-metastatic sublines (Figure 2c). Tyrosine phosphorylation of c-Src, Yes, and Fgr, other members of Src family kinases that were examined, did not correlate

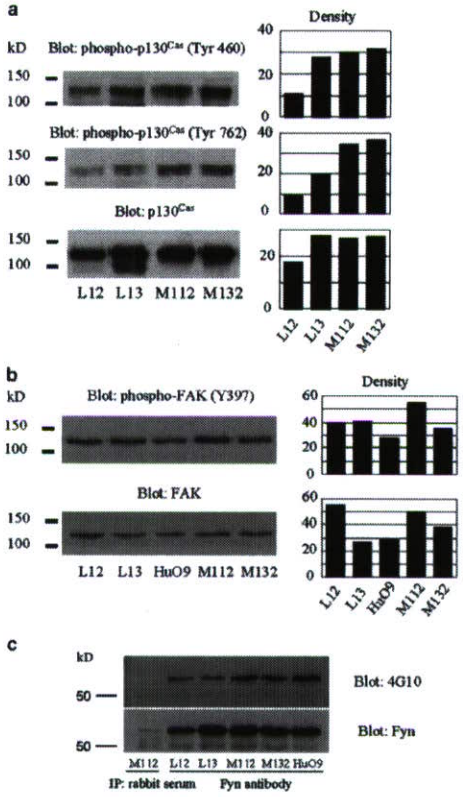

Figure 2 Elevated tyrosine phosphorylation of p130^{Cas} (Tyr 762) in high-metastatic sublines. (**a**) Whole-cell lysates from low-metastatic (L12, L13) and high-metastatic sublines (M112, M132) were immunoblotted for two kinds of anti-phosho-p130^{Cas} antibody (Tyr 460 representing the tandem YDXP motif, and Tyr 762 representing the YDYV motif in Src-binding domain) and p130^{Cas} antibody. Density of each blot was measured as described in Materials and methods. (**b**) Whole-cell lysates from low-metastatic (L12, L13), high-metastatic (M112, M132) and parental HuO9 were immunoblotted for anti-phospho-FAK antibody (Tyr 397) and anti-FAK antibody. Density of each blot was measured as described in Materials and methods. (**c**) Fyn kinase of low- and high-metastatic sublines was immunoprecipitated by anti-Fyn polyclonal antibody and subsequently immunoblotted with anti-phosphotyrosine antibody 4G10 or anti-Fyn antibody

with the metastatic potential (data not shown). However, absorption of Fyn by anti-Fyn antibody from lysates of low- and high-metastatic sublines could not remove the difference in tyrosine phosphorylation around 60 kDa (data not shown), indicating that not only Fyn contributes to the elevation of tyrosine phosphorylation around 60 kDa.

Overexpression and hyperphosphorylation of paxillin in high-metastatic HuO9 sublines

From the molecular size and the broad appearance of the 70 kDa protein, we estimated that this highly phosphorylated protein in high-metastatic sublines was paxillin. Using a specific antibody of phospho-paxillin (Tyr 118) for the blotting of whole-cell lysates, it was confirmed that high-metastatic sublines indeed contained a higher amount of tyrosine-phosphorylated paxillin in high-metastatic sublines (Figure 3A). It was also found that total paxillin expression was elevated in high-metastatic sublines compared with low-metastatic sublines (Figure 3A). As for both total paxillin and phospho-paxillin, high-metastatic sublines were estimated to contain about three to five times as much as low-metastatic sublines using densitometric analysis.

Absorption of paxillin by anti-paxillin antibody from lysates of low- and high-metastatic sublines remove most of the difference in tyrosine phosphorylation around 70 kDa (Figure 3B), indicating that paxillin mainly contributes to the elevation of tyrosine phosphorylation around 70 kDa.

Immunostaining of paxillin revealed that total paxillin and phospho-paxillin (Tyr 118) localize at focal adhesions, which were characterized at both ends of the actin filaments in L12 and M132 cells (Figure 3C). There was no significant change in the localization of paxillin by the metastatic potential of sublines, although the staining of total paxillin and phospho-paxillin were stronger in high-metastatic sublines than those in low-metastatic sublines (Figure 3D).

Src family kinase activity is elevated in the high-metastatic sublines

The general enhancement of tyrosine phosphorylation in high-metastatic sublines (Figure 1) suggests that the activity of some tyrosine kinases were enhanced in high-metastatic sublines. Therefore, we examined which tyrosine kinase is responsible for the high metastatic potential.

First, the difference in Src family kinase activity was investigated using Src-2 antibody, which is known to recognize wide ranges of Src family kinases. As a result, the activity of Src family kinases was elevated in the high-metastatic sublines compared with low-metastatic sublines (Figure 4a). The candidate for the Src family kinase responsible for the elevated kinase activity in high-metastatic sublines might be Fyn, which showed enhanced autophosphorylation in high-metastatic sublines (Figure 2c). We also examined the kinase activity of FAK and c-Abl, which are also reported to phosphorylate the tyrosine residues of paxillin. However, we observed a lack of correlation between kinase activity of FAK or c-Abl and metastatic potential (Figure 4b).

To check the influence of Src family kinase activity on cell motility elevated in high-metastatic sublines, cell migration assay was performed. In the high-metastatic sublines treated with PP2, an inhibitor of Src family kinases, motility was significantly suppressed, while in

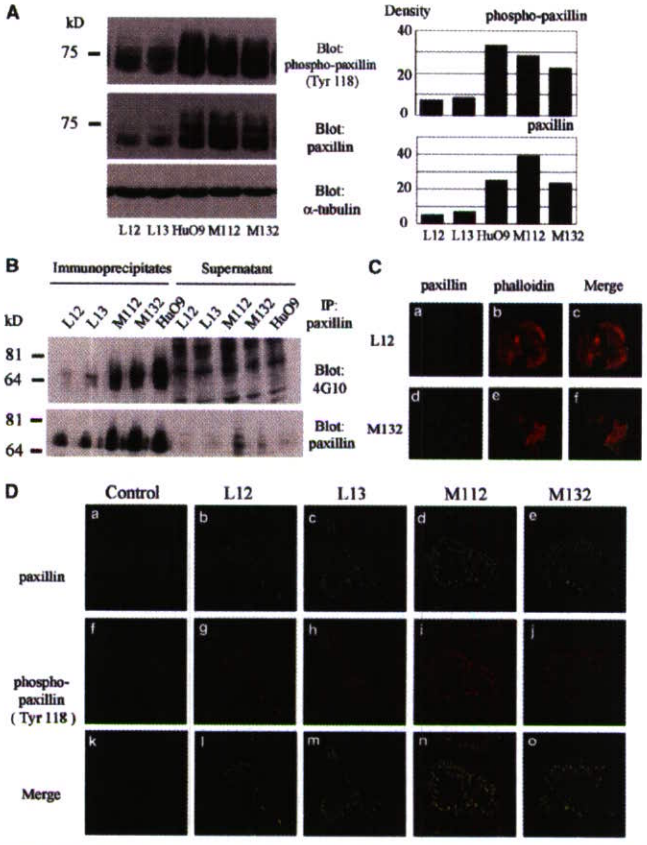

Figure 3 Overexpression and hyperphosphorylation of paxillin in high-metastatic sublines. (**A**) Whole-cell lysates from low-metastatic (L12, L13), high-metastatic (M112, M132) and parental HuO9 were immunoblotted for anti-phospho-paxillin antibody (Tyr 118), paxillin antibody and anti-α-tubulin antibody as an internal control. Densities of paxillin and phospho-paxillin blots are shown on the right. (**B**) Whole-cell lysates of low- and high-metastatic sublines and parental HuO9 cells were immunoprecipitated by monoclonal anti-paxillin antibody. Both immunoprecipitates and supernatants (indicated at the top) were subjected to immunoblotting analysis by anti-phosphotyrosine antibody 4G10 and anti-paxillin antibody. (**C**) L12 and M132 sublines were immunostained with anti-paxillin antibody (a, d: green), and chemically stained with phalloidin (b, e: red) at the same time. (**D**) Low- and high-metastatic sublines were immunostained with the antibody against paxillin (b–e: green) or phospho-paxillin (g–j: red). Superimposed confocal images (l–o: merge) demonstrate the portion of phosphorylated paxillin over the total paxillin. Images without first antibodies (a and f) are shown as negative controls. For comparison, panels were captured with identical gain and iris value and processed in the same way

the cells treated with PP3, inactive structural analog of PP2, their motility was not affected (Figure 4c). The effect of Src family kinase on the tyrosine phosphorylation of paxillin was also evaluated. When, high-metastatic sublines were treated with PP2, the tyrosine phosphorylation of paxillin was almost completely abolished, while the phosphorylation remained unchanged when the cells were treated with PP3 (Figure 4d). These results indicate that, in high-metastatic sublines of HuO9, tyrosine phosphorylation of paxillin and enhanced cell motility are mostly dependent on the activity of Src family kinases.

Cell migration was attenuated by knocking down of paxillin expression in high-metastatic sublines

To evaluate the direct involvement of paxillin in the cell motility of the osteosarcoma cells, paxillin expression was knocked down using RNA interference (RNAi) in high-metastatic HuO9 sublines. Using a novel approach

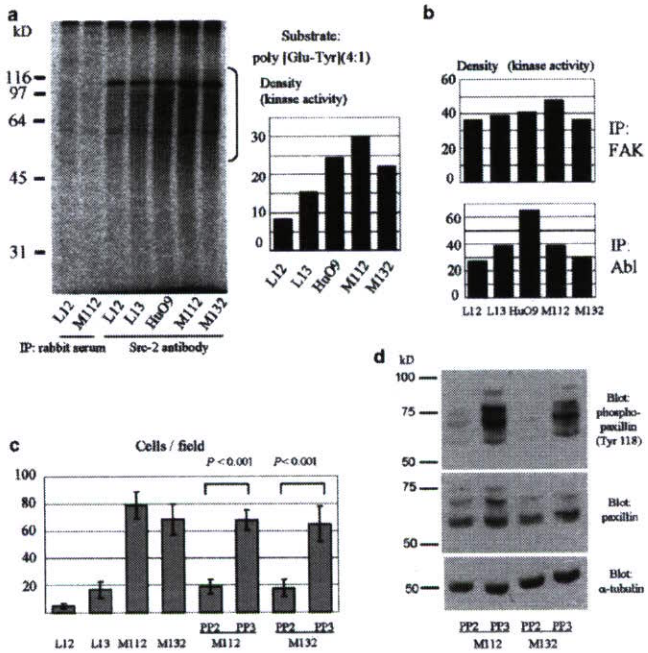

Figure 4 Elevated Src family kinase activity in high-metastatic sublines. (**a**) Elevated Src family kinase activity in high-metastatic sublines. Src family kinases of low- and high-metastatic sublines and parental HuO9 cell lysates were immunoprecipitated by Src-2 antibody. Lysates of L12 and M112 immunoprecipitated with preimmune rabbit serum were used as negative controls. Kinase activity was evaluated by phosphorylation of exogenous synthetic polypeptide poly[Glu-Tyr](4:1). The density of each smear (between 50 and 150 kDa, area shown by a bracket) was quantified. (**b**) FAK or c-Abl of low- and high-metastatic sublines and parental HuO9 were immunoprecipitated by monoclonal antibodies. To evaluate kinase activity, exogenous synthetic polypeptide poly[Glu-Tyr](4:1) was used. The kinase activities were quantified according to the same method as described in (**a**). (**c**) Src family kinase inhibitor PP2 (4-amino-5-(4-chlorophenyl)-7-(t-butyl)pyrazolo[3,4-d]pyrimidine) impairs the motility of high-metastatic sublines. Motility of low- and high-metastatic sublines and parental HuO9 cells was evaluated by migration assay as described in Materials and methods. As for high-metastatic sublines, M112 and M132, motility in the presence of 10 μM of PP2 or 10 μM of PP3 (4-amino-7-phenylpyrazol [3,4-d]pyrimidine) was also evaluated. The cells at the lower side of the filters were stained by Giemsa's stain solution and visualized under microscope at a magnification of $\times$ 200. Each bar represents the mean number of cells $\pm$ s.d. counted in five fields. (**d**) Src family kinase inhibitor PP2 abolishes tyrosine phosphorylation of paxillin. High-metastatic subline M112 and M132 were treated with 10 μM of PP2 or PP3 for 30 min prior to cell lysis. Whole-cell lysates were immunoblotted for anti-phospho-paxillin antibody, anti-paxillin antibody and anti-α-tubulin antibody

called the Dicer method to introduce a series of short interfering RNA (siRNA) into the cells, paxillin expression was suppressed by about 60%, while phospho-paxillin decreased by about 30% compared with LacZ siRNA-treated cells (Figure 5a).

Although the expression of paxillin was not completely suppressed, cell motility was impaired by about two-thirds by treatment with paxillin siRNA when compared with LacZ siRNA-treated cells (Figure 5b). This difference is statistically significant over nonspecific effects of siRNA on cell survival and motility.

This attenuation of motility was not observed when the expression of p130^{Cas} was knocked down using the Dicer method in high-metastatic sublines (Supplementary Figure 2a, b). These results indicate paxillin rather than p130^{Cas} is more closely associated with the motility of osteosarcoma sublines.

Overexpression of paxillin and elevation of Src family kinase activity synergistically enhance the motility of human osteosarcoma

To further examine the role of paxillin and its tyrosine phosphorylation on the motility of osteosarcoma sublines, the effect of transient transfection of GFP-paxillin and its phenylalanine mutant of two tyrosines (2F mutant) was evaluated. In 2F mutant, two critical tyrosine phosphorylation sites at Tyr 31 and Tyr 118 were mutated to phenylalanine, and these tyrosine residues were confirmed to be major phosphorylation sites by transient transfection of GFP-paxillin and GFP-2F mutant to COS-7 cells (Figure 6A).

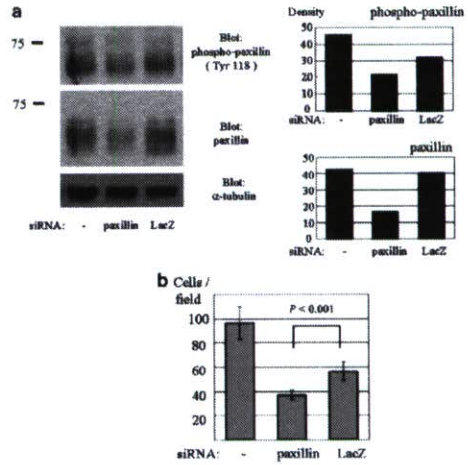

Figure 5 Cell migration was attenuated by knocking down of paxillin expression in high-metastatic sublines. (**a**) M112 subline was transfected with siRNA of paxillin or LacZ, or treated only with lipofection reagent ((−), as indicated at the bottom). Cells were lysed at 72 h from the transfection and whole-cell lysates were immunoblotted with the antibodies indicated. The density of each band is shown on the right. (**b**) M112 subline was transfected with siRNA or treated only with lipofection reagent as described above. Transfected cells were subjected to migration assay as described in Materials and methods

Next, GFP-paxillin and GFP-2F mutant were transiently expressed in the low-metastatic subline, L12 (Figure 6B, arrowhead in lower panel). The tyrosine phosphorylation of GFP-paxillin was detected by phospho-paxillin (Tyr 118) antibody in L12 (Figure 6B, arrowhead in upper panel), although this polyclonal antibody showed slight reactivity even to the 2F mutant of paxillin. Both GFP-paxillin and GFP-2F mutant were confirmed to localize at focal adhesions (Figure 6C).

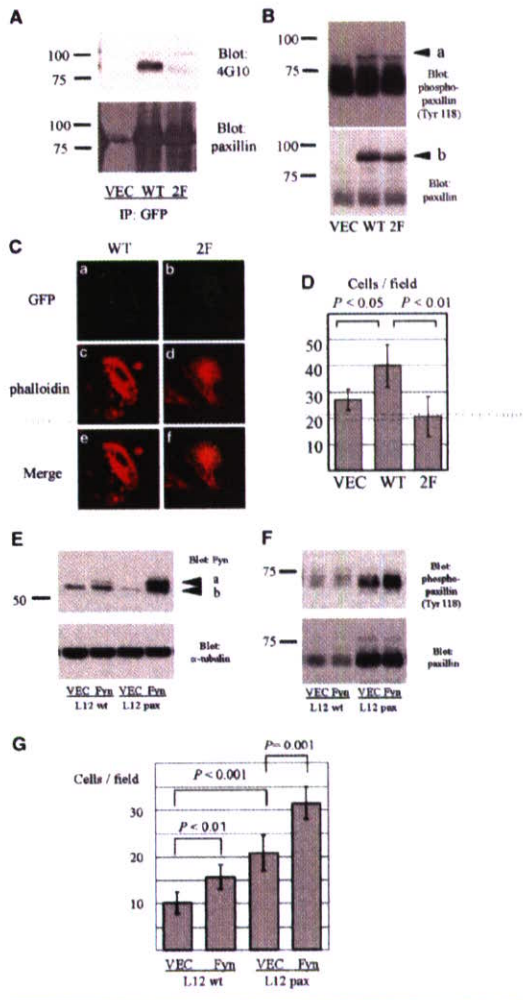

Figure 6 Overexpression of paxillin and elevation of Src family kinase activity synergistically enhance the motility of human osteosarcoma. (**A**) Cos-7 cells were transiently transfected with empty vector (VEC), GFP-paxillin (WT) or GFP-2F (Y31F, Y118F) mutant (2F). Cells were lysed at 48 h from the transfection and immunoprecipitated with anti-GFP antibody. Immunoprecipitates were subjected to immunoblotting analysis by anti-phosphotyrosine antibody 4G10 and anti-paxillin antibody. (**B**) L12 cells were transiently transfected with empty vector (VEC), GFP-paxillin (WT) or GFP-2F mutant (2F). Whole-cell lysates were immunoblotted for anti-phospho-paxillin antibody (Tyr 118) and paxillin antibody. GFP-paxillin and GFP-2F mutant were indicated (arrowhead a and b). (**C**) L12 cells transfected with GFP-paxillin or GFP-2F mutant were chemically stained with phalloidin. GFP (a, b: green) and phalloidin (c, d: red) were visualized with confocal microscopy. (**D**) L12 cells transfected with empty vector, GFP-paxillin or GFP-2F mutant were subjected to migration assay as described in Materials and methods. (**E, F**) L12 cells (L12 wt) or paxillin-FLAG-expressing stable cells (L12 pax) were transiently transfected with empty vector (VEC) or Fyn-FLAG (Fyn). Whole-cell lysates were immunoblotted for the antibodies indicated. Fyn-FLAG (arrowhead a) and endogenous Fyn (arrowhead b) were shown in (**E**) upper panel. (**G**) L12 cells or paxillin-FLAG-expressing stable cells that were transiently transfected with empty vector or Fyn-FLAG were subjected to migration assay as described in Materials and methods

Cell motility was enhanced by the transient expression of GFP-paxillin compared with the transfection of GFP-2F mutant or empty vector (Figure 6D). This indicates that the amount of wild-type paxillin is positively correlated with the motility of osteosarcoma sublines. Considering that GFP-2F mutant could localize at focal adhesions (Figure 6C), the lack of motility-promoting effect of GFP-2F mutant was due to the absence of phosphorylation at Tyr 31 and Tyr 118.

The synergistic effect of paxillin overexpression and Src family kinase activity was examined using a low-metastatic subline, L12. We established L12 cells that stably express more than five times as much an amount of exogenous paxillin as the wild-type L12 subline, which is a similar level of endogenous paxillin in the high-metastatic sublines. FLAG epitope-tagged Fyn was transiently transfected to wild-type L12 cells and paxillin-overexpressing L12 cells (Figure 6E). Enhancement of tyrosine phosphorylation of paxillin was observed in Fyn-FLAG-transfected cells compared with mock-transfected cells in both wild-type L12 and paxillin-overexpressing L12 cells (Figure 6F). Cell migration assay reveals that overexpression of both Fyn-FLAG and paxillin-FLAG significantly enhances the cell motility of L12 cells (Figure 6G). This result of cell migration was correlated with the amount of phospho-paxillin in the cells (Figure 6F, upper panel), which suggests that overexpression of paxillin and Fyn contributes to the enhanced motility through the tyrosine phosphorylation of paxillin.

Discussion

We have shown the general enhancement of tyrosine phosphorylation in high-metastatic HuO9 sublines, and the elevated activation of Src family kinase. Among the substrates of Src family kinase, prominent phosphorylation of paxillin along with elevated expression of paxillin was observed in the high-metastatic sublines.

Since human osteosarcoma cell lines suitable for metastatic study were not available, results of previous biochemical analysis on metastatic osteosarcoma were derived from murine models (Khanna *et al.*, 2001, 2004; Iwaya *et al.*, 2003). The present study is the first biochemical analysis on human metastatic osteosarcoma. We used four independent, but genetically close sublines of osteosarcoma that are excellent tools for analysis of signal alteration in the process of acquiring metastatic potential. The high-metastatic sublines were established by *in vivo* selection and the low-metastatic sublines by the dilution plating method. Considering that malignant tumors contain subpopulations of different metastatic capabilities, these selection methods resemble authentic events during the progression of osteosarcoma. Moreover, these sublines were established without any manipulation of genes, which minimizes the artificial effects on our study.

In these sublines of human osteosarcoma, the results of cell motility assay clearly reflected metastatic potential (Nakano *et al.*, 2003). This is reasonable because the properties of cancer cells measured by cell migration assay such as cell movement and ability to interact with extracellular matrix are critical factors during tumor metastasis. Therefore in this study, cell motility was used as an indicator of metastatic potential.

Elevation of Src family kinase activity in metastases was reported in human colorectal cancer (Talamonti *et al.*, 1993) and in human melanoma (Marchetti *et al.*, 1998). According to these reports, there is clear difference in the activated member of Src family kinase among types of tumors. Talamonti *et al.* showed increased activity of c-Src in liver metastases compared to primary tumor. Marchetti *et al.* used brain metastatic sublines and found that kinase activity of Yes, not c-Src, was elevated compared to low-metastatic cells. We recently reported that, in a metastatic model of murine melanoma cell lines, kinase activity of Fyn was elevated in high-metastatic sublines, and interacted with cortactin (Huang *et al.*, 2003). Although not as significant as in the case of murine melanoma, Fyn will also be a candidate for the responsible kinase for metastatic potential of human osteosarcoma. Other members of Src family kinase with relatively low expression, such as c-Src, or with relatively low kinase activity do not appear to be involved in regulation of metastatic potential.

In osteosarcoma, elevated phosphorylation of YDYV motif in $p130^{Cas}$ in high-metastatic sublines (Figure 2a) is a possible clue to Src family activation because phosphorylated YDYV motif in $p130^{Cas}$ stabilizes the active form of Src family kinases by binding with the SH2 domain of Src family kinases (Nakamoto *et al.*, 1996; Burnham *et al.*, 2000). This type of molecule may function as a regulator of Src family kinases that causes activation of Src family kinases in osteosarcoma cells, although the contribution of phosphorylated $p130^{Cas}$ may be low considering the small effect of RNAi on the cell motility.

Although this is the first report on hyperphosphorylation of paxillin in a metastatic tumor, some studies investigated the relationship of cell motility and tyrosine phosphorylation of paxillin. Tyr 31 and Tyr 118 of paxillin are phosphorylated upon cell adhesion (Burridge *et al.*, 1992) and Src family tyrosine kinases (Klinghoffer *et al.*, 1999), FAK (Schaller and Parsons, 1995), and c-Abl (Lewis and Schwartz, 1998) are reported to phosphorylate these sites. The roles of phospho-paxillin on cell motility are still controversial. Migration-promoting effect of phospho-paxillin was demonstrated by using Nara bladder tumor II (NBTII) cells (Petit *et al.*, 2000), while migration-inhibitory effect was shown by using NMuMG cells, MM-1 cells and Cos 7 cells (Yano *et al.*, 2000; Tsubouchi *et al.*, 2002). Our results have added another example of the migration-promoting effects of phospho-paxillin.

The migration-promoting effect of phospho-paxillin might be due to interaction with Crk (Schaller and Parsons, 1995). Crk interacts with a cellular protein DOCK180, which binds directly and activates small GTPase Rac1 (Kiyokawa *et al.*, 1998). Activation of this pathway provides a link between paxillin–Crk association and cell motility.

The binding partners of phospho-paxillin seem to vary among tumor types and may provide some clue for the controversy between migration-promoting and inhibitory effect of phospho-paxillin. In NMuMG cells, in which phosho-paxillin exerts migration inhibitory effect, phospho-paxillin was shown to bind p120Ras-GAP and RhoA activity was suppressed as a downstream of signal transduction (Tsubouchi *et al.*, 2002). Therefore, it is also possible that SH2 domain-containing molecule other than Crk may function as a binding partner of phospho-paxillin and send a positive signal for cell motility in osteosarcoma cells.

We observed the impaired motility by knocking down the expression of paxillin and showed the direct effect of paxillin on cell migration. Paxillin-knocked-down cells showed 67% migration activity compared to LacZ siRNA-treated cells. One reason for this rather weak motility suppression is the partial effect of RNAi, as 40% of paxillin and 68% of phospho-paxillin remained after the treatment with paxillin siRNA compared to LacZ siRNA-treated cells. Another possible reason is the existence of other factors that enhance the metastatic potential independently of paxillin. However, considering the partial effect of RNAi, it can be estimated that paxillin has a significant contribution to high-metastatic phonotype.

We examined the contribution of $p130^{Cas}$, which is another substrate of Src family kinase and involved in the integrin signaling. As a result, suppression of $p130^{Cas}$ expression did not affect the motility of high-metastatic osteosarcoma cells, which supports the relative importance of paxillin in the motility of osteosarcoma cells.

FAK is also known as a binding partner and a substrate of Src family kinase. However, in the osteosarcoma sublines, the tyrosine phosphorylation of FAK was not correlated with the activity of Src family kinase. This may suggest that, in the case of human osteosarcoma, the phosphorylation of FAK reflects other kinase activity including autophosphorylation and is not strongly associated with metastatic potentials.

We have shown the migration-promoting effect of phosho-paxillin by overexpression of GFP-paxillin and its mutant. Expression of exogenous GFP-paxillin enhanced the cell motility in the low-metastatic subline, while expression of GFP-2F mutants did not. Furthermore, we showed paxillin overexpression and Src family activity could contribute to the high metastatic potential of osteosarcoma. Expression of Fyn-FLAG and paxillin-FLAG at the same time in the L12 subline promoted the motility synergistically, although it did not enhance the motility to the extent of high-metastatic sublines, probably because of the existence of other factors which contribute to the high-metastatic potential of osteosarcoma. These results strongly suggest that this cooperative function of Src family kinase and paxillin also works in endogenously expressed proteins and play a major role in high-metastatic phenotype of osteosarcoma cells.

Then, what is the mechanism of overexpression of paxillin in high-metastatic sublines of human osteosarcoma? The locus of paxillin, 17p8q, is not included in the areas where comparative genomic hybridization (CGH) analysis revealed that gene amplification is frequent in human osteosarcoma (Batanian *et al.*, 2002; Squire *et al.*, 2003; Lau *et al.*, 2004). Paxillin mRNA in high-metastatic sublines is at most 1.7 times compared to that in low-metastatic sublines by cDNA microarray analysis (Nakano *et al.*, personal communication). Considering high-metastatic sublines express about five times as much paxillin as low-metastatic sublines, paxillin may be highly stable and degraded slowly in high-metastatic sublines.

In conclusion, this study provides information on the importance of phospho-paxillin during metastasis of human osteosarcoma. We have shown that enhancement of Src family kinase activity and overexpression of paxillin synergistically contribute to the high metastatic potential of human osteosarcoma through hyperphosphorylation of paxillin. Further biochemical analysis is needed to clarify the phosphotyrosine-dependent binding partner with paxillin, since the downstream pathway specific to tumor metastasis is a potential therapeutic target. If Src family kinases are activated by a specific mechanism in metastatic osteosarcoma, that would also be an attractive therapeutic target. These themes deserve investigation to improve the extremely poor prognosis of metastatic osteosarcoma.

Materials and methods

Antibodies and reagents

Anti-phosphotyrosine antibody 4G10 was purchased from Upstate Biotechnology. Phospho-specific antibodies against Tyr 460 and Tyr 762 of $p130^{Cas}$ were raised by immunizing rabbits with peptide CAEDVYDVP and CMEDYDYVHL, respectively, and affinity purified. As anti-$p130^{Cas}$ antibody, polyclonal Cas2 antibody was used as described previously (Sakai *et al.*, 1994). Monoclonal antibody against FAK was from BD Transduction Laboratories. Polyclonal antibody against phospho-FAK (Tyr 397) was purchased from Upstate Biotechnology. Monoclonal antibody against c-Src (GD11) was from Upstate Biotechnology. Polyclonal antibodies against Fyn (Fyn-3), Fgr (N-47) and pan-Src (Src-2) were from Santa Cruz Biotechnology. Monoclonal antibodies against Yes, Hck, Lck and Lyn were purchased from BD Transduction Laboratories. Monoclonal antibody against paxillin was from Zymed Laboratories Inc. Polyclonal antibody against phospho-paxillin (Tyr 118) was purchased from Cell Signaling. Anti-α-tubulin antibody (B-5-1-2) was purchased from SIGMA. Monoclonal antibody against Abl was from BD Biosciences. Polyclonal antibody against GFP (598B) was from Medical and Biological Laboratories. HRP-conjugated anti-mouse antibody was purchased from Amersham Pharmacia. Alexa Fluor 488 goat anti-mouse IgG, Alexa Fluor 594 goat anti-rabbit IgG and Alexa Fluor 546 phalloidin were purchased from Molecular Probe. Normal rabbit serum was from DakoCytomation. Src family kinase inhibitor PP2 and the structural analog PP3 were purchased from Calbiochem-Novabiochem Ltd.